

A Field Device to Rapidly Determine the Bending Strength of Maize Stalks

A Thesis

Presented in Partial Fulfillment of the Requirements for the

Degree of Master of Science

with a

Major in Mechanical Engineering

in the

College of Graduate Studies

University of Idaho

by

Taylor W. Spence

Approved by:

Major Professor: Daniel Robertson, Ph.D., PE

Committee Members: Michael Maughan, Ph.D., PE; Joel Perry, Ph.D., PE

Department Administrator: Gabriel Potirniche, Ph.D., PE

December 2021

## Abstract

Billions of dollars' worth of maize are destroyed across the world every year by high winds, hail, and other natural phenomena. Historically, plant breeders and farmers have been unable to prevent these losses using selective breeding because no reliable method for determining stalk strength was available. Recent innovations have seen several devices and methods created to determine stalk strength, but each has its downsides. One of the more promising methods is the use of puncture tests, which puncture maize stalks with a needle and record the displacement and force of the needle. The data from these tests are then analyzed to extract important information about the stalk geometry. Experiments have shown that this method for determining stalk strength is highly correlated with more direct and destructive methods of stalk strength analysis. However, these tests have only been performed in a lab setting with heavy and expensive equipment.

The Stalk Puncture Device (SPuD) is a novel handheld, battery-operated, unit capable of performing nearly 100 puncture tests per hour. This device costs a fraction of the price of standard lab equipment and allows users to test stalks *in vivo*. Initial tests of the device during validation are promising and show strong correlation with data from lab equipment. Hardware and software improvements were identified during validation that will likely improve these correlations further in the future.

### Acknowledgements

I would like to thank Dr. Robertson for his support, guidance, and inspiration to pursue this degree.

My sincere thanks to Dr. Christopher Stubbs for his assistance, advice, and encouragement throughout my research.

I would like to thank my committee members, Dr. Michael Maughan and Dr. Joel Perry, for bringing their expertise not only to my research, but to my education here as well.

I would also like to extend my gratitude to Andrew Stucker, Hunter Casteel, and Austin Bebee for their advice and help throughout my project.

Lastly, I would like to thank the University of Idaho and especially the Mechanical Engineering Department staff for providing me with the resources, support, and care that has made gaining an education here a joy.

Funding for this research was provided by the National Science Foundation grant #1826715.

**Dedication**

I dedicate this work to my wife Ruthie, my son Roran, and my daughter Arden. Your patience and support made this work possible.

## Chapter 1: Table of Contents

Abstract .....	ii
Acknowledgements .....	iii
Dedication .....	iv
List of Tables.....	vii
List of Figures .....	viii
Chapter 1: Background.....	1
1.1 Introduction .....	1
1.2 Stalk lodging.....	1
1.3 Selective breeding .....	3
1.4 Devices to predict lodging resistance .....	4
1.5 Methods to explain lodging resistance .....	5
1.6 Determining stalk geometry .....	6
1.7 Rind puncture tests .....	6
1.8 Stalk Puncture Device (SPuD) .....	8
Chapter 2: Stalk Puncture Device (SPuD).....	10
2.1 Abstract .....	10
2.2 Repository Files.....	10
2.3 Bill of Materials.....	11
2.3.1 Purchased Components .....	11
2.3.2 3D Printed Components .....	12
2.3.3 Laser Cut Components .....	13
2.3.4 Machined Components .....	13
2.3.5 Hardware .....	13
2.3.6 SPuD Total Cost.....	14
2.4 Build Instructions .....	15
2.4.1 Case Assembly .....	15

2.4.2 Backside Assembly .....	17
2.4.2 Linear System Assembly.....	26
2.4.4 Attaching Linear System and Backside to Case.....	29
2.4.5 Adding Electrical Components.....	32
2.4.6 Lid Assembly.....	38
2.4.7 Wiring.....	46
2.4.8 Load Cell and Needle Mounting .....	54
2.4.9 Shoulder Strap Setup .....	58
2.5 User Interface .....	60
2.5.1 Main Menu .....	60
2.5.2 Settings Menu.....	60
2.5.3 Hardware Check Screen .....	63
2.5.4 Testing Menu.....	64
2.5.5 Setting Zero and Start Positions .....	65
2.5.6 Setting Plot, Stalk, and Node.....	67
2.5.7 Testing .....	68
2.6 Validation.....	70
2.6.1 Methods .....	70
2.6.2 Validation Results .....	71
Chapter 3: Conclusion .....	76
3.1 Design Challenges .....	76
3.2 Next Steps.....	77
3.3 Conclusion.....	78
Literature Cited.....	79

**List of Tables**

Table 2.1 Repository file names and descriptions.....	10
Table 2.2 Purchased components bill of materials.....	11
Table 2.3 3D printed components bill of materials.....	12
Table 2.4 Laser cut components bill of materials.....	13
Table 2.5 Machined components bill of materials .....	13
Table 2.6 Hardware bill of materials.....	13
Table 2.7 SPuD total cost.....	14

## List of Figures

Figure 1.1 [10] A group of lodged maize stalks.....	2
Figure 1.2 [11] Mid-season versus late-season failure methods in maize.....	2
Figure 1.3 Maize stalk geometry.....	3
Figure 1.4 [11] a) Guo's Device b) DARLING Device.....	4
Figure 1.5 [22] Rind puncture resistance device.....	5
Figure 1.6 Puncture test graph shows how different geometry is determined from the graph.....	7
Figure 1.7 [29] Puncture test being run on Instron.....	8
Figure 1.8 CAD model render of SPuD.....	9
Figure 2.1 Case assembly components.....	15
Figure 2.2 Outer case assembled.....	16
Figure 2.3 Bottom cover and legs attached.....	16
Figure 2.4 Case assembled with bottom buttons installed.....	17
Figure 2.5 Load cell cover assembly components.....	18
Figure 2.6 Screw inserted on slide and pre-threaded on nut.....	18
Figure 2.7 Slider moved into position on load cell cover part.....	19
Figure 2.8 Allen wrench positioned to tighten front slider screw.....	19
Figure 2.9 Slider moved forward and nut inserted in cutout.....	20
Figure 2.10 Allen positioned to tighten rear slider screw.....	20
Figure 2.11 Slide pushed forward with holder head attached.....	21
Figure 2.12 Shoulder bolt threaded into interior of slide.....	21
Figure 2.13 Load cell cover with both sliders installed.....	22
Figure 2.14 Nuts inserted into openings on back of load cell cover.....	22
Figure 2.15 Fully assembled load cell cover.....	23
Figure 2.16 Motor cover assembly components.....	24
Figure 2.17 Motor cover showing spring and plunger insertion.....	25
Figure 2.18 Linear system assembly components.....	26
Figure 2.19 Linear system with load cell mount attached.....	27
Figure 2.20 Linear scale cut to length and with wire shortened.....	27
Figure 2.21 Linear scale with linear system interface mounted.....	28
Figure 2.22 Linear scale aligned for assembly to linear system.....	28
Figure 2.23 Linear system assembly complete.....	29
Figure 2.24 Linear system assembly and load cell cover attached to case.....	29
Figure 2.25 Front bolts attaching load cell cover and linear system to case.....	30

Figure 2.26 Motor cover attached to case. ....	30
Figure 2.27 Bolts connecting motor case to case assembly.....	31
Figure 2.28 Right case cover removed to show rear motor case bolts. ....	31
Figure 2.29 Case with linear system, load cell case, and motor case assembled. ....	32
Figure 2.30 Motor driver with required fasteners.....	32
Figure 2.31 Motor driver attached to case with fasteners.....	33
Figure 2.32 Stepper motor wired to motor driver.....	33
Figure 2.33 Arduinos with required fasteners. ....	34
Figure 2.34 Arduinos attached to case with fasteners. ....	34
Figure 2.35 Load cell wiring components. ....	35
Figure 2.36 (Left) Placement for compliant clip on load cell wire cover. (Right) Fully seated compliant clip. ....	36
Figure 2.37 Load cell with wire routed through gap and into hole in bottom cover. ....	36
Figure 2.38 Load cell wire cover snapped in place. ....	37
Figure 2.39 Nut inserted in bottom of wire spool part. ....	37
Figure 2.40 Load cell wire spooled around part.....	38
Figure 2.41 Load cell wire spool cover bolted down and load cell wired to load cell amp. ....	38
Figure 2.42 DC power panel mount assembly components. ....	39
Figure 2.43 DC plug to discreet wire part and nuts set into mount. ....	39
Figure 2.44 Top cover of DC panel mount part added.....	40
Figure 2.45 DC power components mounted to lid with screws and wired.....	40
Figure 2.46 Panel mount touch screen assembly components. ....	41
Figure 2.47 Touch screen frame with screws mounted to top cover. ....	42
Figure 2.48 Touchscreen mounted to the bottom of top cover with nuts. ....	42
Figure 2.49 Panel mount SD port assembly components. ....	43
Figure 2.50 SD breakout board and nuts inserted into mount part. ....	43
Figure 2.51 SD breakout board bolted to mounting part. ....	44
Figure 2.52 SD breakout mount being held and fastened to top cover.....	44
Figure 2.53 USB splitter panel assembly components. ....	45
Figure 2.54 Cut grommet placed on USB splitter cable. ....	45
Figure 2.55 USB splitter routed through top cover. ....	46
Figure 2.56 Pre-wiring layout of case. ....	47
Figure 2.57 Wiring from Arduino Uno to Arduino Mega.....	47
Figure 2.58 Wiring Arduino Uno to motor driver. ....	48

Figure 2.59 Example Dupont connector cable.	48
Figure 2.60 Wiring Dupont connector to Arduino Mega.	49
Figure 2.61 Wiring components.	50
Figure 2.62 Wiring common ground for motor driver.	50
Figure 2.63 Limit switches mounted and wired.	51
Figure 2.64 Wiring left and right push buttons.	51
Figure 2.65 Linear assembly cover installed.	52
Figure 2.66 Top lid components wired.	52
Figure 2.67 Top cover mounted and hook and loop tape applied.	53
Figure 2.68 Hook and loop tape applied to batteries.	53
Figure 2.69 Batteries attached to case using hook and loop tape and plugged in.	54
Figure 2.70 Needle chuck assembly components.	55
Figure 2.71 Needle chuck being assembled.	55
Figure 2.72 Main menu screen (left) and the hardware check screen (right).	56
Figure 2.73 Slide stop part slid over load cell mount and secured with screws.	56
Figure 2.74 Load cell secured to load cell mount with screw.	57
Figure 2.75 Needle chuck threaded onto loadcell.	58
Figure 2.76 Camera straps looped through sling mounts.	58
Figure 2.77 Sling mounts secured to both sides of device.	59
Figure 2.78 Fully assembled SPuD being held by shoulder harness.	59
Figure 2.79 Main menu screen.	60
Figure 2.80 Settings menu screen.	61
Figure 2.81 Load cell recalibration screens A) Record zero screen B) Enter known weight screen C) Record known weight screen D) Save calibration screen.	62
Figure 2.82 Settings menu with alternate theme colors.	63
Figure 2.83 Hardware check screen.	64
Figure 2.84 Testing menu screen.	65
Figure 2.85 Set zero position screen.	66
Figure 2.86 Set start position screen.	67
Figure 2.87 Set plot number screen.	68
Figure 2.88 SPuD during test.	69
Figure 2.89 Post-test screen.	70
Figure 2.90 Stalk holder for validation tests.	71

Figure 2.91 Three graphs comparing SPuD and Instron data for the same internodes. A) Graph with high error between SPuD and Instron area under the curve values; likely caused by incorrect zero on SPuD. B) Median error graph of all tests. C) Graph with low error.....	73
Figure 2.92 Scatter plot comparing minor diameter calculations for the Instron and SPuD.....	74
Figure 2.93 Scatter plot comparing SPuD and Instron IPS values.....	75

## Chapter 1: Background

### 1.1 Introduction

Humans are dependent on only a few staple crops for most of our sustenance. Maize, rice, and wheat make up more than 50% of total caloric intake for humans worldwide [1]. A significant portion of maize is also utilized as a primary ingredient in livestock feed [1], [2]. Ever increasing amounts of maize are also being grown to make biofuels as the demand for these fuels continues to grow [1], [3].

As the world population rapidly expands, demand for maize has increased. However, the total amount of farmland has been decreasing [4]. Because of this, it is becoming increasingly vital that we guarantee the yield of farmlands producing maize. A large obstacle on our path to ensuring high yield is stalk lodging.

The purpose of this thesis is to describe a handheld device that will help improve the yield of maize crops by identifying the geometric features of stalks that increase stalk lodging resistance.

### 1.2 Stalk lodging

Stalk lodging is the buckling or breakage of a plant stalk which typically occurs as a result of high winds, hail, rain, or other natural phenomena. Late season maize stalks tend to fail through Brazier buckling of the internodes [5], which are the long pith filled sections of the stalk separated by solid nodes. Early season stalks tend to fail by snapping at the node [6]. Lodging early in the growth of a plant may kill it or decrease the grain quality of the plant if it survives [7], [8]. Late season lodging typically results in the plant being unable to be harvested by conventional means [9].



Figure 1.1 [10] A group of lodged maize stalks.

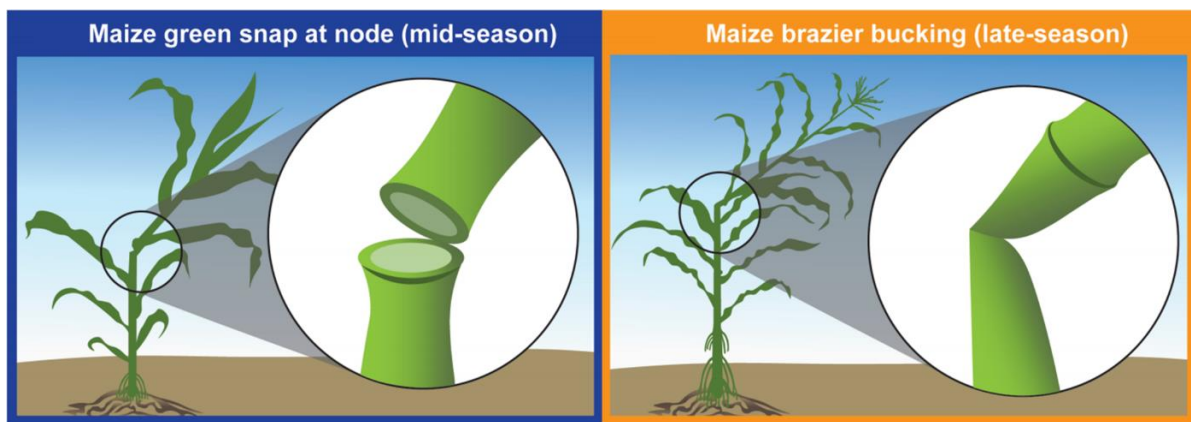


Figure 1.2 [11] Mid-season versus late-season failure methods in maize.

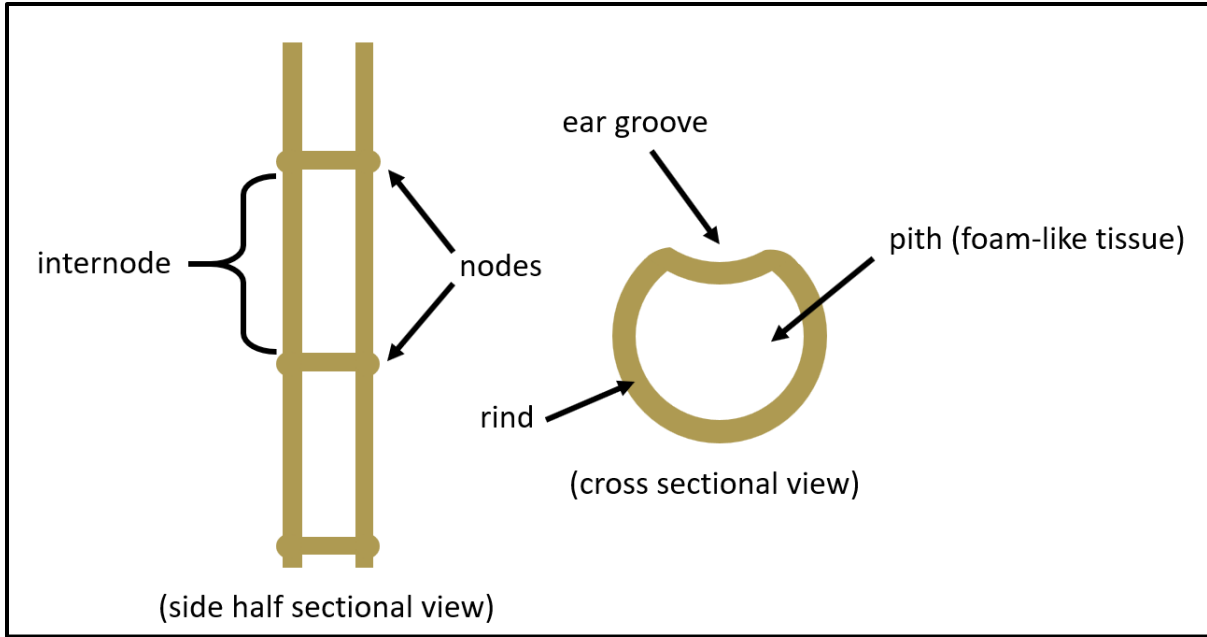


Figure 1.3 Maize stalk geometry.

Maize is not the only plant to have significant yield losses as a result of stalk lodging. Other large grains such as sorghum [12] and small grains like wheat [13] lose a significant portion of their yield to this phenomenon. Another similar phenomenon called root lodging, which is the toppling of a plant as a result of the breakage or pulling out of the roots occurs in many of these plants as well.

In the United States between 5-20% of the total maize yield is lost as a result of lodging every year [14]. This equates to 3.8 billion dollars of lost yield every year [15]. Not only does this loss effect farmers, but it also negatively impacts consumers who see an increase in the prices of their food, feed, and fuel. There is therefore a demand for maize plants with improved stalk lodging resistance.

### 1.3 Selective breeding

The most widespread method for actively increasing stalk lodging resistance in maize is through the process of selective breeding, purposefully selecting and interbreeding plants with preferred traits in an effort to promote the traits further. Selective breeding has successfully been practiced for thousands of years, but it requires the identification of preferred phenotypes. As stalk lodging is not consistently observable, it has been a historically challenging phenotype to breed for. Thus, the need for proxy measurements, phenotypes that co-vary with stalk lodging, has emerged.

#### 1.4 Devices to predict lodging resistance

Devices have been used in the past to determine maize stalk lodging resistance. One such device, called Guo's device, works by attaching a line to the stalk and pulling on that line to bend it to specific angles while recording the maximum equivalent force. This maximum equivalent force was shown to have a negative correlation with incidences of stalk lodging in maize [16], [17].

Another device called the DARLING (Device for Assessing Resistance to Lodging in Grains) works by setting it next to a stalk and then leaning it forward, from the hinged base, to push a stalk to failure with a load cell backed head. During the test the angle and force are continually measured and the maximum force is determined. This maximum force was also shown to correlate well with lodging resistance [18], [19].

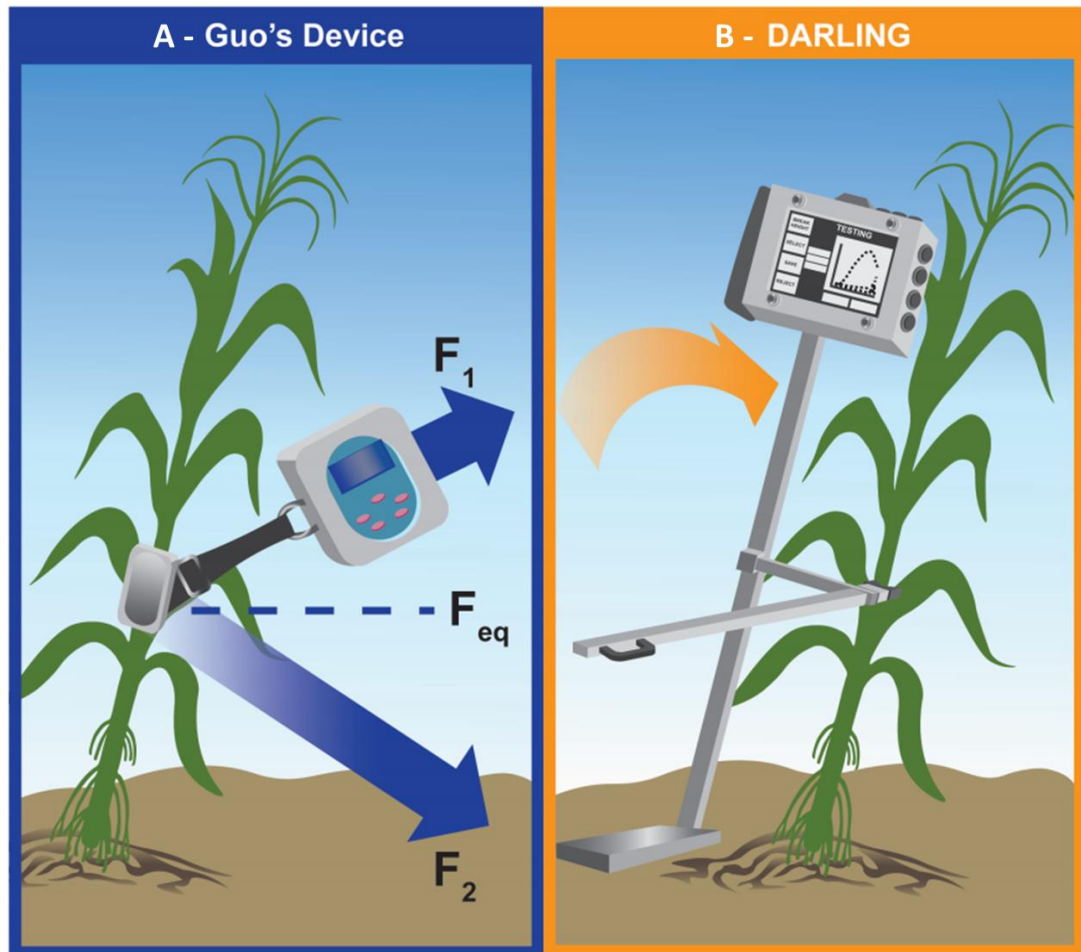


Figure 1.4 [11] a) Guo's Device b) DARLING Device.

The pros and cons of these tests are further discussed in [11], but a main method these two devices share is the use of bending stiffness and bending strength as a proxy phenotype for lodging

resistance. While these tests have been shown to predict lodging resistance, they do not address the mechanistic relationship between lower level phenotypes (e.g., tissue and morphological parameters) and stalk lodging resistance. For plant breeders to understand this relationship, methods that utilize lower level phenotypes as proxy measurements must be utilized.

### 1.5 Methods to explain lodging resistance

One of the oldest attempts to correlate lower level phenotypes of a stalk with increased lodging resistance was through the use of Rind Penetration Resistance (RPR) tests. RPR tests use rind hardness as a proxy measurement for lodging resistance. These tests began in the 1930s [20] and are performed by puncturing a needle through the rind of a maize stalk and measuring the maximum force required during the puncture. Modern day RPR tests are performed using custom handheld devices with load cell backed needles [21], [22].



Figure 1.5 [22] Rind puncture resistance device.

An emerging method to determine the cause of lodging resistance is light spectroscopy. Light spectroscopy analyzes the wavelengths of light reflected by plant tissue to identify concentrations of chemicals bonds in a plant that could be correlated with lodging resistance [23].

However, both methods have limitations. RPR tests yield promising correlations between rind hardness and lodging resistance [24], [25], but selectively breeding for higher RPR test values ultimately resulted in hard skinny stalks with inferior lodging resistance [22], [26]. Light spectroscopy test results have yet to be published, but similar tests which used ground samples of

stalks to perform metabolic analysis yielded no correlation between the chemistry of the plant and historical lodging resistance [27].

The diameter being reduced in the selectively RPR bred stalks ultimately led to decreased strength, and therefore reduced lodging resistance. So using cross-sectional geometry as a proxy measurement for stalk lodging is logical.

### **1.6 Determining stalk geometry**

Two prominent methods that have been utilized to assess stalk cross sections are imaging and CT scans. Imaging is done by harvesting stalks and cutting them into thin cross sections. Those cross sections are then dyed and photographed. Then software can analyze those photos and extract major and minor diameter, rind thickness, and other relevant information.

CT scans require stalks to be harvested and then scanned within a CT scan machine. Data from these scans can then be analyzed with software to extract cross sectional geometry information.

Unfortunately, these methods are cumbersome, low throughput, and time consuming. The process of cutting the stalks into cross sections for imaging must be done carefully or else risk ruining the pictures. The process of sectioning, dying, and imaging a single corn stalk can take between two and three hours to complete [28]. Stalks must also be harvested for the CT scans and the scans can take approximately 6 hours to complete per maize stalk. Additionally, the cost of a CT scanning machine makes this a costly method to use. Lastly, imaging and CT scanning cross section values can vary for the same stalk since the change from rind to pith is a gradient rather than a defined line. This also makes both tests subjective since the rind thickness values can vary depending on the software programming with either method. An alternative to these methods is the rind puncture test method.

### **1.7 Rind puncture tests**

Rind puncture tests are similar to RPR tests but have a few major differences. Instead of just puncturing through the rind of a stalk, as in RPR tests, puncture tests go through the entire stalk. Puncture tests also record more information throughout the process. Rather than just recording the maximum force on the needle they continually record both the force on the needle and the displacement of the needle throughout the test. This information can then be plotted as a graph with displacement on the x-axis and force on the y-axis. A typical puncture test will appear to have two prominent peaks separated by a valley between them. Each peak in the force represents a rind being punctured through while the valley in between shows the force on the needle as it passes through the pith of the stalk. The maximum height (i.e., force) of these peaks is equivalent to the stalk's rind

penetration resistance. If the needle's displacement is zeroed against the backplane, where the back of the stalk rests during testing, then additional geometric information can be gathered from the graph. Stalk diameter can be identified by locating the leftmost point of the first force peak and calculating its distance from the established zero. Rind thickness is assessed by finding the second peak's leftmost point's distance from zero. Further discussion on these graphs can be found in [29].

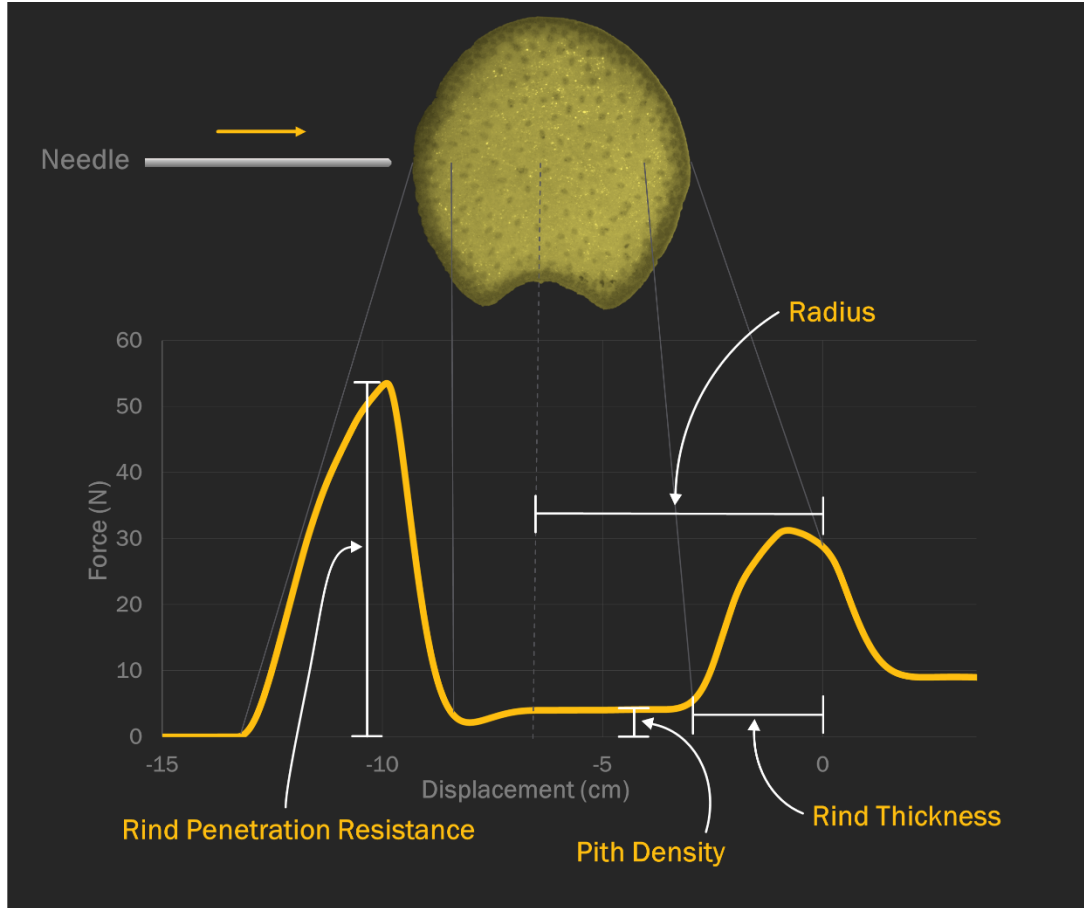


Figure 1.6 Puncture test graph shows how different geometry is determined from the graph.

A previous study found that rind puncture tests effectively captured the geometric information necessary to predict maximum bending strength in maize stalks [30]. This study used a Universal Testing System (Instron, model # 5944, Norwood MA) along with a custom rind puncture test fixture to compare the rind puncture test results of 1774 stalks to the maximum bending moment found from 3 point bending tests on the same stalks. To interpret the geometric information contained within the puncture tests researchers used a custom Matlab program to convert each graph into a number, known as an Integrated Puncture Score, further details on this can be found in [30]. This Integrated Puncture Score was found to have a positive correlation with the stalk bending strength

with an  $R^2$  value between 0.67 and 0.74 depending on the type of hybrid. The results from this study are positive, but the process is still cumbersome.



Figure 1.7 [29] Puncture test being run on Instron.

The instrumentation used for taking these rind puncture measurements is expensive. The Instron Universal Testing System setup used costs around \$50,000 [29]. A likely more prohibitive characteristic of this method though is its inability to accommodate *in vivo* testing. Every maize stalk tested in this study was harvested, individually labeled, and transported to the lab for testing. This adds cost, time, and complexity to the method. An individual rind puncture test takes only a few seconds once stalks are prepared, but transporting the stalks adds days to the process and increases the risk of handoff mistakes and damage during transportation. The process would be simpler and faster if a device could be used to take *in vivo* rind puncture measurements.

### **1.8 Stalk Puncture Device (SPuD)**

To summarize, RPR tests ultimately failed to produce stronger stalks when used as a selective breeding index and light spectroscopy tests have too low of correlations to be used effectively. Imaging and CT scans both yield promising results for determining stalk geometry, which is correlated with stalk strength, but both methods are slow and unsuited for rapid *in vivo* implementation. Rind puncture tests are quick and have good correlations with stalk strength but require expensive lab-based instrumentation. So, this research has been to design and validate a portable rind puncture test device capable of performing tests *in vivo*. The Stalk Puncture Device, or SPuD for short, is the device designed to fulfill this need.

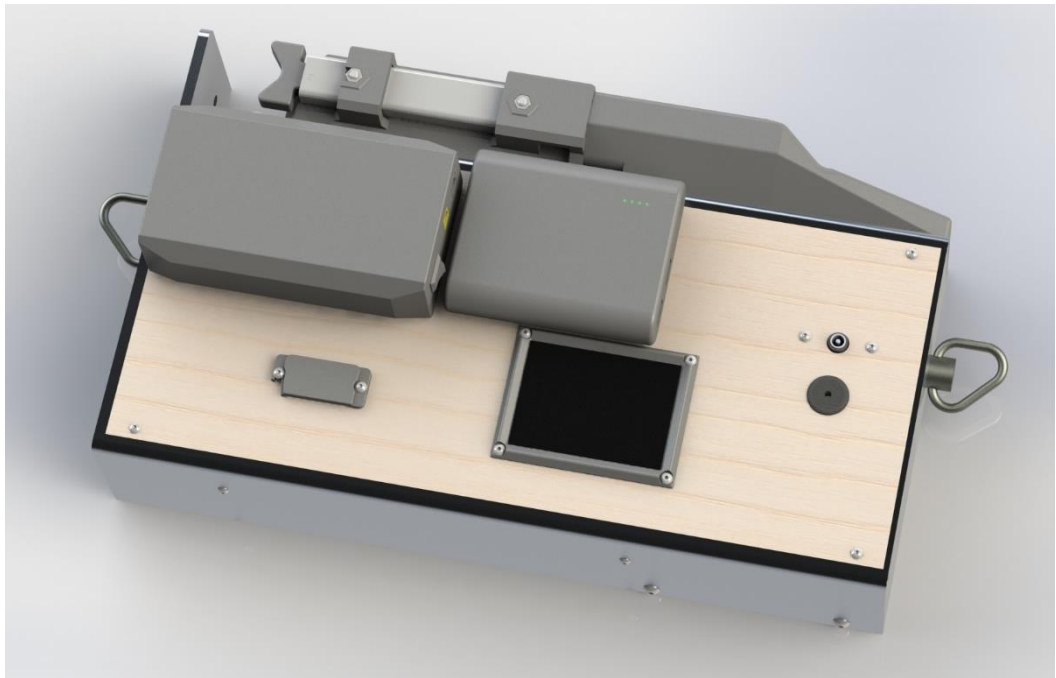


Figure 1.8 CAD model render of SPuD.

## Chapter 2: Stalk Puncture Device (SPuD)

### 2.1 Abstract

The Stalk Puncture Device (SPuD) is a portable, battery operated, rind puncture device. It takes the puncture test capabilities of the Instron and packs them into a handheld device for less than one twentieth the price of the Instron Universal Testing Machine setup. A SPuD costs approximately \$2300 in materials and can perform nearly 100 in vivo puncture tests per hour. The device has an intuitive user interface that is controlled via a touchscreen and two mounted safety buttons. The screen can provide real time device measurements and provides users with post test graphs of acquired data. Test data is stored on a micro SD card for easy data transfer.

The SPuD and the puncture analysis method are patented: Method and Apparatus for Analyzing Stalk Strength. US patent 17/109,989. Issued June 3, 2021. Inventors are: Robertson D.J., Cook D., Seegmiller W., Spence T., Seegmiller K., Stucker A.

### 2.2 Repository Files

The SPuD is a complex device with many supporting documents and files that could not be reasonably added into this thesis. A repository for these files has been uploaded to GitHub:

<https://github.com/TaylorSpence/SPuD>

Table 2.1 Repository file names and descriptions.

File Name	File Description
3D Print STLs.zip	Contains all STL files for 3D printing.
Laser Cut DXFs.zip	Contains all DXF files for laser cutting.
Mill Drawing PDFs.zip	Contains all engineering drawing PDFs for milled parts.
SPuD Wiring V3.pdf	Wiring schematic for SPuD device.
SPuD CAD Renders.zip	Contains SolidWorks renders of the SPuD.
SPuD CAD 1-4.zip	Contains SolidWorks assemblies, parts, and drawings.
SPuD BOM.xlsx	Bill of materials with full info on all parts in the SPuD.
Raw SPuD Data.zip	Raw CSV files for every internode tested with SPuD.
Raw Instron Data.zip	Raw CSV files for every internode tested with Instron.
Minor Diameter Analysis.zip	Graphic/data outputs of minor diameter analysis.
IPS Analysis.zip	Contains Matlab code and graphic/data outputs of IPS analysis.
Final SPuD Arduino Code.zip	Contains Arduino code for the Arduino Mega and Arduino Uno.
Instron & SPuD Naming... .xlsx	Shows alignment of Instron bar codes to SPuD file names.

## 2.3 Bill of Materials

A fully detailed bill of materials can be found within the repository. The tables below collectively contain every item in the full bill of materials, but contain less information on each individual item and are divided by component types.

### 2.3.1 Purchased Components

Table 2.2 Purchased components bill of materials.

Item Description	Designator	Qty.	Cost	Item Total*
2.8" LCD Touchscreen	Touchscreen	1	\$ 29.95	\$ 37.77
24V Rechargeable Battery	24V Battery	1	\$ 62.99	\$ 62.99
3M Double Sided Foam Tape	Double Sided Tape	1	\$ 12.99	\$ 12.99
3M Dual Lock Velcro Tape	Velcro Tape	1	\$ 10.95	\$ 10.95
Al. Extruded Case, 6"W x 14" L	Extruded Case	1	\$ 116.74	\$ 131.84
5V Rechargeable Battery	5V Battery	1	\$ 35.00	\$ 35.00
Arduino Mega	Arduino Mega	1	\$ 38.00	\$ 38.00
Arduino Uno R3	Arduino Uno	1	\$ 18.85	\$ 18.85
Arduino Wires Kit	Arduino Wires Kit	2	\$ 6.98	\$ 13.96
Chest Harness Camera Strap	Camera Strap	1	\$ 14.99	\$ 14.99
DC Power Adapter M-M 1"	DC Power Adapter	1	\$ 7.99	\$ 7.99
Digital Linear Slide Scale 12"	Linear Slide Scale	1	\$ 68.95	\$ 68.95
Dupont Conn Kit w/ Wires	Dupont Connector Kit	1	\$ 17.97	\$ 17.97
Hx711 (load cell driver)	Load Cell Driver	1	\$ 9.95	\$ 9.95
Linear Axis w/ Motor	Linear System	1	\$ 528.29	\$ 528.29
Logic Level Converter	Logic Level Converter	1	\$ 2.95	\$ 9.95
M4 Shoulder Bolt	Shoulder Bolt	2	\$ 4.20	\$ 8.40
MicroB USB Breakout Board	USB Breakout Board	1	\$ 2.50	\$ 2.50
MicroSD Card 64 GB	MicroSD Card	1	\$ 11.99	\$ 11.99
MicroSD Card Breakout Board	SD Card Breakout Board	1	\$ 7.50	\$ 15.84
Mini 100 lb Load Cell	Load cell	1	\$ 675.00	\$ 731.75
Mini Limit Switch Rollers	Limit Switch	1	\$ 2.49	\$ 2.49
Nylon Spacer #4 .25"	Nylon Spacer	1	\$ 10.09	\$ 10.09
Perma-Proto 1/4 breadboard	Breadboard	1	\$ 8.50	\$ 8.50
Push Button Sling Swivel Set	Sling Mount	1	\$ 17.79	\$ 22.79
Resistor Assortment Kit	10k Ohm Resistor	1	\$ 11.99	\$ 11.99
Rubber Grommet	Rubber Grommet	1	\$ 5.03	\$ 5.03
Spring 3" L .6" OD	Spring	1	\$ 7.26	\$ 7.26
3A Stepper Motor Driver	Stepper Motor Driver	1	\$ 9.99	\$ 9.99
Telescoping Slide	Slider	2	\$ 102.41	\$ 204.82
USB Splitter	USB Splitter	1	\$ 13.95	\$ 13.95
Weather-proof push button	Push Button	2	\$ 7.50	\$ 23.00
			<b>Total</b>	<b>\$ 2,110.83</b>

\*Item total includes shipping costs in some cases.

### 2.3.2 3D Printed Components

All parts printed from onyx material were printed on a Markforged Mark Two 3D printer with a triangular infill pattern, 37% infill density, 4 roof layers, and 2 wall layers. Most of these onyx parts were printed with a layer height of 0.1 mm, except the load cell cover body (CAD06), motor cover body (CAD08), and slide cover (CAD15) which were printed at a 0.3 mm layer height to reduce print duration.

The ABS linear assembly cover (CAD05) was printed on a Sindoh 2X printer with a rectilinear infill pattern, 20% infill density, 3 roof layers, 3 wall layers, and a layer height of 0.2 mm.

Table 2.3 3D printed components bill of materials.

Item Description	Designator	Material	Mass (g)	Qty.	Cost*	Item Total
Bottom DC Panel Mount	CAD01	Onyx**	9g	1	\$ 1.88	\$ 1.88
Compliant Clips	CAD02	Onyx	1g	2	\$ 0.10	\$ 0.20
Device Feet	CAD03	Onyx**	7g	4	\$ 1.48	\$ 5.92
Linear System Adapter	CAD04	Onyx**	13g	1	\$ 2.65	\$ 2.65
Linear Assembly Cover	CAD05	ABS	70g	1	\$ 2.99	\$ 2.99
Load Cell Cover Body	CAD06	Onyx**	118g	1	\$ 30.31	\$ 30.31
Load Cell Wire Cover	CAD07	Onyx**	30g	1	\$ 6.03	\$ 6.03
Motor Cover Body	CAD08	Onyx**	146g	1	\$ 41.44	\$ 41.44
Plunger	CAD09	Onyx**	5g	2	\$ 1.04	\$ 2.08
Pusher Heads	CAD10	Onyx	4g	2	\$ 0.74	\$ 1.48
Screen Frame	CAD11	Onyx**	5g	1	\$ 0.94	\$ 0.94
SD Panel Mount Base	CAD12	Onyx**	10g	1	\$ 2.15	\$ 2.15
SD Panel Mount Cover	CAD13	Onyx**	2g	1	\$ 0.53	\$ 0.53
Slide Catch	CAD14	Onyx	5g	1	\$ 1.12	\$ 1.12
Slide Cover	CAD15	Onyx**	29g	1	\$ 6.08	\$ 6.08
Top DC Panel Mount	CAD16	Onyx**	3g	1	\$ 0.70	\$ 0.70
Wire Spool	CAD17	Onyx**	8g	1	\$ 1.59	\$ 1.59
Wire Spool Cover	CAD18	Onyx**	9g	1	\$ 1.91	\$ 1.91
					Total	\$ 110.00

\*Cost for Onyx parts is calculated within the Markforged slicer. ABS price is calculated at \$29.99 per 700g spool.

\*\*These Onyx components could likely be printed out of ABS to save money, but were made of Onyx due to the increased fidelity and minimal cleanup of the Markforged printer compared to other accessible ABS printers at the time.

### 2.3.3 Laser Cut Components

Table 2.4 Laser cut components bill of materials.

Item Description	Designator	Material	Qty.	Cost*	Item Total
Bottom Cover	LASER01	1/8" Birch Plywood	1	\$ 0.50	\$ 0.50
Top Cover	LASER02	1/8" Birch Plywood	1	\$ 0.50	\$ 0.50
					<b>Total</b> \$ 1.00

\*Cost calculated at \$20 per 5' x 5' sheet.

### 2.3.4 Machined Components

Table 2.5 Machined components bill of materials.

Item Description	Designator	Material	Qty.	Cost*	Item Total
Left Cover	MILL01	6061 Aluminum	1	\$ 3.00	\$ 3.00
Right Cover	MILL02	6061 Aluminum	1	\$ 0**	\$ 0
Back Cover	MILL03	6061 Aluminum	1	\$ 0**	\$ 0
Front Cover	MILL04	6061 Aluminum	1	\$ 0**	\$ 0
Linear Scale Bottom Mount	MILL05	6061 Aluminum	2	\$ 0.75	\$ 1.50
Linear Scale Top Mount	MILL06	6061 Aluminum	2	\$ 0.75	\$ 1.50
Load Cell Mount	MILL07	6061 Aluminum	1	\$ 8.00	\$ 8.00
Needle Chuck	MILL08	6061 Aluminum	1	\$ 0.25	\$ 0.25
Test Needle	MILL09	17-4 PH SS	1	\$ 6.04	\$ 6.04
					<b>Total</b> \$ 20.29

\*6061 Aluminum part costs estimated by \$10 per kg. Test needle cost determined by McMaster-Carr part number 3180T31.

\*\*These components are included in the extruded case purchase which is already listed under the purchased parts bill of materials, Table 2.1.

### 2.3.5 Hardware

Table 2.6 Hardware bill of materials.

Item Description	Designator	Qty.	Cost*	Item Total
2-56 Machine Nut	2-56 Nut	4	\$ 0.50	\$ 2.00
4-40 Machine Nut	4-40 Nut	16	\$ 0.50	\$ 8.00
6-32 Machine Nut	6-32 Nut	3	\$ 0.50	\$ 1.50
8-32 Machine Nut	8-32 Nut	2	\$ 0.50	\$ 1.00
Button Head Cap Screw 4-40 .25"	BHCS 4-40 .25"	4	\$ 0.50	\$ 2.00
Button Head Cap Screw 4-40 .3125"	BHCS 4-40 .3125"	4	\$ 0.50	\$ 2.00
Button Head Cap Screw 4-40 .5"	BHCS 4-40 .5"	6	\$ 0.50	\$ 3.00
Button Head Cap Screw 4-40 .75"	BHCS 4-40 .75"	4	\$ 0.50	\$ 2.00
Button Head Cap Screw 6-32 .5"	BHCS 6-32 .5"	2	\$ 0.50	\$ 1.00
Button Head Cap Screw 6-32 .75"	BHCS 6-32 .75"	2	\$ 0.50	\$ 1.00
Button Head Cap Screw 8-32 .5"	BHCS 8-32 .5"	2	\$ 0.50	\$ 1.00
Button Head Cap Screw M4 6mm	BHCS M4 6mm	2	\$ 0.50	\$ 1.00

Button Head Cap Screw M6 25mm	BHCS M6 25mm	2	\$ 0.50	\$ 1.00
Button Head Cap Screw M6 50mm	BHCS M6 50mm	2	\$ 0.50	\$ 1.00
Button Head Cap Screw M6 75mm	BHCS M6 75mm	2	\$ 0.50	\$ 1.00
Flat Head Cap Screw 6-32 .375"	FHCS 6-32 .375"	8	\$ 0.50	\$ 4.00
Flat Head Cap Screw M3 4mm	FHCS M3 4mm	4	\$ 0.50	\$ 2.00
Flat Head Cap Screw M4 10mm	FHCS M4 10mm	4	\$ 0.50	\$ 2.00
Flat Head Cap Screw M6 18mm	FHCS M6 18mm	4	\$ 0.50	\$ 2.00
M4 Machine Nut	M4 Machine Nut	4	\$ 0.50	\$ 2.00
M6 Machine Nut	M6 Machine Nut	2	\$ 0.50	\$ 1.00
Set Screw M3 8mm	Set Screw M3 8mm	1	\$ 0.50	\$ 0.50
Socket Head Cap Screw 2-56 .125"	SHCS 2-56 .125"	1	\$ 0.50	\$ 0.50
Socket Head Cap Screw 2-56 .375"	SHCS 2-56 .375"	8	\$ 0.50	\$ 4.00
Socket Head Cap Screw 4-40 .75"	SHCS 4-40 .75"	2	\$ 0.50	\$ 1.00
Socket Head Cap Screw 4-40 1"	SHCS 4-40 1"	4	\$ 0.50	\$ 2.00
Socket Head Cap Screw 6-32 1"	SHCS 6-32 1"	1	\$ 0.50	\$ 0.50
Socket Head Cap Screw M3 6mm	SHCS M3 6mm	1	\$ 0.50	\$ 0.50
Socket Head Cap Screw M6 10mm	SHCS M6 10mm	4	\$ 0.50	\$ 2.00
Socket Head Cap Screw M6 12mm	SHCS M6 12mm	2	\$ 0.50	\$ 1.00
<b>Total</b>			<b>\$ 53.50</b>	

\*The cost of all hardware components is estimated at \$0.50 per a component based on local hardware store prices.

### 2.3.6 SPuD Total Cost

Table 2.7 SPuD total cost.

Purchased Components Total	\$ 2,110.83
3D Printed Components Total	\$ 110.00
Laser Cut Components Total	\$ 1.00
Machined Components Total	\$ 20.29
Hardware Components Total	\$ 53.50
<b>SPuD Total Cost</b>	<b>\$ 2,295.62</b>

The total component cost to create a SPuD, \$2296, is less than one twentieth the price of the Instron Universal Testing System setup that has previously been used to perform these puncture tests.

## 2.4 Build Instructions

### 2.4.1 Case Assembly

As seen in Figure 2.1, the main portion of the case is assembled using the following components: A: Left cover (MILL01). B: Right cover (MILL02). C: Back cover (MILL03). D: Front cover (MILL04). E: Bottom cover (LASER01). F: Four device feet (CAD03). G: Four 4-40 button head cap screws 0.75 inches long. H: Eight 6-32 flat head cap screws 0.375 inches long. I: Two push buttons (not pictured).

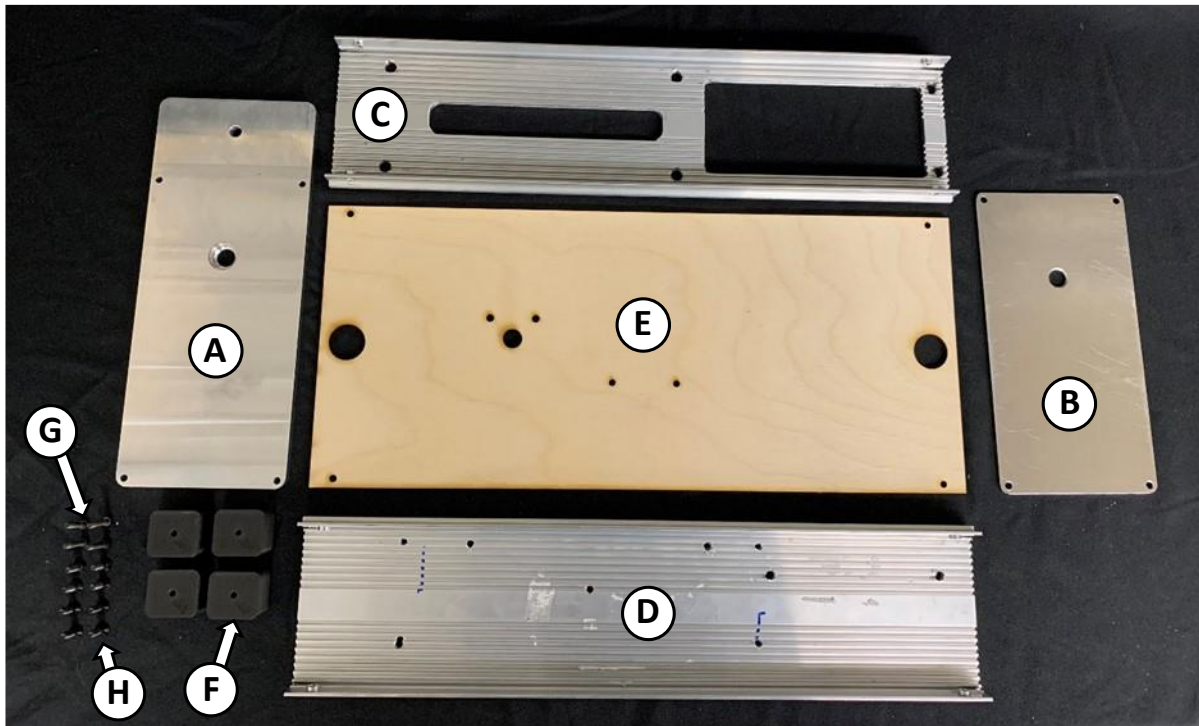


Figure 2.1 Case assembly components.

Begin the case assembly by attaching both the front and back cover to the left cover using four of the flat head cap screws (two for the front cover and two for the back cover). Attach the right cover similarly using the remaining four flat head cap screws. Make sure the large hole in the right cover is closer to the back of the device, similar to the layout in Figure 2.1.



Figure 2.2 Outer case assembled.

Flip the case over and attach the base cover by passing the button head cap screws through the feet, through the bottom cover, and screwing them into the front and back covers. Make sure to orient the legs so that the slight ridge on the face touching the bottom cover faces toward the rounded edge. This ridge is to help prevent the feet from turning.

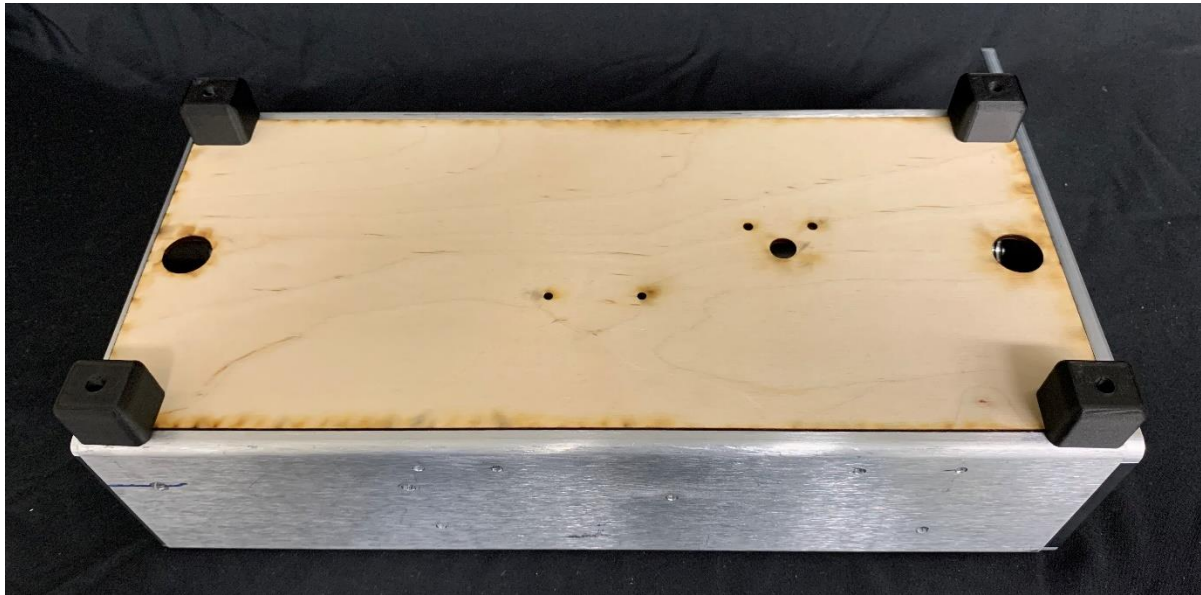


Figure 2.3 Bottom cover and legs attached.

To finish the case assembly install both of the push buttons in the bottom cover of the case.

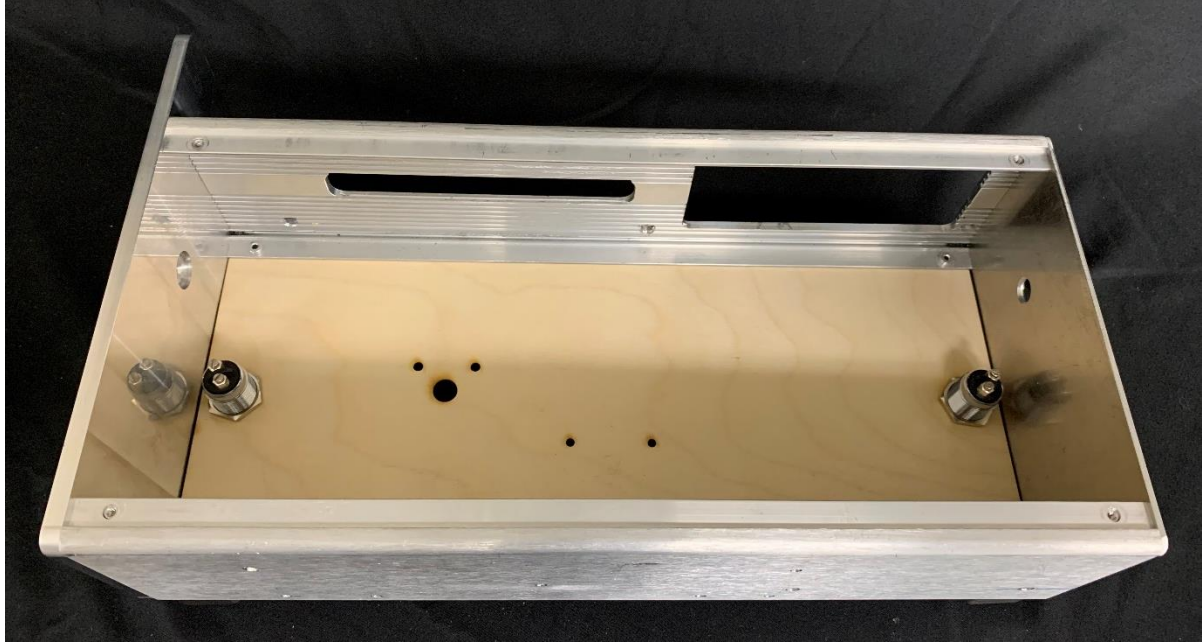


Figure 2.4 Case assembled with bottom buttons installed.

#### 2.4.2 Backside Assembly

The back side of the SPuD has two sub-assemblies, the load cell cover and the motor cover. Assembly begins with the load cell cover. As seen in figure 2.5 below, load cell assembly begins with the following components: A: Load cell cover body (CAD06). B: Slide cover (CAD15). C: Two pusher heads (CAD10). D: Two sliders. E: Two M4 shoulder bolts. F: Four M4 flat head cap screws 10 millimeters long. G: Two M4 button head cap screws 6 millimeters long. H: Two 4-40 flat head cap screws 0.75 inches long. I: Four M4 nuts. J: Two 4-40 nuts.

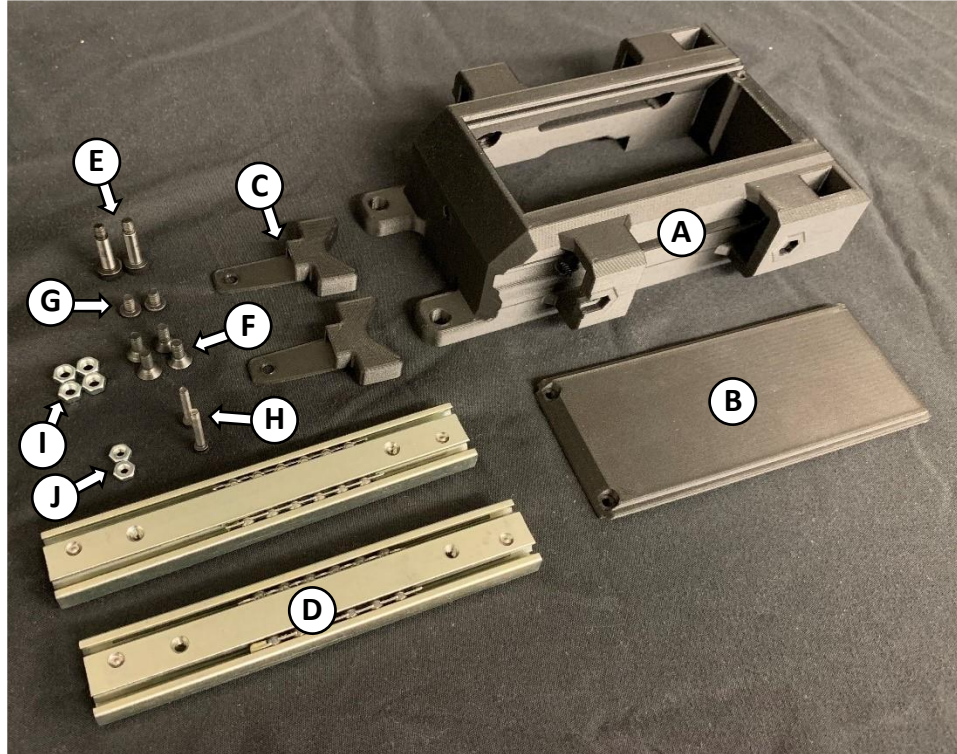


Figure 2.5 Load cell cover assembly components.

Pull the slide back enough on the slider to insert one of the flat head cap screws into place. Begin threading one of the M4 nuts. It should look like Figure 2.6 once this is complete.



Figure 2.6 Screw inserted on slide and pre-threaded on nut.

Pull the slide back over the flat head cap screw and slot the slider into place on the load cell cover body, as seen in Figure 2.7.



Figure 2.7 Slider moved into position on load cell cover part.

If the slider is positioned correctly and the slide is pulled back completely an Allen wrench can pass through the threaded hole to tighten the flat head cap screw underneath, see Figure 2.8.



Figure 2.8 Allen wrench positioned to tighten front slider screw.

Once the front screw is tightened insert an M4 nut into the cutout and pull the slide forward, as shown in Figure 2.9.



Figure 2.9 Slider moved forward and nut inserted in cutout.

Keep the slide forward as you rotate the cover to the position shown in Figure 2.10. Insert a flat head cap screw through the hole indicated and tighten it using an Allen wrench.



Figure 2.10 Allen positioned to tighten rear slider screw.

Rotate the cover back and attach the pusher head to the end of the slide by bolting it in place with a button head cap screw.



Figure 2.11 Slide pushed forward with holder head attached.

Lastly, pull the slide back and thread the shoulder bolt into the threaded hole on the interior of the slide.



Figure 2.12 Shoulder bolt threaded into interior of slide.

Repeat this process to mount the slider mechanism onto the opposite side.



Figure 2.13 Load cell cover with both sliders installed.

Insert the two 4-40 nuts into the back of the load cell cover body.

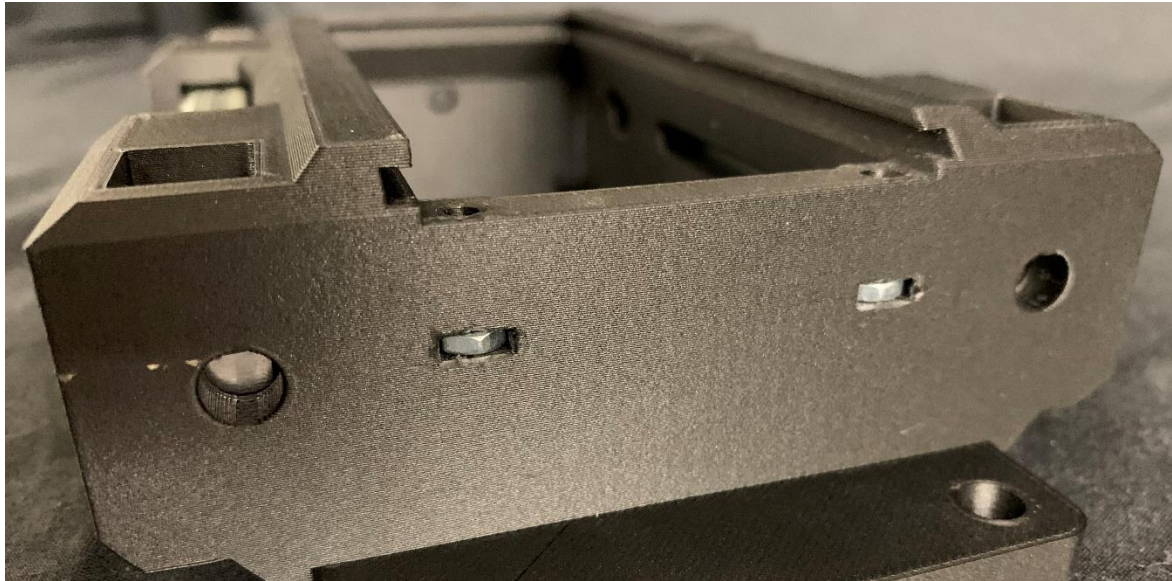


Figure 2.14 Nuts inserted into openings on back of load cell cover.

Finally, slide the slide cover into place from the back side and secure it with the two flat head cap screws.



Figure 2.15 Fully assembled load cell cover.

As seen in Figure 2.16, the motor cover assembly includes the following components: A: Motor cover body (CAD08). B: Two plungers (CAD09). C: Two springs.

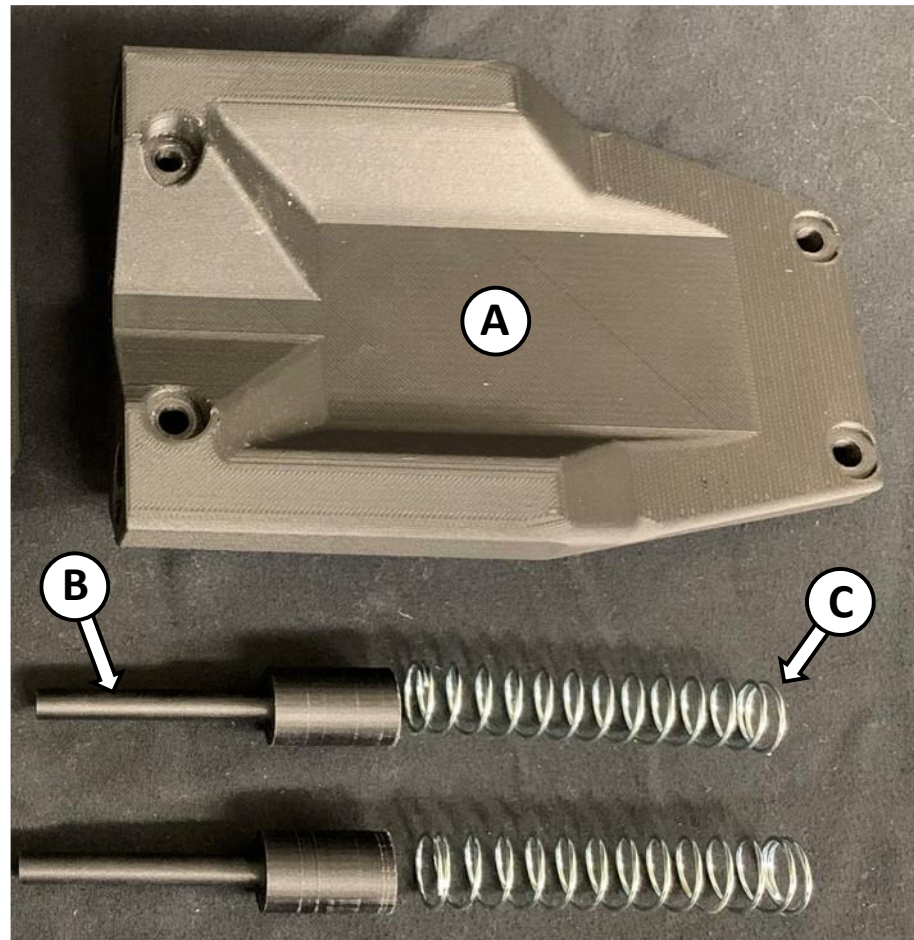


Figure 2.16 Motor cover assembly components.

Insert the two springs into the holes in the motor cover body. Insert the plungers into the same holes. Make sure the plungers fit smoothly into the hole, if they do not, try cleaning any excess support material residue from the holes or trimming the bottom perimeter of the plunger until it slides into the hole easily.

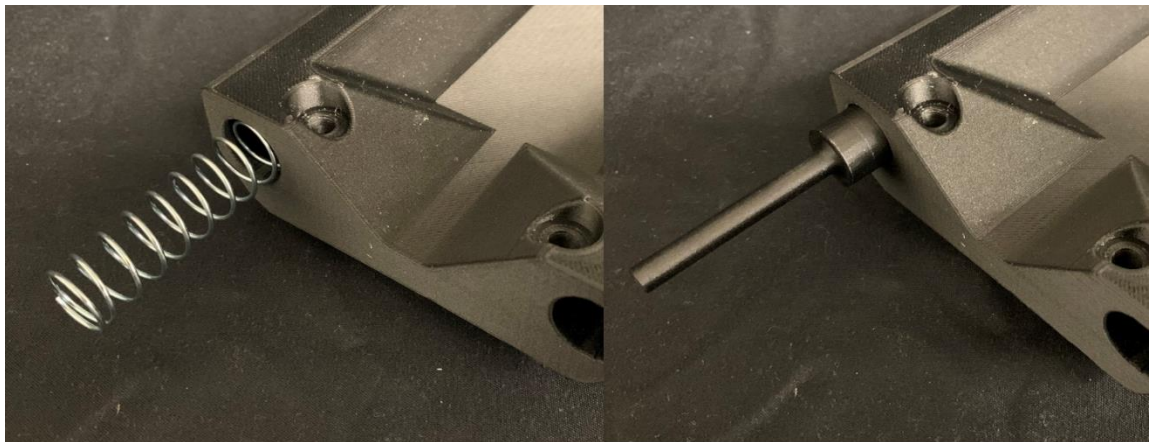


Figure 2.17 Motor cover showing spring and plunger insertion.

#### 2.4.2 Linear System Assembly

As seen in Figure 2.18, the linear system sub-assembly is assembled from the following components: A: Linear system. B: Linear slide scale. C: Load cell mount (MILL07). D: Linear system adapter (CAD04). E: Two linear scale bottom mounts (MILL05). F: Four M6 socket head cap screws 10 millimeters long. G: Four M6 flat head cap screws 18 millimeters long. H: Four M3 flat head cap screws 4 millimeters long.

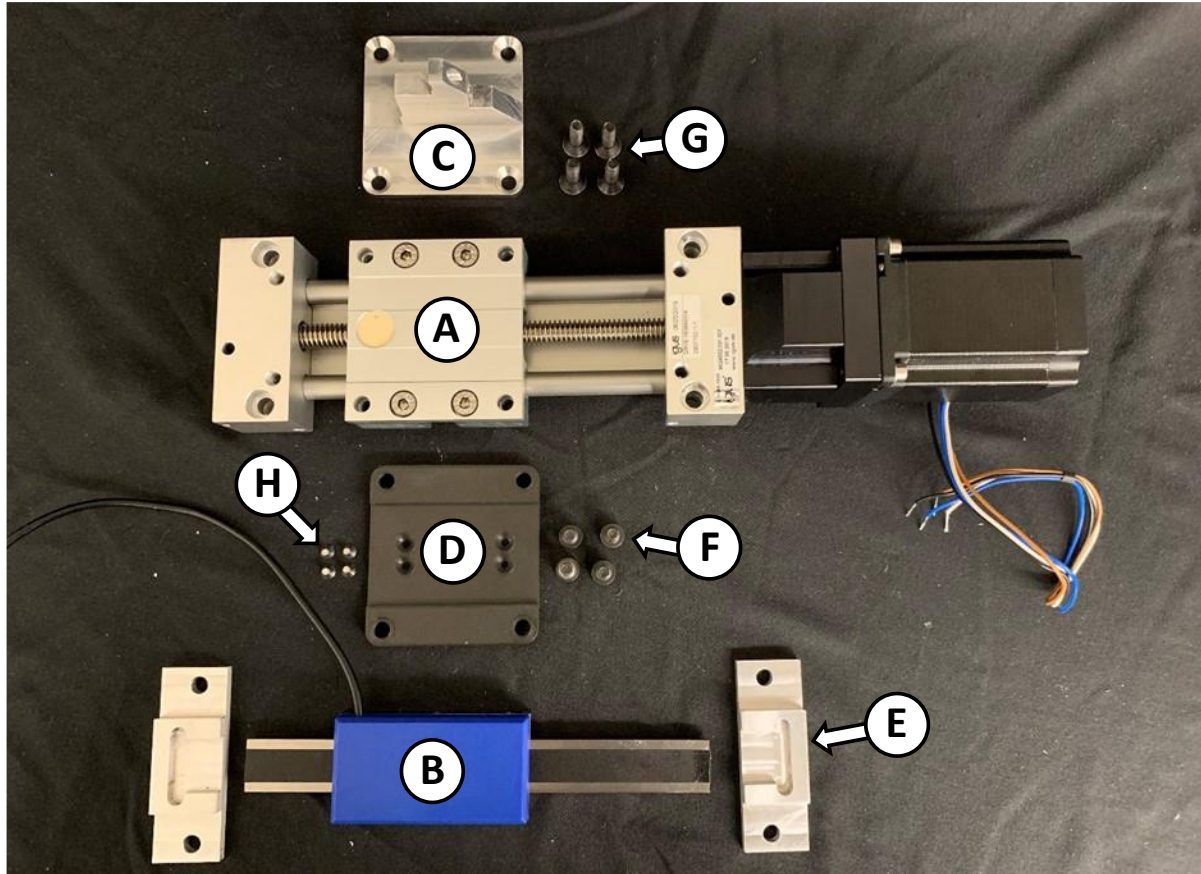


Figure 2.18 Linear system assembly components.

Begin assembly of the linear system by attaching the load cell mount to the linear system using the four 18 millimeter long M6 flat head cap screws as shown in Figure 2.19.



Figure 2.19 Linear system with load cell mount attached.

Before attaching anything to the linear scale it should be cut down to 7 inches in length. The scale packaging includes directions for how to cut it to length. Make sure not to clamp onto the portion of the scale you plan to keep, additionally using a hacksaw is suggested since the metal is difficult to machine. It is also suggested that you cut and resolder the wire down to a total length of 12 inches, as seen in figure 2.20.

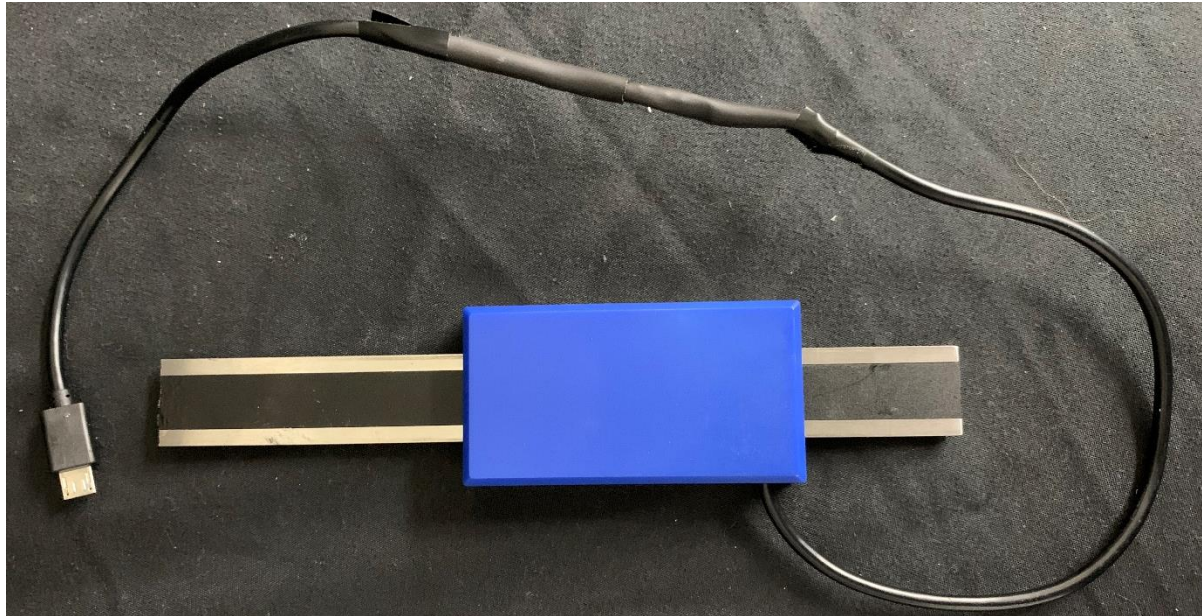


Figure 2.20 Linear scale cut to length and with wire shortened.

Attach the linear system interface to the bottom of the linear scale using the four M3 flat head cap screws.



Figure 2.21 Linear scale with linear system interface mounted.

Place the two linear scale bottom mounts onto the back side of the linear system and temporarily keep them in place with some of the M6 button head cap screws needed for later in the assembly process (these screws cannot be threaded in this way, just slotted in to keep the bottom mounts in place). Set the linear scale in place and align the holes as seen in Figure 2.22. Make sure to match the orientation of the wire to the Figure as well.

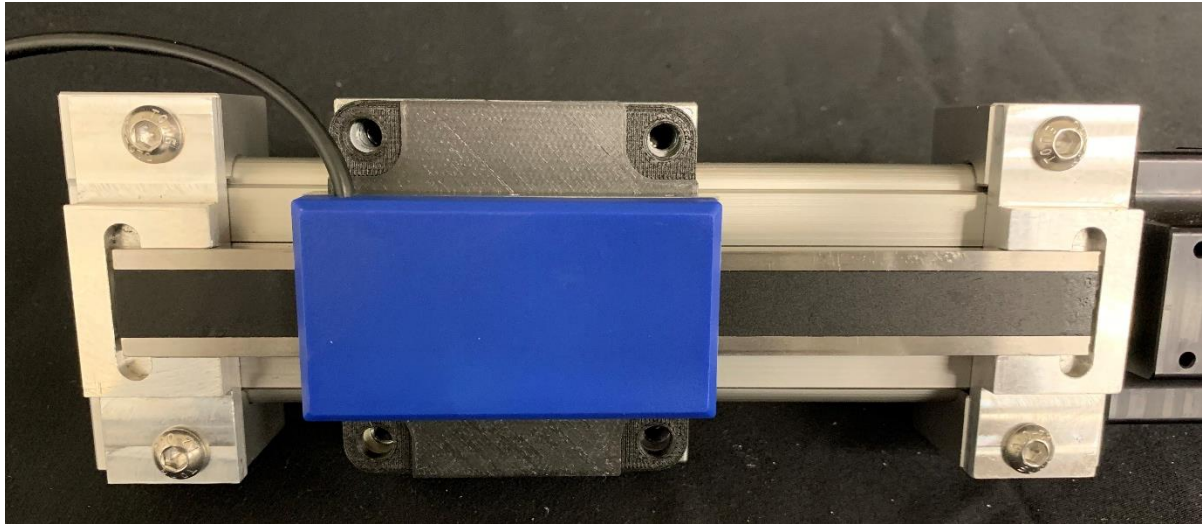


Figure 2.22 Linear scale aligned for assembly to linear system.

Attach the interface block to the linear system using the four socket head cap screws. The temporary button head cap screws can now be removed.

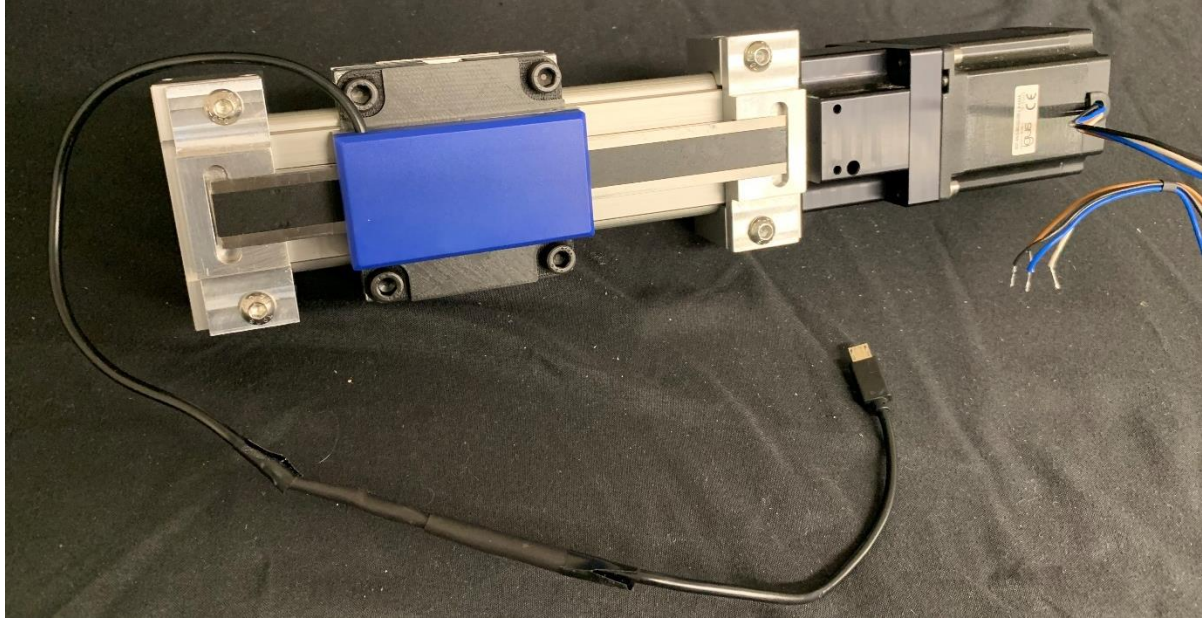


Figure 2.23 Linear system assembly complete.

#### 2.4.4 Attaching Linear System and Backside to Case

Begin attaching the back components by aligning the linear system on the inside of the case and the load cell cover on the outside of the case. Run two M6 button head cap screws 50 millimeters long through the front tabs of the load cell cover all the way through the linear scale bottom mounts. This should keep them aligned, but to secure them in place set the linear scale top mount in place and tighten the screws. See Figures 2.24 and 2.25.

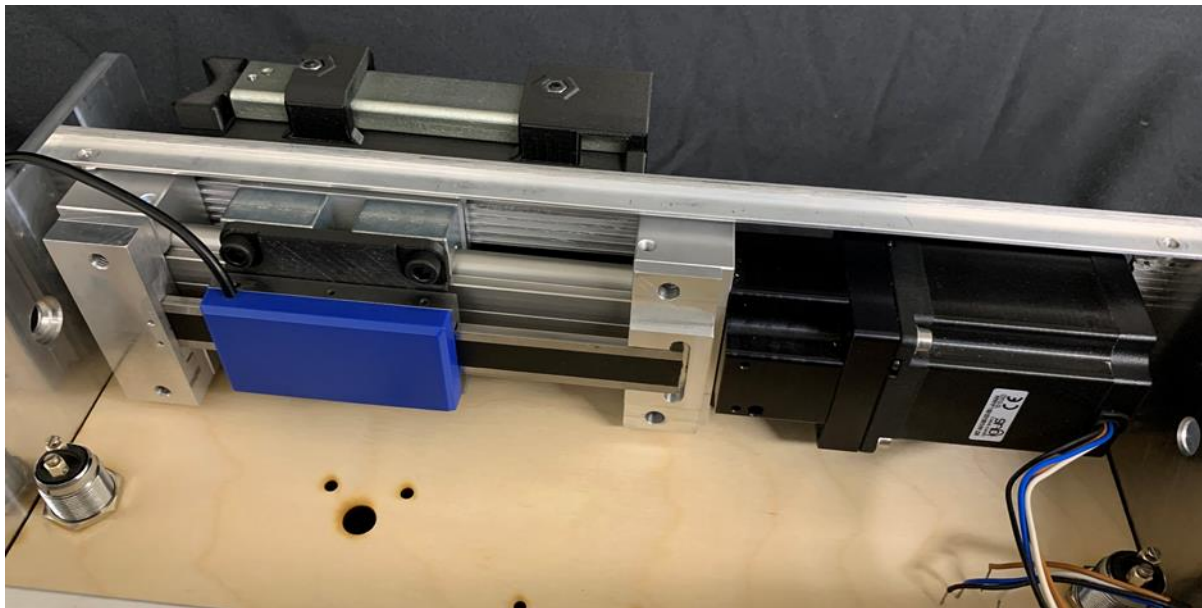


Figure 2.24 Linear system assembly and load cell cover attached to case.



Figure 2.25 Front bolts attaching load cell cover and linear system to case.

Slide the motor cover assembly into place behind the load cell cover. Make sure that the plungers stick through the corresponding holes in the back of the load cell cover. Hold the motor cover assembly in place by running two M6 button head cap screws 75 millimeters long through the front two holes on the motor cover all the way through to the linear scale bottom mounts. Secure it in place by setting the linear scale top mount in place and tightening the screws. See Figures 3.26 and 3.27.

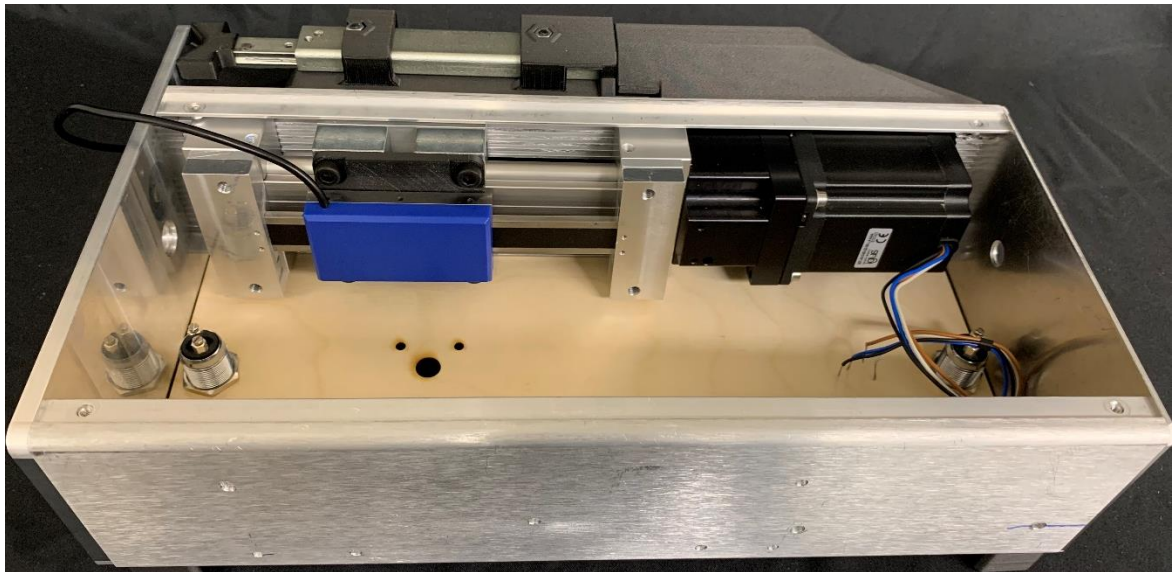


Figure 2.26 Motor cover attached to case.



Figure 2.27 Bolts connecting motor case to case assembly.

Finish securing the motor cover in place by running two M6 button head cap screws 25 millimeters long through the back two holes and securing them on the inside of the case using two M6 nuts. The right cover may be removed to gain easier access to the nuts.

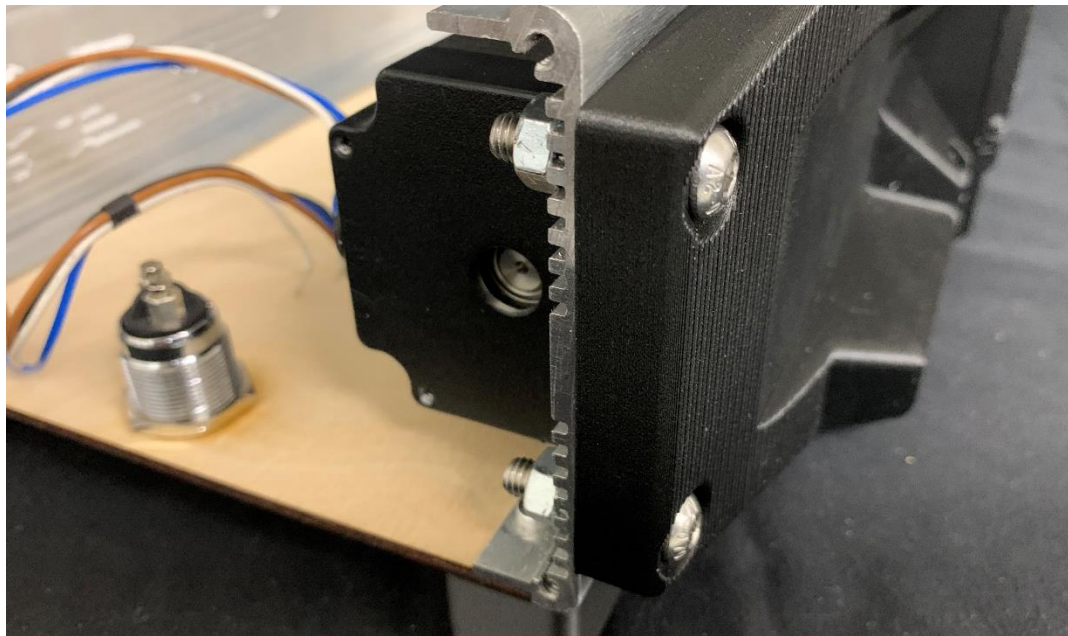


Figure 2.28 Right case cover removed to show rear motor case bolts.

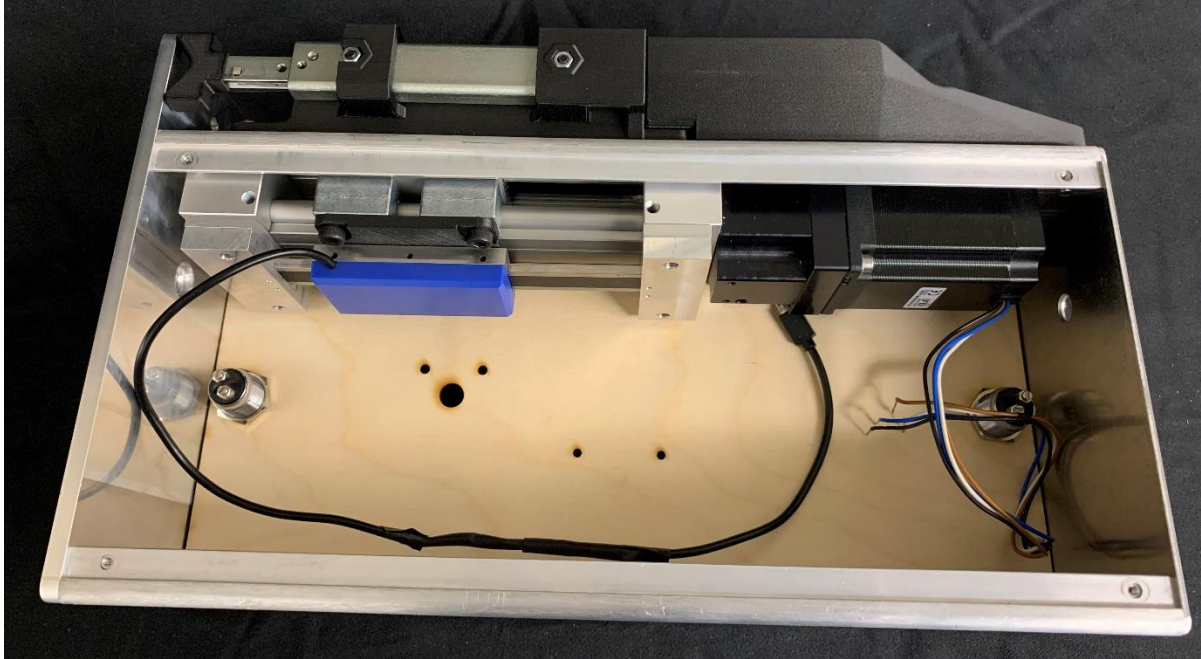


Figure 2.29 Case with linear system, load cell case, and motor case assembled.

#### 2.4.5 Adding Electrical Components

As seen in Figure 2.30, begin electrical component assembly by gathering the motor driver, two 8-32 button head cap screws 0.5 inches long, and two 8-32 nuts.

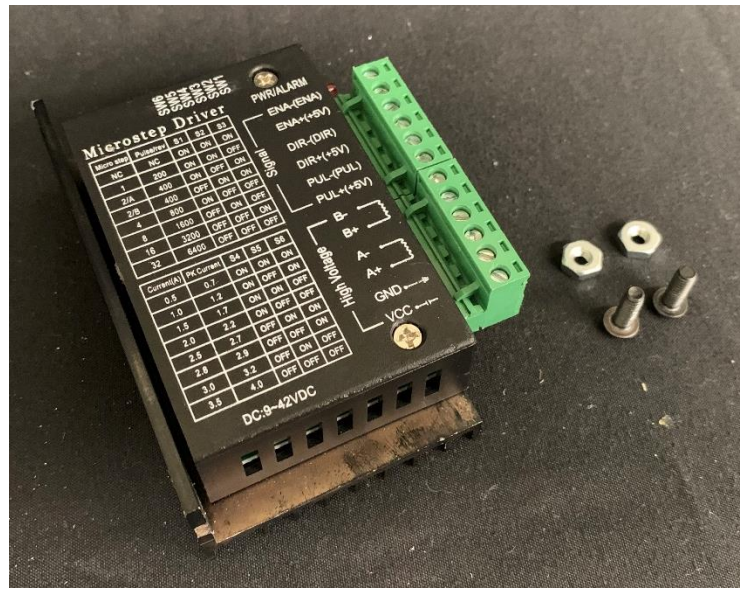


Figure 2.30 Motor driver with required fasteners.

Attach the motor driver in place by passing the bolts through the two larger holes in the front cover. Place the motor driver on the inside of the cover and use the nuts to hold it in place.

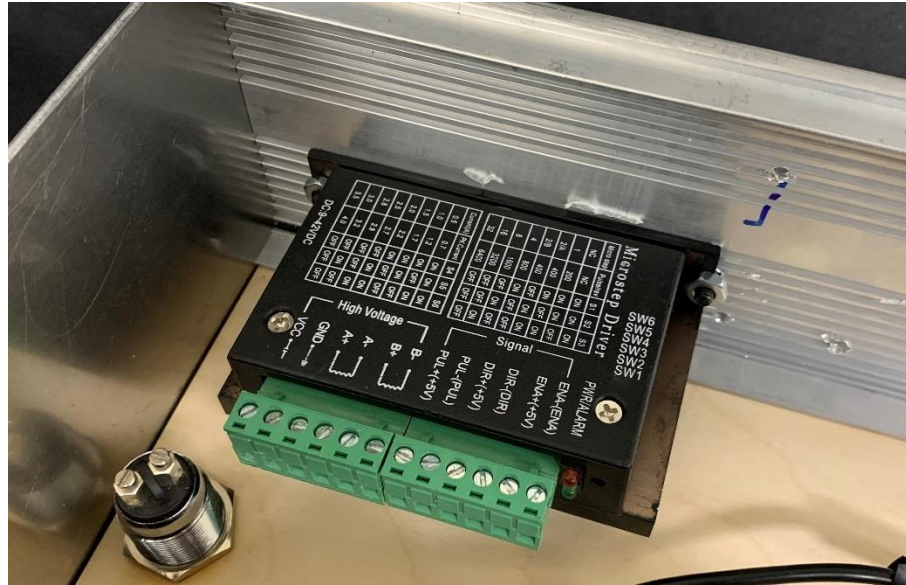


Figure 2.31 Motor driver attached to case with fasteners.

Then wire the stepper motor to the motor driver by wiring the black wire to B-, the blue wire to B+, the brown wire to A-, and the white wire to A+.

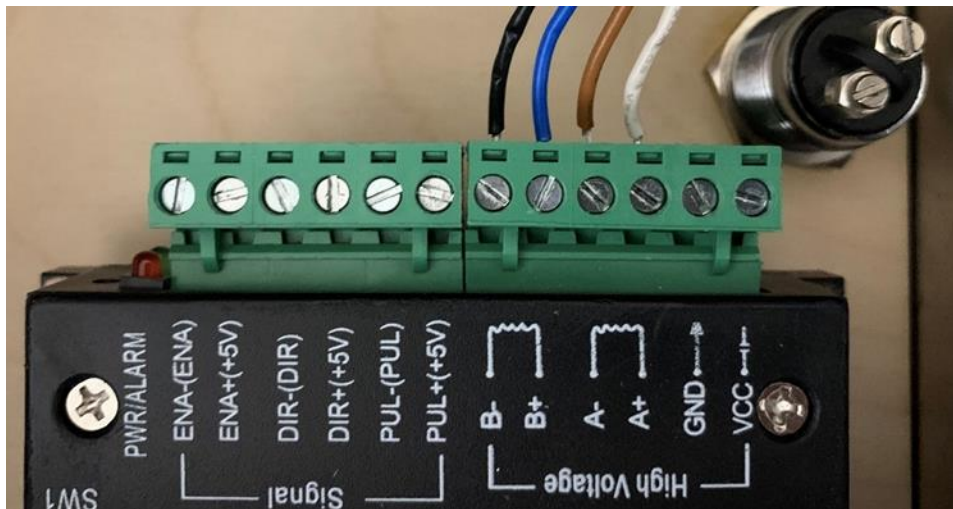


Figure 2.32 Stepper motor wired to motor driver.

As seen in Figure 2.33, to mount the Arduinos gather an Arduino Mega, Arduino Uno, four 4-40 button head cap screws 0.5 inches long, and four 4-40 nuts.

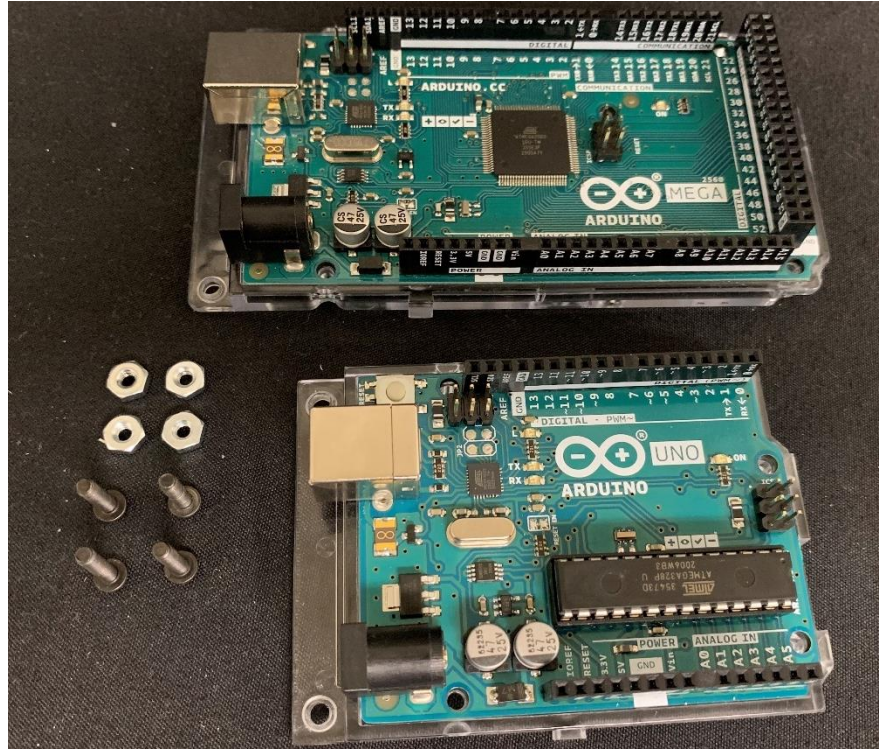


Figure 2.33 Arduinos with required fasteners.

Attach the Arduinos in place by passing the bolts through the two larger holes in the front cover. Place the Arduinos on the inside of the cover and use the nuts to hold them in place.

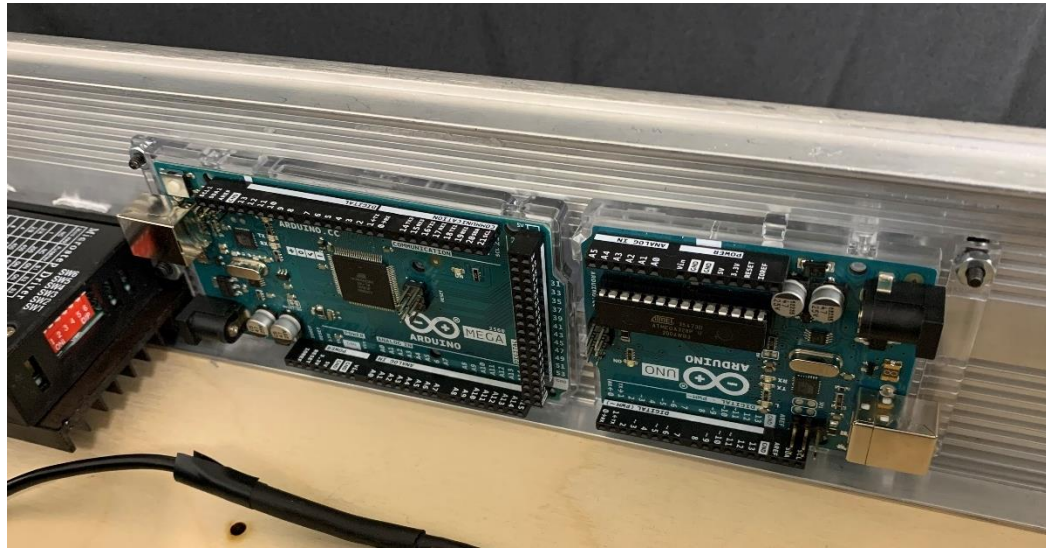


Figure 2.34 Arduinos attached to case with fasteners.

As seen in Figure 2.35, to wire the load cell gather the following components: A: Load cell. B: Load cell wire cover (CAD07). C: Two compliant clips (CAD02). D: Wire spool part (CAD17). E:

Wire spool cover (CAD18). F: Load cell amp. G: Two 6-32 button head cap screws 0.75 inches long. H: One 6-32 flat head cap screw 1 inch long. I: Three 6-32 nuts. Note that the load cell wire has been broken into its discreet wires and soldered to wires with female Dupont connectors on the ends. The reading rate of the load cell amplifier should also be increased from 50 Hz to 80 Hz by cutting the small lead between the two “rate” pads on the bottom side of the load cell amplifier using a razor.

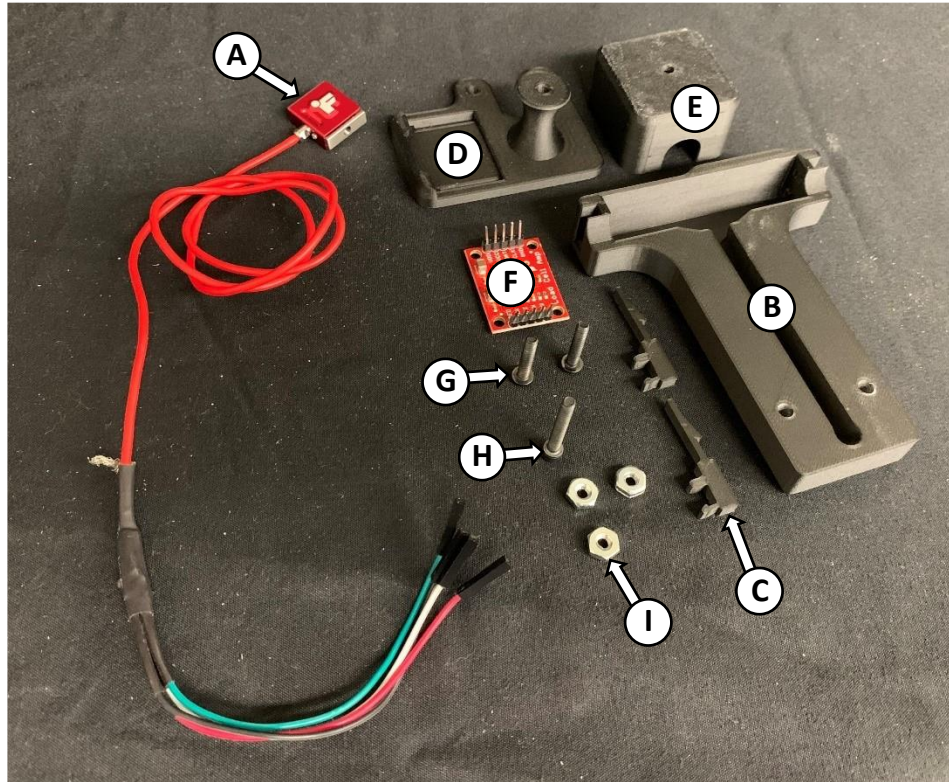


Figure 2.35 Load cell wiring components.

Install the compliant clips into both sides of the load cell wire cover. Seating them completely may require tapping them in with a hammer.



Figure 2.36 (Left) Placement for compliant clip on load cell wire cover. (Right) Fully seated compliant clip.

Remove the sliding cover on the load cell cover and place the load cell inside. Do not mount the load cell yet. Route the wire through the gap in the bottom of the cover and through the large hole in the bottom cover.

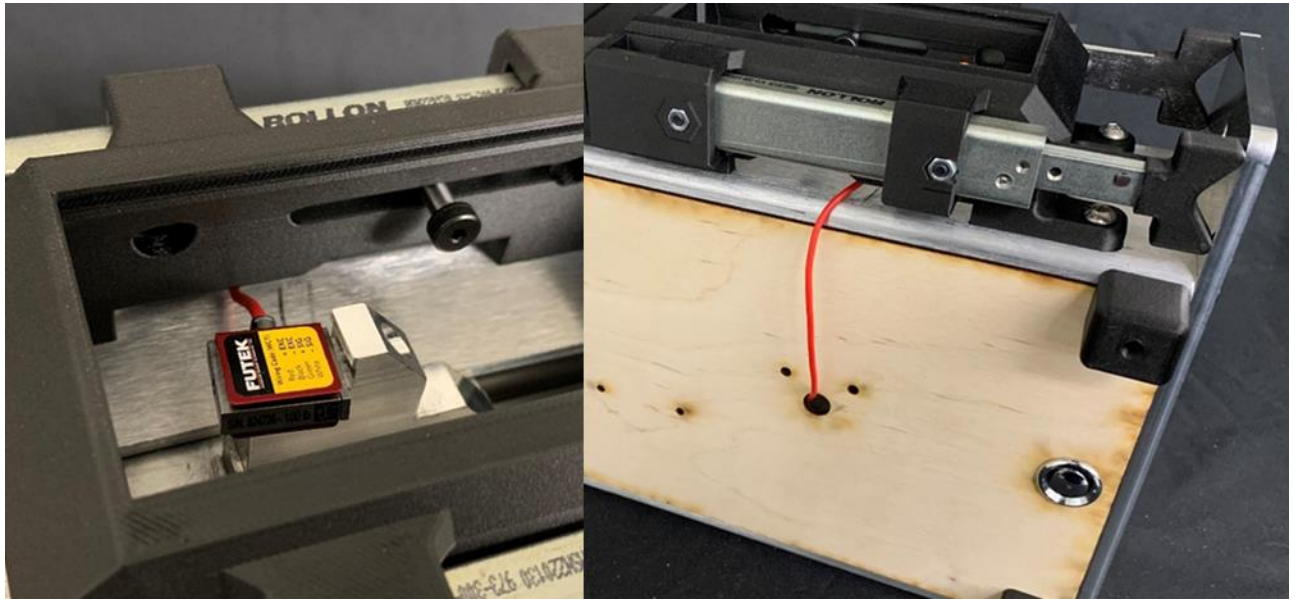


Figure 2.37 Load cell with wire routed through gap and into hole in bottom cover.

Make sure the wire is straight between the hole and the gap in the load cell cover and carefully, making sure not to pinch the load cell wire, clip the load cell wire cover in place. The compliant clips should now be locked into the inside of the load cell cover, but can be pinched inward to remove the load cell wire cover, if needed.



Figure 2.38 Load cell wire cover snapped in place.

Insert a 6-32 nut into the bottom of the wire spool part. Set the wire spool part in place and run the two 6-32 button head cap screws through the load cell wire cover and up through the wire spool part. Set the two 6-32 nuts in place and tighten it down.



Figure 2.39 Nut inserted in bottom of wire spool part.

Drop the load cell amp in place and slide it to the left side. Make sure there is enough slack for the load cell to move in the load cell cover by carefully pulling more through if needed. Spool most of the remaining wire around the spool.

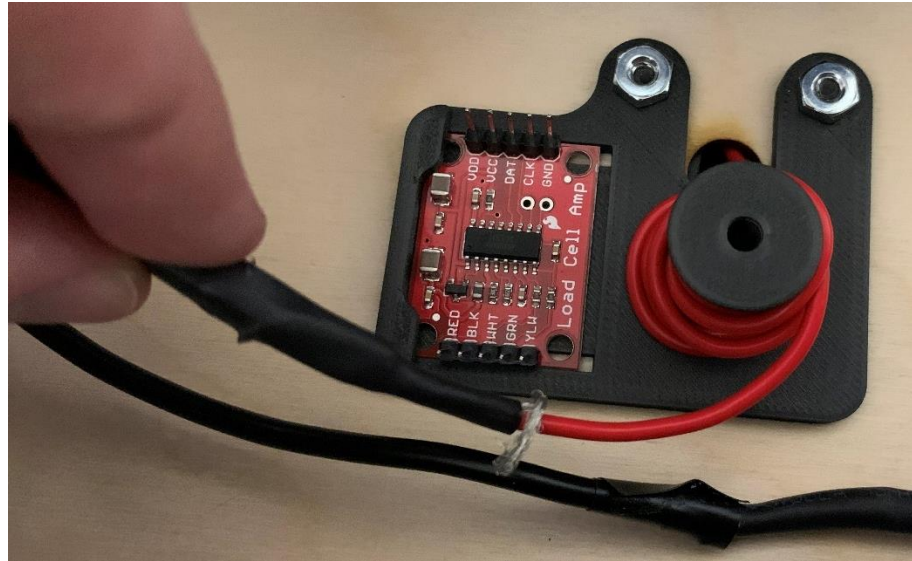


Figure 2.40 Load cell wire spooled around part.

Place the wire spool cover in place and secure it using the flat head cap screw. Note that there is a slight ridge on one of the bottom edges of the cover that should go on the side of the load cell amp. Wire the load cell to the load cell amp.

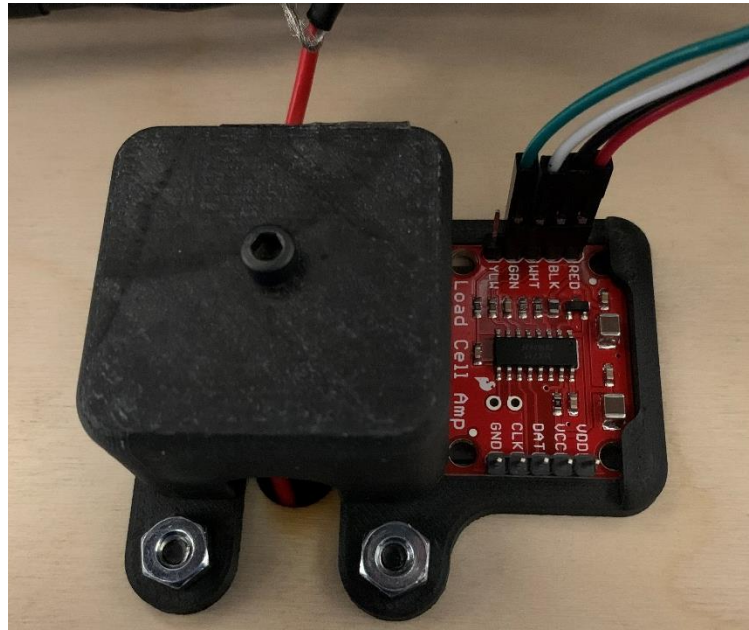


Figure 2.41 Load cell wire spool cover bolted down and load cell wired to load cell amp.

#### 2.4.6 Lid Assembly

As seen in Figure 2.42, to begin lid assembly gather the following components: A: Top cover (LASER02). B: Bottom DC panel mount part (CAD01). C: Top DC panel mount part (CAD16). D:

DC plug to discreet wire converter. E: Two 4-40 flat head cap screws 1 inch long. F: Two 4-40 nuts. G: Wires.

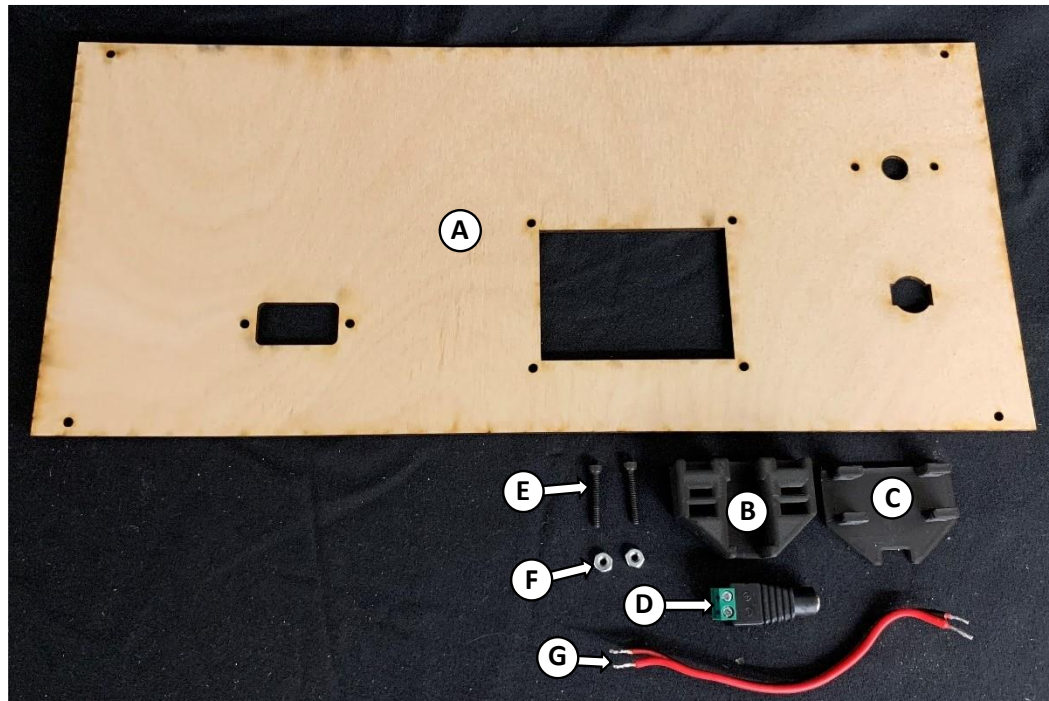


Figure 2.42 DC power panel mount assembly components.

Set the DC plug to discreet wire converter into the bottom panel mount part and the two nuts into the slot on the same part, as shown in Figure 2.43.

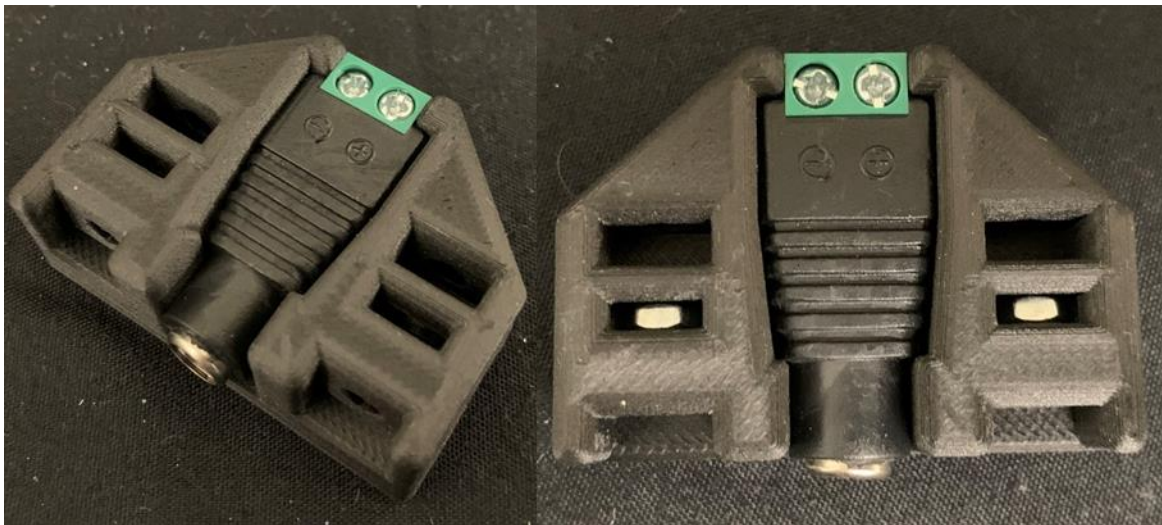


Figure 2.43 DC plug to discreet wire part and nuts set into mount.

Add the top cover of the DC panel mount as seen in Figure 2.44.



Figure 2.44 Top cover of DC panel mount part added.

Attach the DC power panel mount assembly to the inside of the top cover using the two flat head cap screws. Then wire it as seen in Figure 2.45.

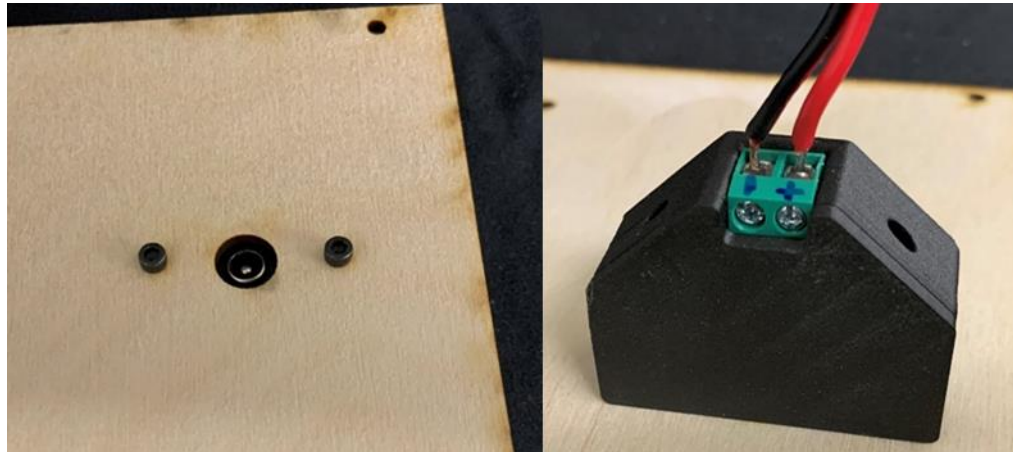


Figure 2.45 DC power components mounted to lid with screws and wired.

As seen in Figure 2.46, to mount the screen gather the following components: A: Top cover assembly. B: The screen. C: The screen frame (CAD11). D: Four 4-40 button head cap screws 0.3125 inches long. E: Four 4-40 nuts. Note that headers have been soldered to both sides of the screen, see Figure 2.48. Only the 8-bit side will be wired but soldering the header onto the SPI side may help the screen mount evenly.

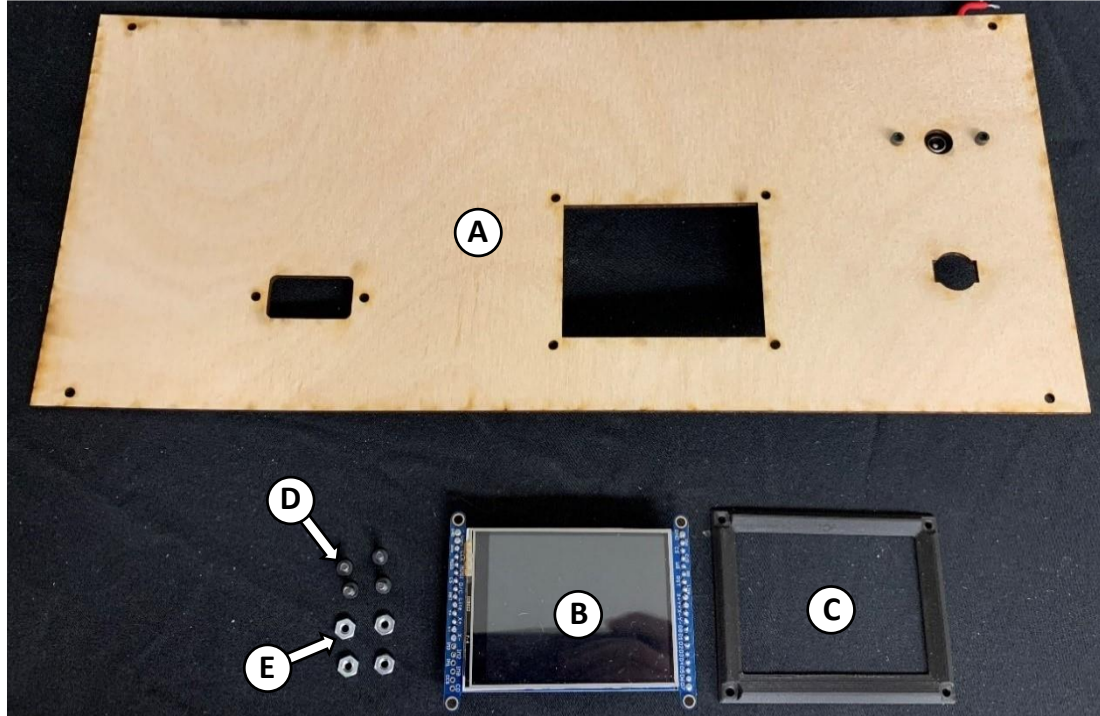


Figure 2.46 Panel mount touch screen assembly components.

Set the frame on the outside of the top cover. Make sure the “Top” text on the frame can be read from the front of the cover. Then pass the button head cap screws through the frame and through the screen on the back side. Note that the SPI connections on the screen should be on the left side of Figure 2.47.



Figure 2.47 Touch screen frame with screws mounted to top cover.

Then secure the screen in place using the 4-40 nuts.

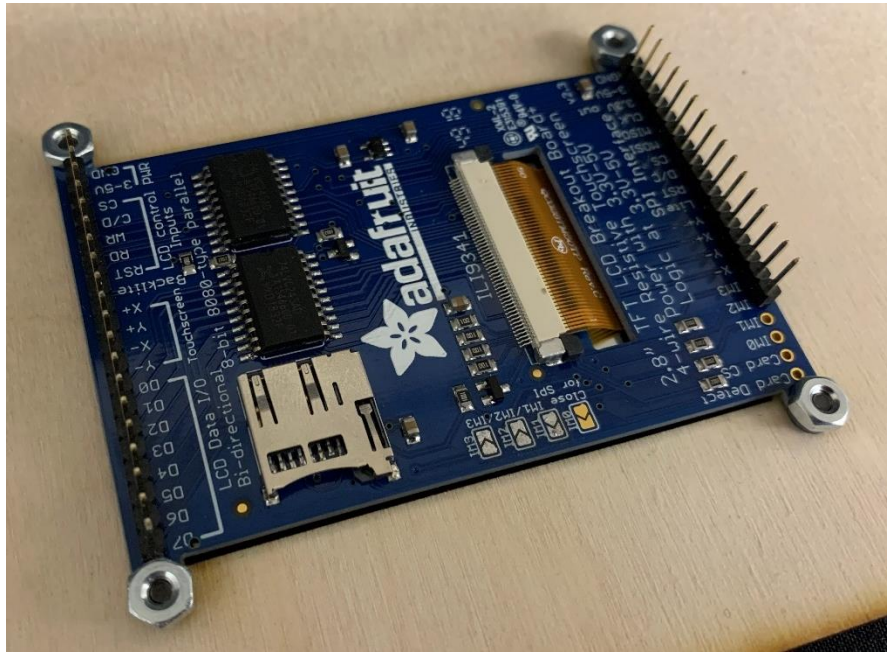


Figure 2.48 Touchscreen mounted to the bottom of top cover with nuts.

As seen in Figure 2.49, to panel mount the SD breakout board gather the following components: A: Top cover assembly. B: SD panel mount base (CAD12). C: SD panel mount cover (CAD13). D: SD breakout board. E: Micro SD card. F: Two 4-40 socket head cap screws 1 inch long. G: Four 2-56 socket head cap screws 0.375 inches long. H: Two 4-40 nuts. I: Four 2-56 nuts.

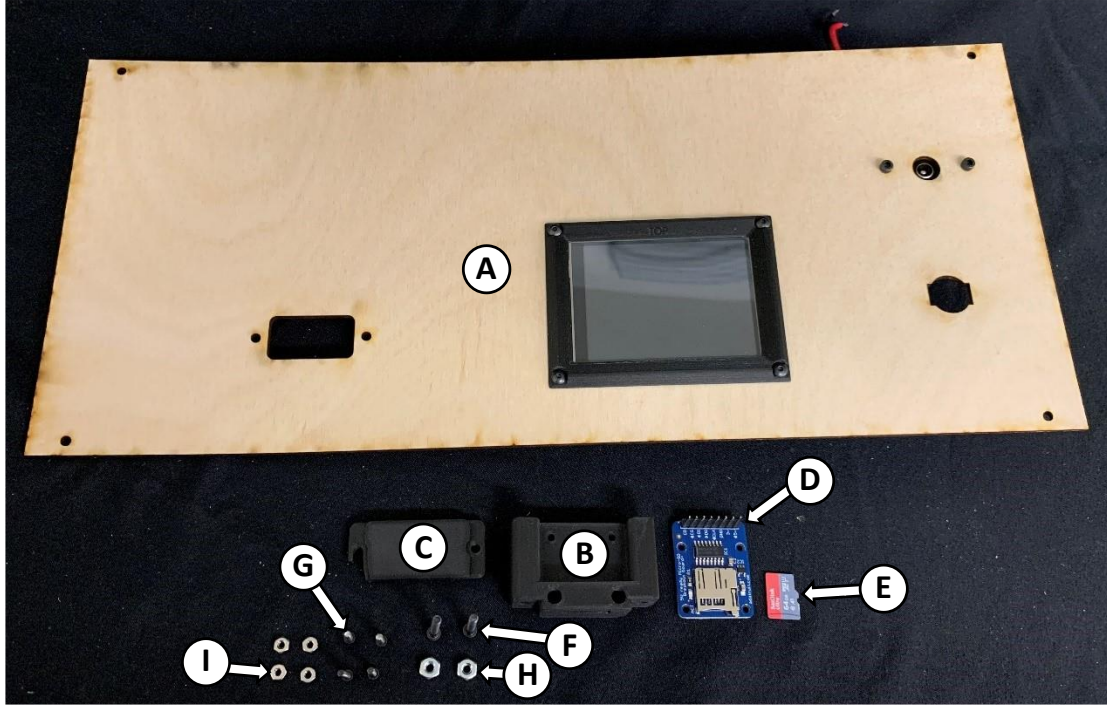


Figure 2.49 Panel mount SD port assembly components.

Set the SD breakout board into the SD panel mount base, flip it over, and set the 2-56 nuts into the base.

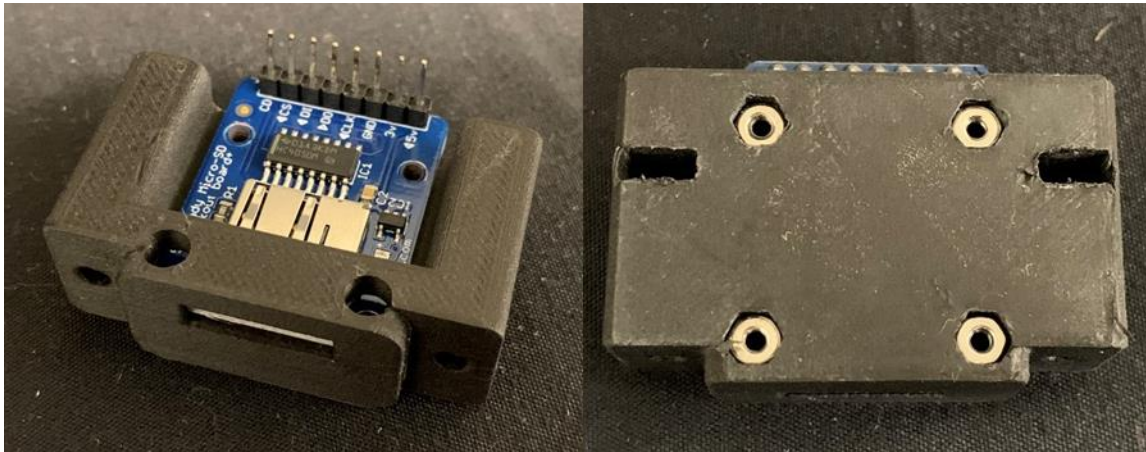


Figure 2.50 SD breakout board and nuts inserted into mount part.

Secure the SD breakout board in place using the four socket head cap screws. And insert the 4-40 nuts into the slots in the bottom of the panel mount base.

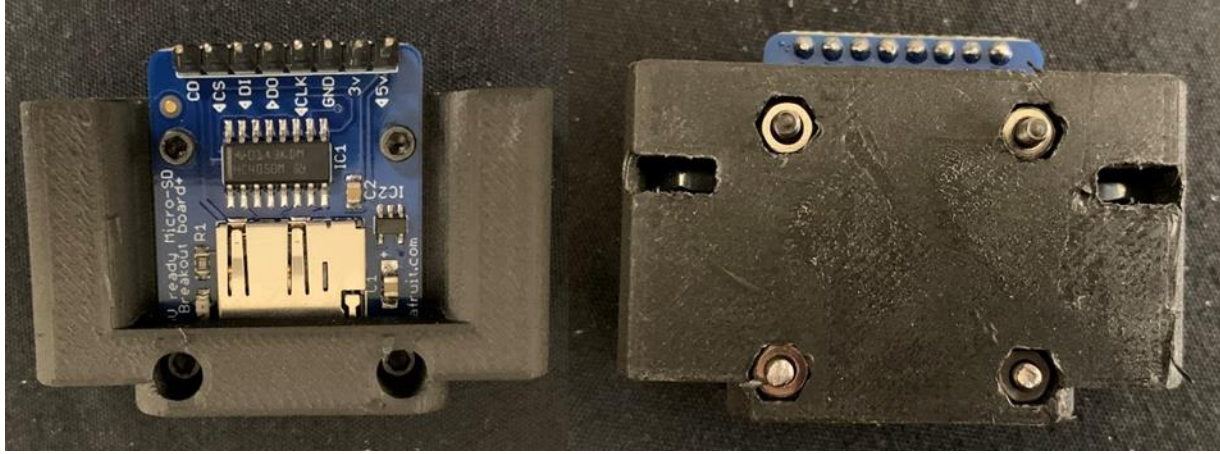


Figure 2.51 SD breakout board bolted to mounting part.

Set the SD breakout base into the cutout on the inside of the top cover and the SD panel mount cover on the outside of the top cover. Secure it in place using the two 4-40 socket head cap screws as seen in Figure 2.52.

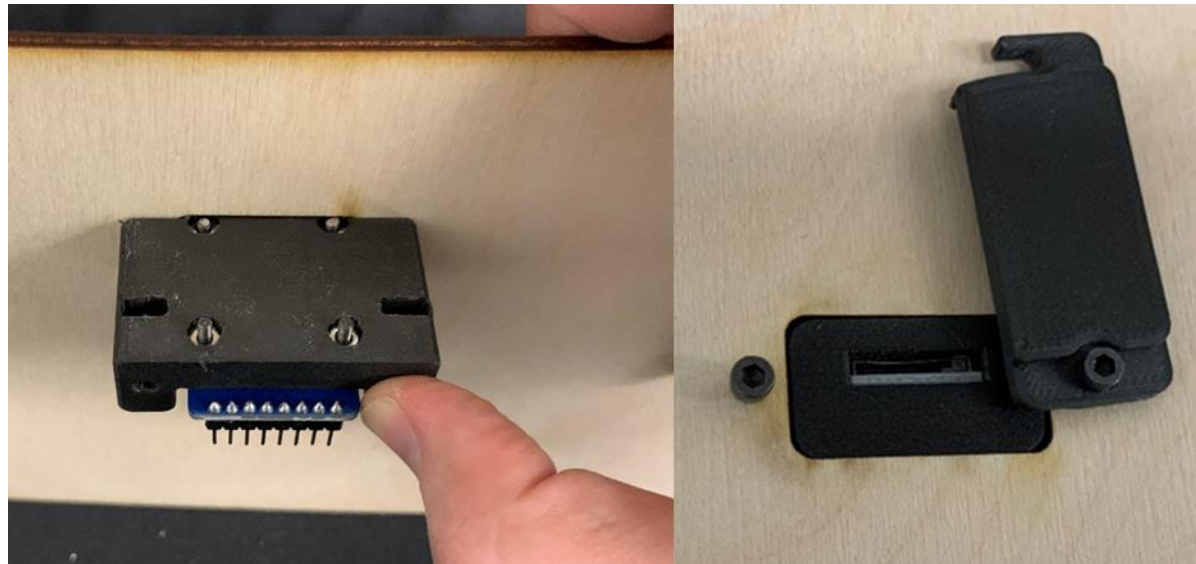


Figure 2.52 SD breakout mount being held and fastened to top cover.

To add the USB splitter onto the top cover gather the USB splitter, the rubber grommet, and some double-sided tape.

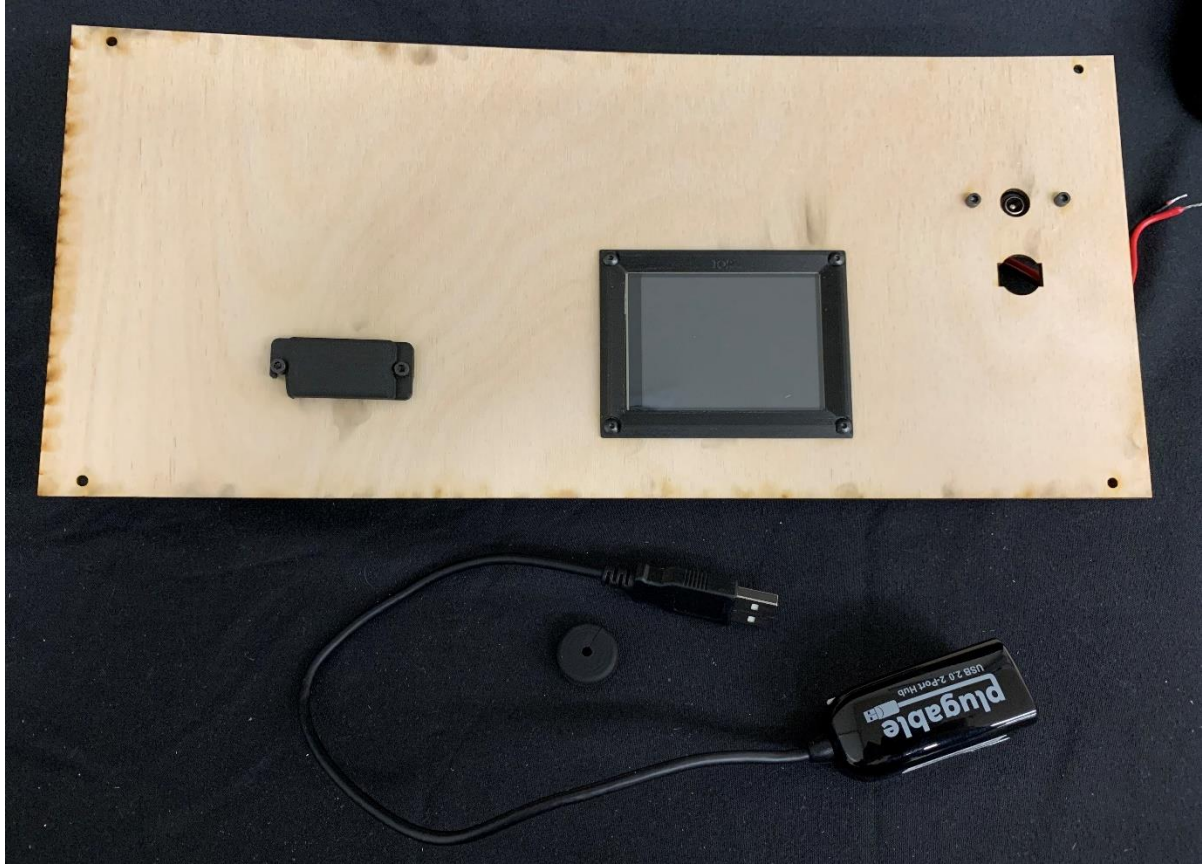


Figure 2.53 USB splitter panel assembly components.

Begin by cutting the grommet and inserting the USB splitter cable into the grommet as seen in Figure 2.54.



Figure 2.54 Cut grommet placed on USB splitter cable.

Run the USB cable through the back of the cover and secure the grommet in the hole. Then attach the USB splitter to the inside of the cover using double sided tape in the same position as seen in Figure 2.55.

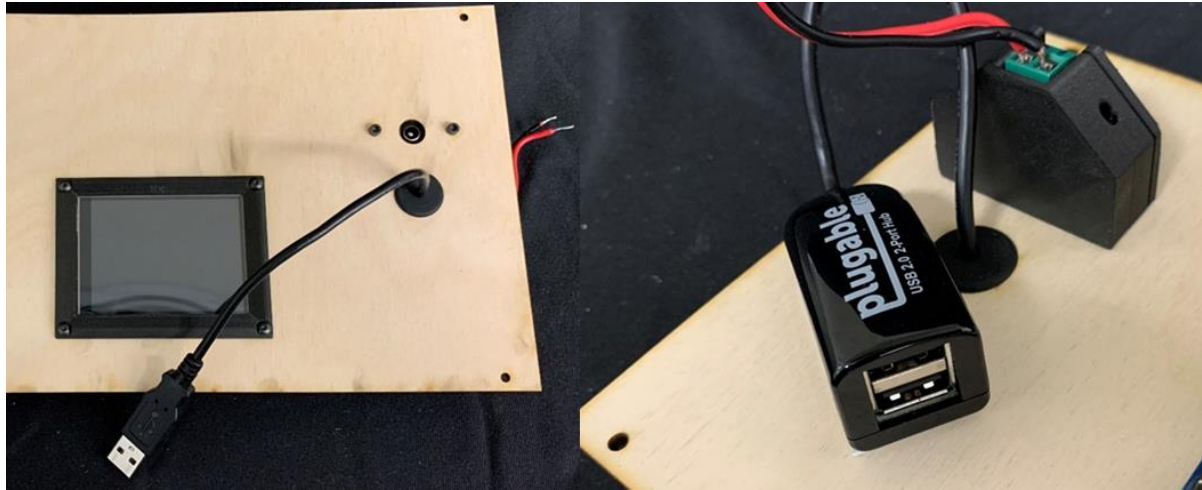


Figure 2.55 USB splitter routed through top cover.

#### 2.4.7 Wiring

At this point the only wired components are the load cell to the load cell driver and the motor to the motor driver. In this section we will cover the additional components that need to be wired and some of the strategies for wiring them. This section will not cover specific wiring steps for every connection, but the full SPuD wiring schematic can be found in the repository.

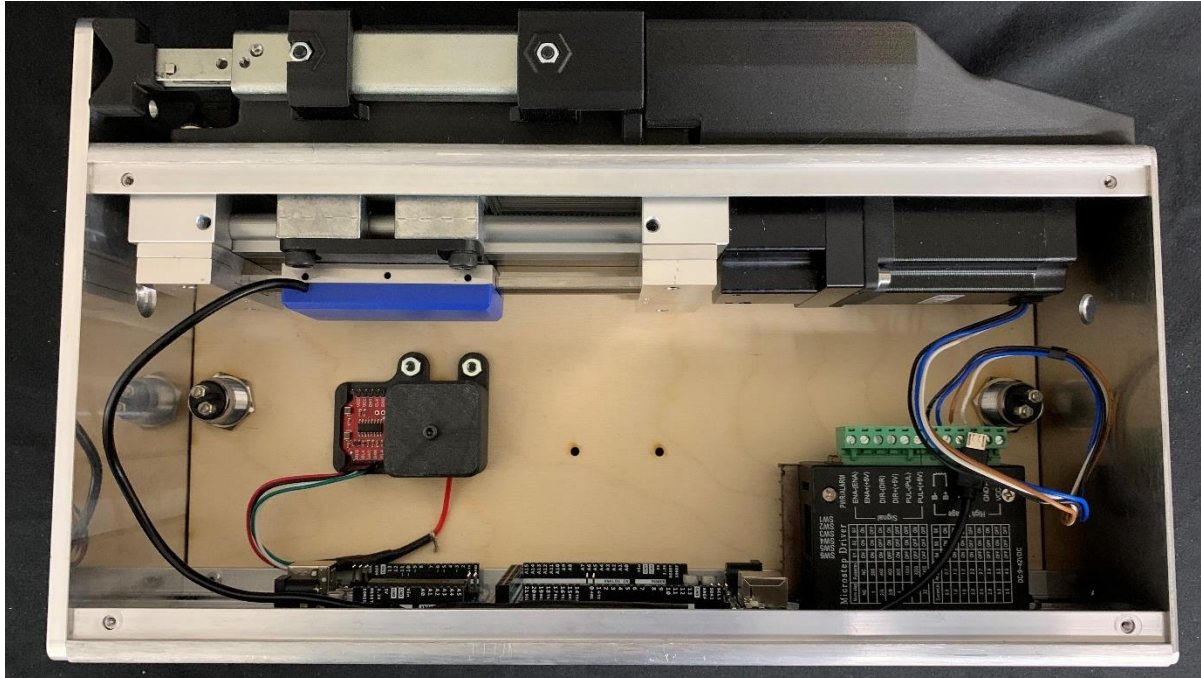


Figure 2.56 Pre-wiring layout of case.

Most of the wiring will be done from the Arduino Mega since the Arduino Uno is only required to drive the stepper motor and communicate back and forth with the Arduino Mega. Figure 2.57 shows the wiring necessary for the communication between Arduinos. See the wiring schematic for specific wiring.

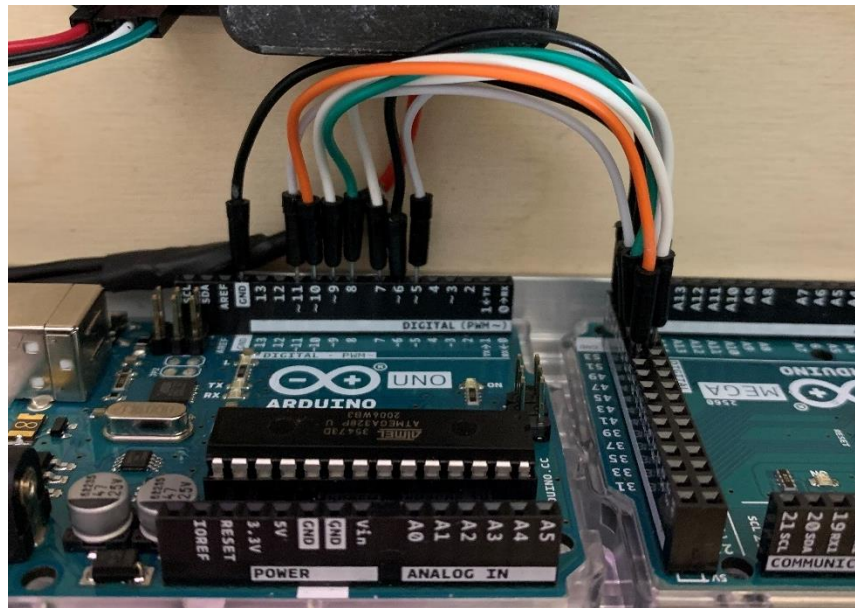


Figure 2.57 Wiring from Arduino Uno to Arduino Mega.

The only other connections wired to the Arduino Uno are the three connections to the motor driver shown in Figure 2.58.

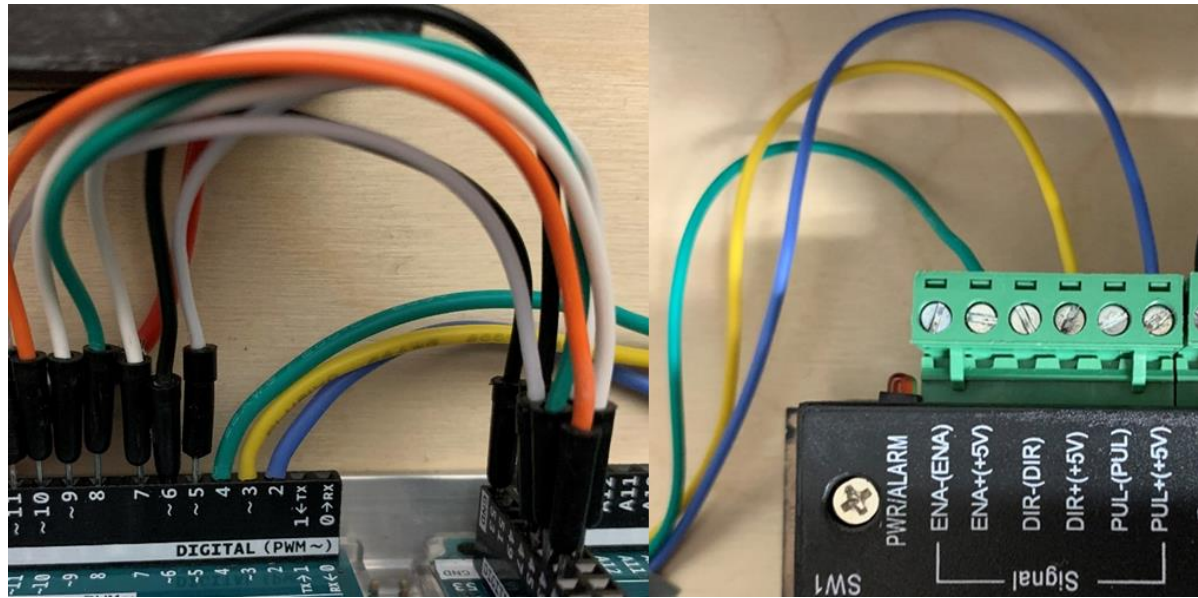


Figure 2.58 Wiring Arduino Uno to motor driver.

The Arduino Mega is wired to many components, so it can be helpful to use methods that assist with wire organization. One method utilized in the wiring of the SPuD is to use Dupont connectors where possible.

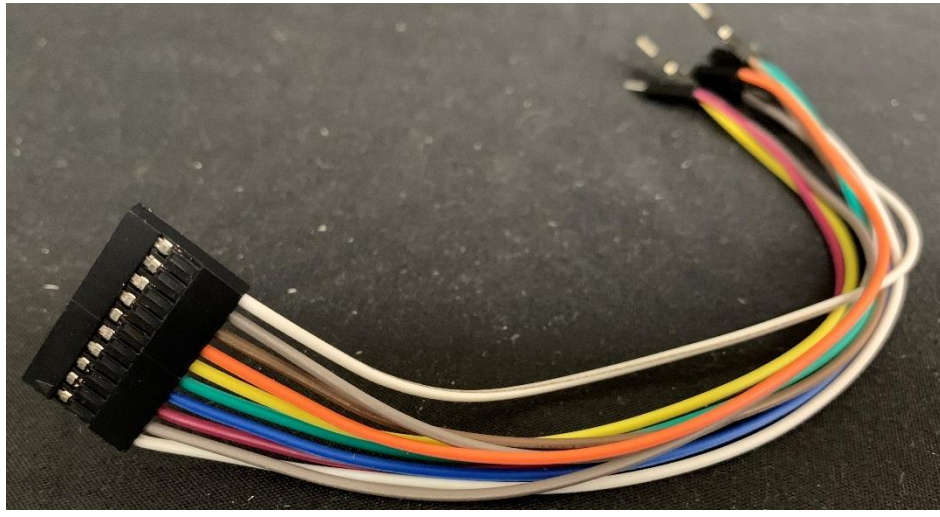


Figure 2.59 Example Dupont connector cable.

The Dupont connector seen in Figure 2.60 provides half of the necessary connections for the LCD screen that will later be added. This not only organizes the wires but allows the screen to be quickly detached for easy lid removal.

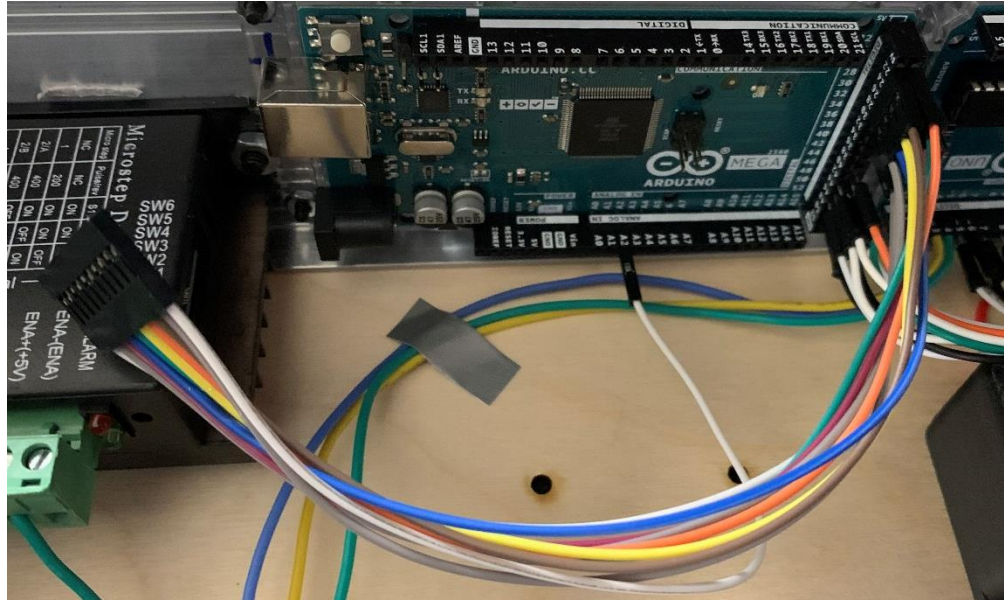


Figure 2.60 Wiring Dupont connector to Arduino Mega.

As seen in Figure 2.61, additional components should be gathered for the wiring of this device. Components include: A: Two limit switches. B: USB breakout board. C: Logic level converter. D: Breadboard. E: Four  $10\text{ k}\Omega$  resistors (not pictured). F: Two #4 0.25 inch long nylon spacers. G: Two 4-40 button head cap screws 0.5 inches long. H: Four 2-56 flat head cap screws 0.375 inches long (not pictured). I: Two 4-40 nuts. The breadboard is included in this wiring assembly to assist with some of the connections necessary in the wiring schematic, such as linking common grounds and as a place to mount resistors. Figures 2.62-2.64 show examples of components that may benefit by being wired to the breadboard.

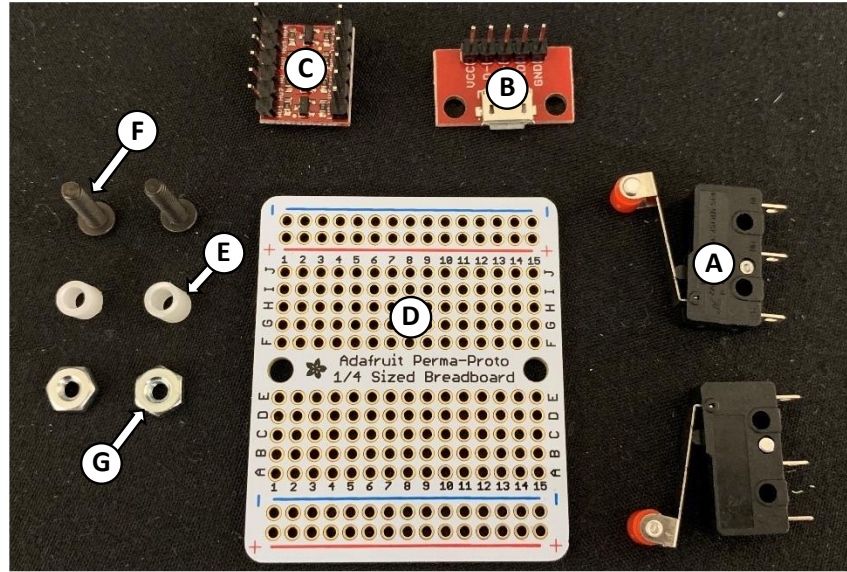


Figure 2.61 Wiring components.

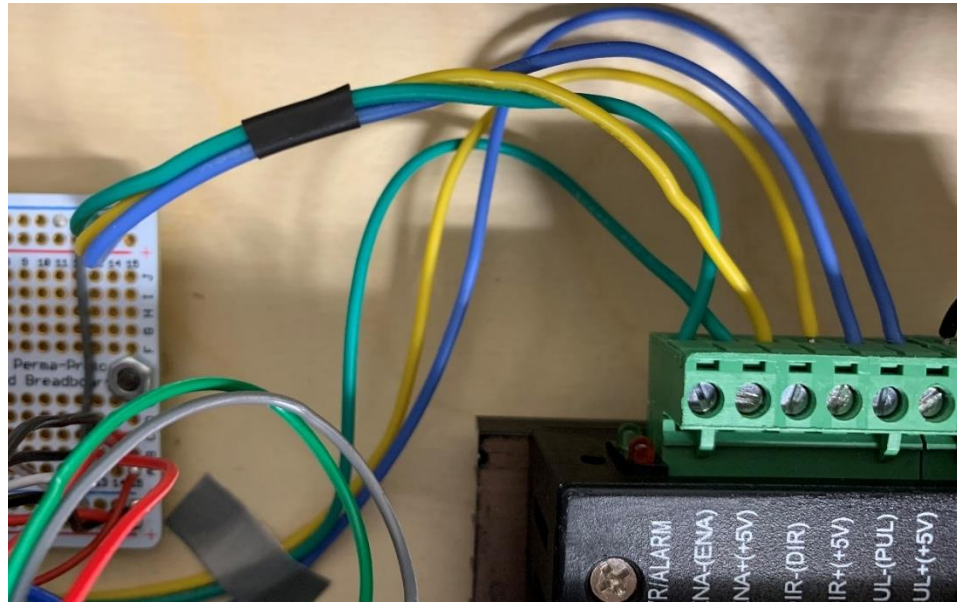


Figure 2.62 Wiring common ground for motor driver.

Limit switches are mounted to both linear scale bottom mounts using the four flat head cap screws, as seen in Figure 2.63.

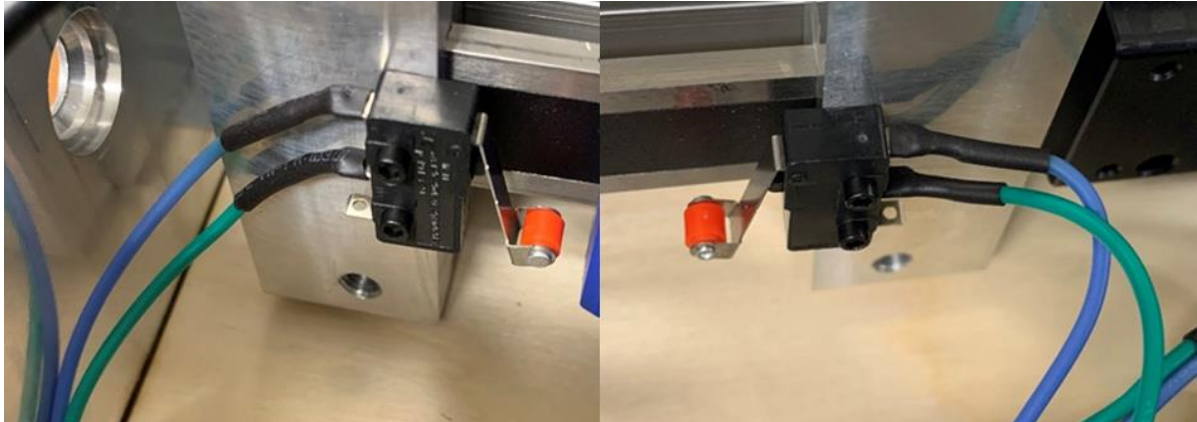


Figure 2.63 Limit switches mounted and wired.

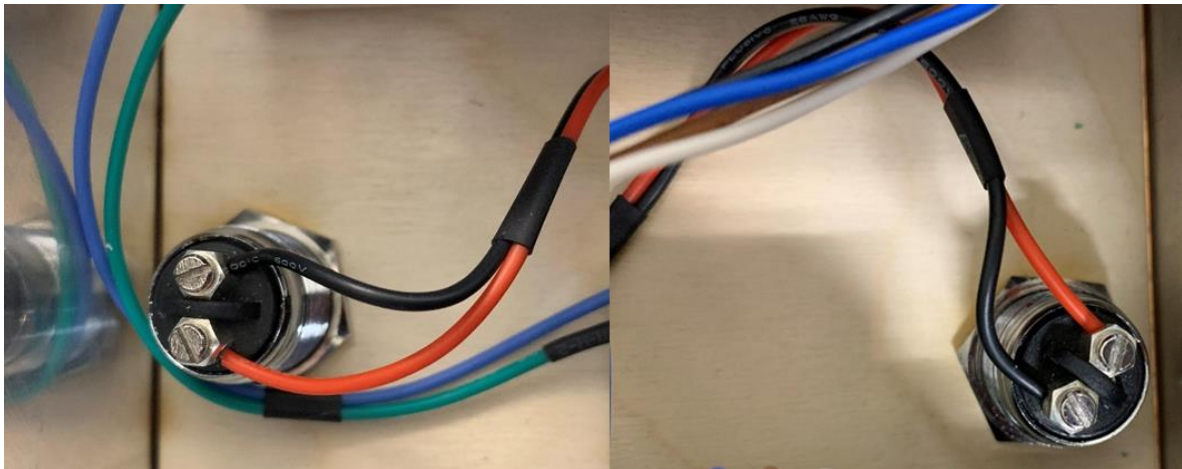


Figure 2.64 Wiring left and right push buttons.

Once the breadboard has been wired it can be mounted to the two remaining holes in the bottom cover by running the button head cap screws up through the bottom of the cover, through the spacers, through the breadboard, and securing them in place with the 4-40 nuts.

Once wiring is complete gather the linear assembly cover (CAD05) and four M6 flat head cap screws 12 millimeters long. Mount it in place by screwing the bolts into the linear scale bottom mounts, as seen in Figure 2.65. This cover will prevent any wires from being caught in the motion of the linear system. At this point make sure that Arduino Uno and Mega have the proper sketches uploaded, both sketches can be found in the appendices.

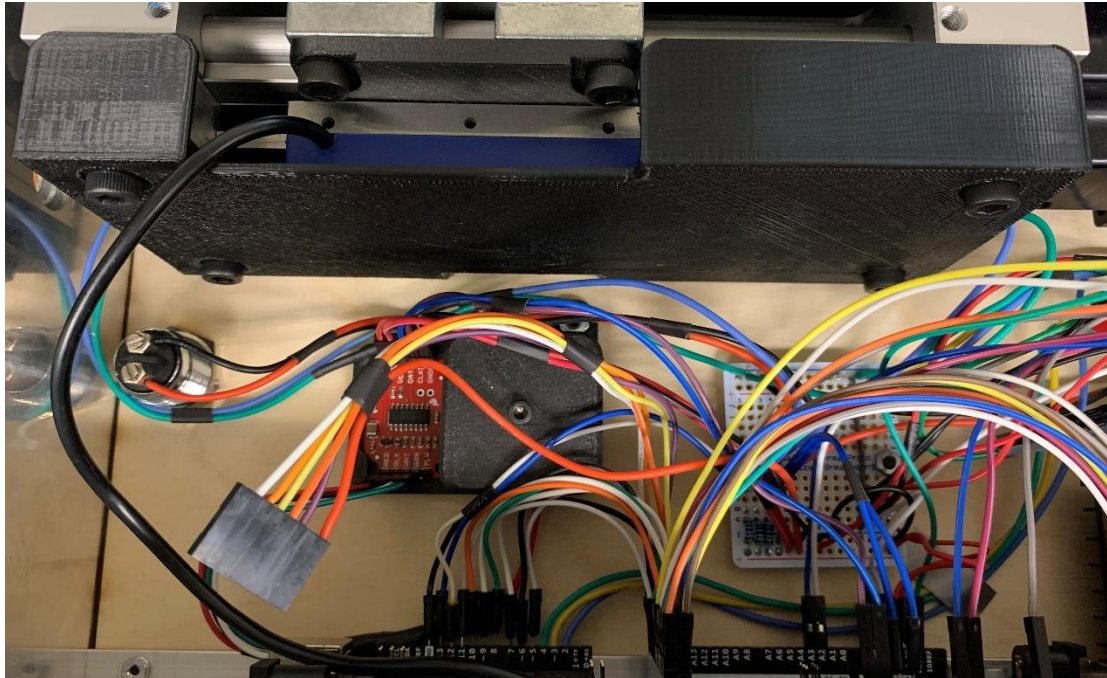


Figure 2.65 Linear assembly cover installed.

Finally, the top cover can be brought over to the device and wired. As mentioned before, the wiring for this SPuD is such that the SD breakout board and LCD are attached with Dupont connectors that allow for quick removal of the lid. The Arduinos are powered using the included cables which are plugged into the USB splitter. The DC power wires must be wired into the motor driver.

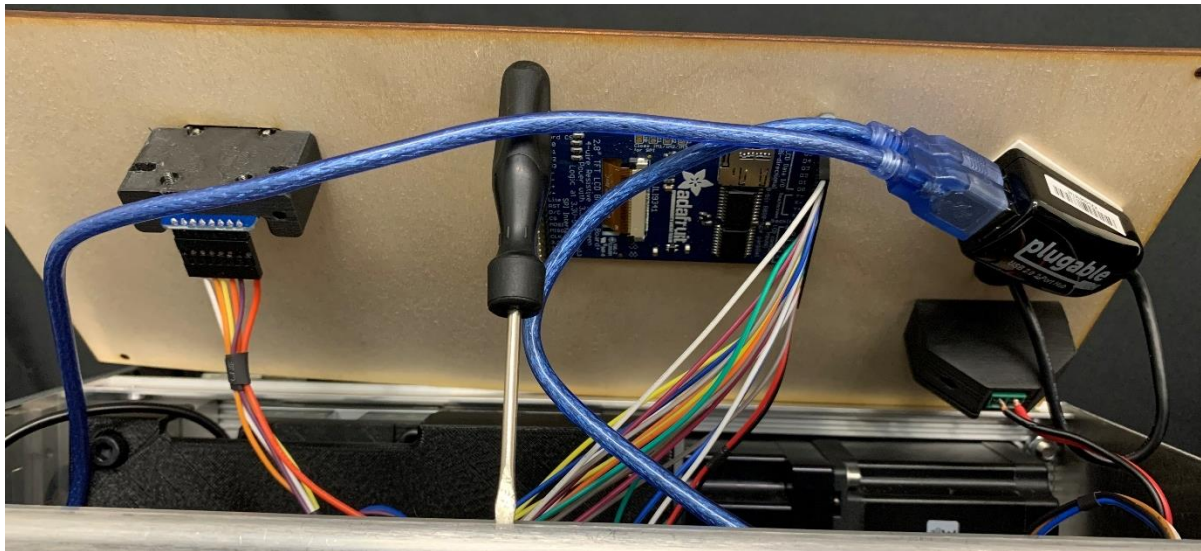


Figure 2.66 Top lid components wired.

After wiring, the top cover can be mounted using four 4-40 button head cap screws 0.25 inches long. Hook and loop tape should also be applied to the top cover as pictured in Figure 2.67.

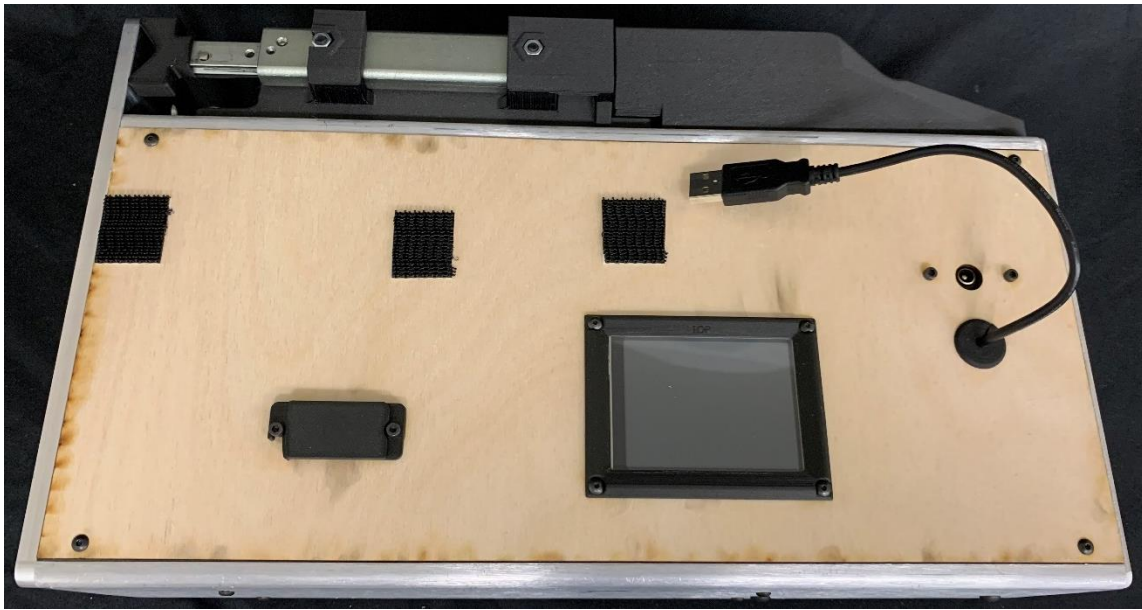


Figure 2.67 Top cover mounted and hook and loop tape applied.

Attach hook and loop tape to the two batteries, making sure the tape position matches that of the case.



Figure 2.68 Hook and loop tape applied to batteries.

The batteries can be attached to the case using the matching hook and loop tape and plugged in. The USB should be plugged into the smaller 5 V battery and the larger 24 V battery should be

wired from the 24 V port to the DC panel mount port using a 1 foot male to male DC power cable. Do not plug both the USB and DC plugs into the 24V battery. Doing this initially seems to work but causes the linear system's readings to become unsteady and will ruin test data.



Figure 2.69 Batteries attached to case using hook and loop tape and plugged in.

#### 2.4.8 Load Cell and Needle Mounting

Now that the device is up and running, we will be mounting the load cell and needle to the device. As seen in Figure 2.70, gather the following components: A: The needle chuck (MILL08). B: Slide catch (CAD14). C: Test needle (MILL09). D: Two 6-32 button head cap screws 0.5 inches long. E: One M3 socket head cap screw 6 millimeters long. F: One 2-56 socket head cap screw 0.125 inches long. G: One M3 set screw 8 millimeters long.

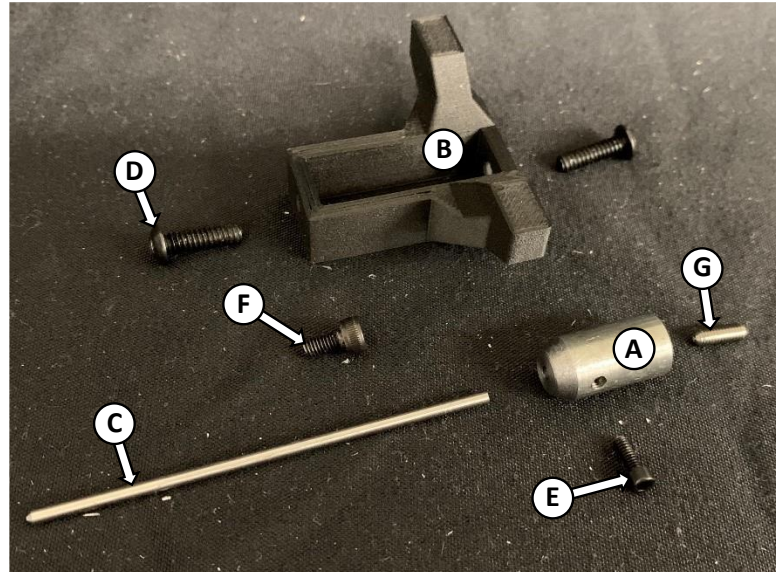


Figure 2.70 Needle chuck assembly components.

Begin assembly by threading the set screw into the back of the chuck. Insert the needle in the front of the chuck and secure it in place with the 2-56 socket head cap screw.



Figure 2.71 Needle chuck being assembled.

Now power up the SPuD if it is not already powered. The main menu screen shown on the left of Figure 2.72 should now be on the screen. Navigate to the Hardware Check screen by pressing the corresponding blue box on the LCD. This screen, seen on the right of Figure 2.72, allows the user to move the shuttle left and right which will aid in the assembly of the load cell and needle. Before moving the shuttle at all, remove the slide cover from the load cell cover and make sure that the unmounted load cell and its wire are in a safe location. Move the shuttle to the far left and allow movement to be stopped by the limit switch.

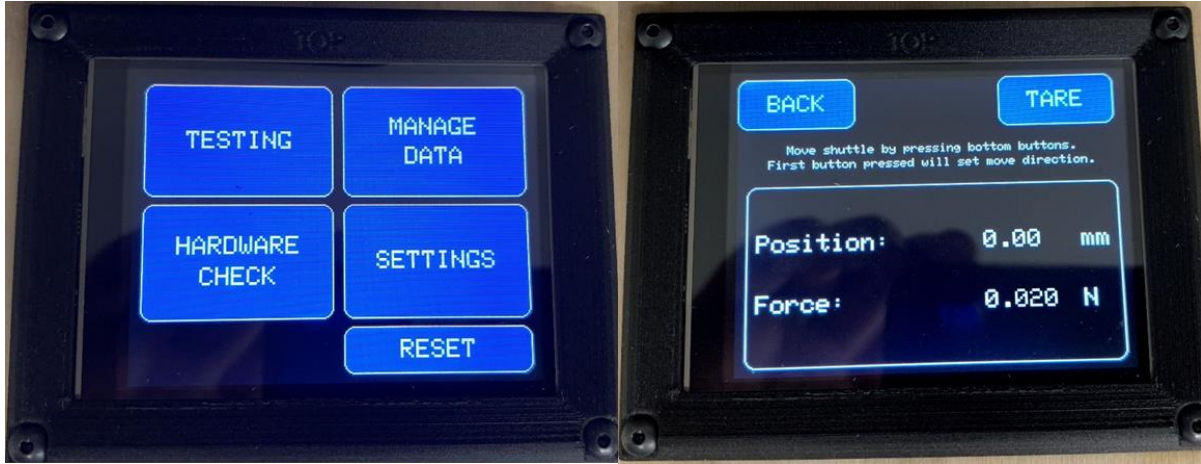


Figure 2.72 Main menu screen (left) and the hardware check screen (right).

Once the shuttle is in the far left position set the slide stop part over the load cell mount and secure it in place with one of the button head cap screws in the right mounting hole. Move the shuttle to the far right and allow movement to be stopped by the limit switch. Use the second button head cap screw to secure the left mounting hole.

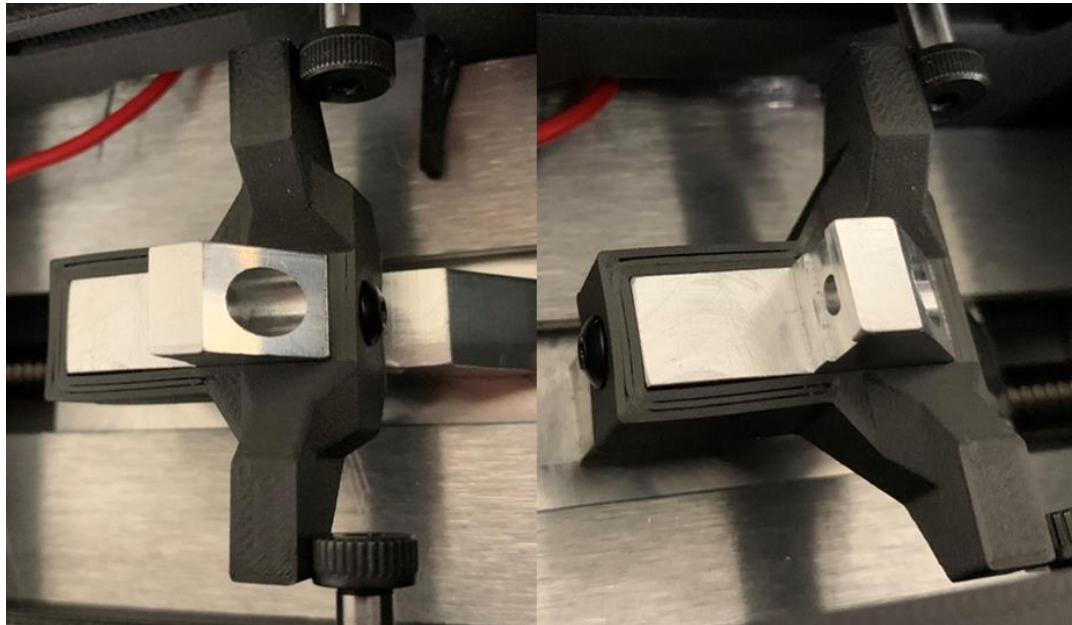


Figure 2.73 Slide stop part slid over load cell mount and secured with screws.

Move the shuttle as necessary and use the M3 flat head cap screw to attach the load cell to the load cell mount in the orientation shown in Figure 2.74. After mounting the load cell double check the amount of slack in the load cell wire to ensure it does not get pinched or stretched throughout the full motion of the shuttle; adjust this if necessary.



Figure 2.74 Load cell secured to load cell mount with screw.

Move the shuttle as necessary and attach the needle chuck to the load cell by threading it on by hand. Secure the load cell slide cover back in place.

Now check that the test needle is aligned with the center of the hole on the left cover. If the needle is misaligned in the direction perpendicular to the stalk being tested it should be adjusted towards the center of the hole. Methods to adjust the position of the needle include checking the seating of the needle in the chuck, ensuring that the needle is straight, loosening mounting hardware to move components within the clearance hole tolerances, and placing shims between the linear system and the load cell mount (MILL07). Be careful not to shim too much or the load cell mount could begin to scrape along the inside of the case during movement. Remaining misalignment in this direction would likely cause the SPuD to underpredict the minor diameter of the stalks being tested. There is no need to adjust the needle if it is off center in either direction parallel to the length of the stalk being tested unless it is severe enough not to pass through the hole.



Figure 2.75 Needle chuck threaded onto loadcell.

#### 2.4.9 Shoulder Strap Setup

To get the shoulder harness ready simply loop the camera straps through the sling mounts as shown in Figure 2.76.



Figure 2.76 Camera straps looped through sling mounts.

Secure the sling mounts to the left and right covers of the device by pressing the button in the center of the sling mount and pushing them into their respective holes. The buttons should pop back up once they are inserted to show they are locked in place.

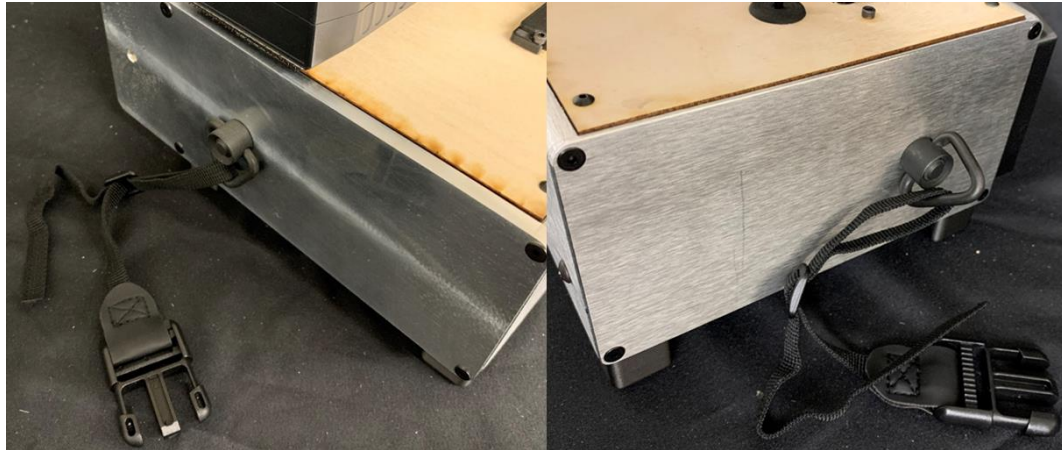


Figure 2.77 Sling mounts secured to both sides of device.

Put on the shoulder harness and clip into the buckles.



Figure 2.78 Fully assembled SPuD being held by shoulder harness.

## 2.5 User Interface

### 2.5.1 Main Menu

The SPuD device is controlled via the LCD touchscreen and the two buttons mounted on the bottom cover. This section details navigation through the user interface.

When the device is powered it should immediately display the **main menu** screen shown in Figure 2.79. From this screen the user can access the **settings menu** to change screen colors or recalibrate the load cell, access the **hardware check** screen to see hardware functionality, access the **testing menu** to setup and begin testing, and **reset** the device. There is also a **MANAGE DATA** button on the **main menu**, but that functionality has not yet been programmed. Press any of the onscreen buttons to navigate.



Figure 2.79 Main menu screen.

### 2.5.2 Settings Menu

Pressing SETTINGS on the **main menu** screen should take you to the **settings menu** screen shown in Figure 2.80. At the top of the screen the current calibration slope is displayed. From this screen the user can recalibrate the load cell, swap the theme colors, or navigate back to the **main menu** using the BACK button.



Figure 2.80 Settings menu screen.

To begin recalibrating the load cell press the RECALIBRATE LOAD CELL button on the **settings menu** screen. Follow along with the instructions on the **record zero** screen, seen in Figure 2.81a. These instructions tell the user to remove the needle chuck from the device and remove the load cell from the load cell mount. Open the device and unspool the load cell wire to pull extra through so the load cell can be sat upright, the threaded holes facing up and down, on a flat surface. Press the RECORD ZERO button while the load cell is on the surface without any weight. Pressing this will move to the **enter known weight** screen, but pressing CANCEL on any of the recalibration screens will return the user to the **settings menu** without making any changes to the calibration.

On the **enter known weight** screen, seen in Figure 2.81b, the user inputs the mass in grams of a known weight that they will be placing on the load cell using the on-screen keypad. The user can then hit ENTER and be taken to the **apply known weight** screen, seen in Figure 2.81c, where they will apply the known weight to the load cell and press RECORD VALUE.

After pressing RECORD VALUE the user will see the **save calibration** screen, seen in Figure 2.81d, which shows the new calibration slope that has been calculated and provides one final option to cancel before setting the new calibration. If the user proceeds the new calibration will

overwrite the old one in the Arduino Mega's EEPROM and return them to the **settings menu** screen, which will display the new calibration.

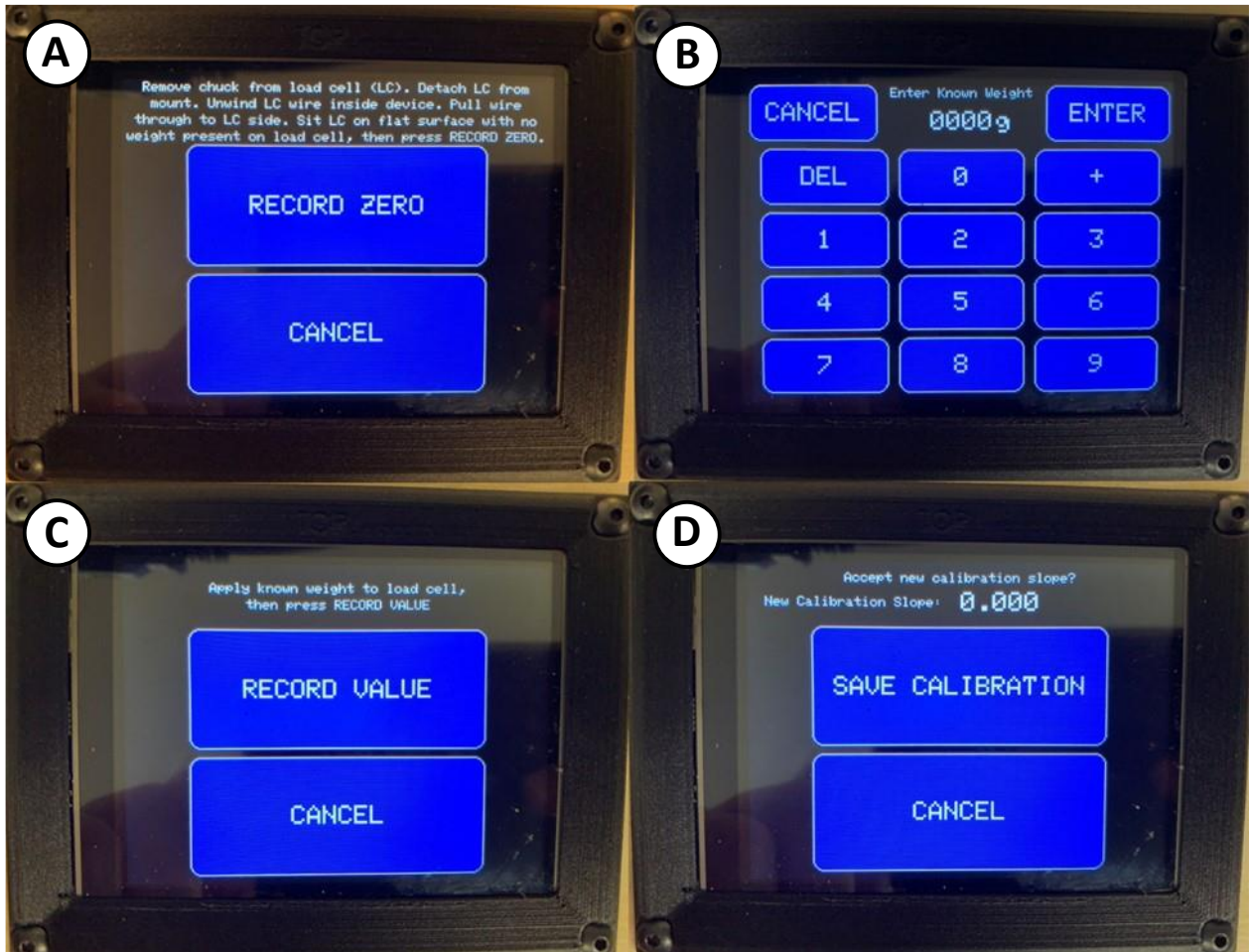


Figure 2.81 Load cell recalibration screens A) Record zero screen B) Enter known weight screen C) Record known weight screen D) Save calibration screen.

To change the theme colors press the **SWITCH THEME** button on the **settings menu** screen. Pressing this will change the theme colors for the device, as seen in Figure 2.82. To change the theme back press the **SWITCH THEME** button again.

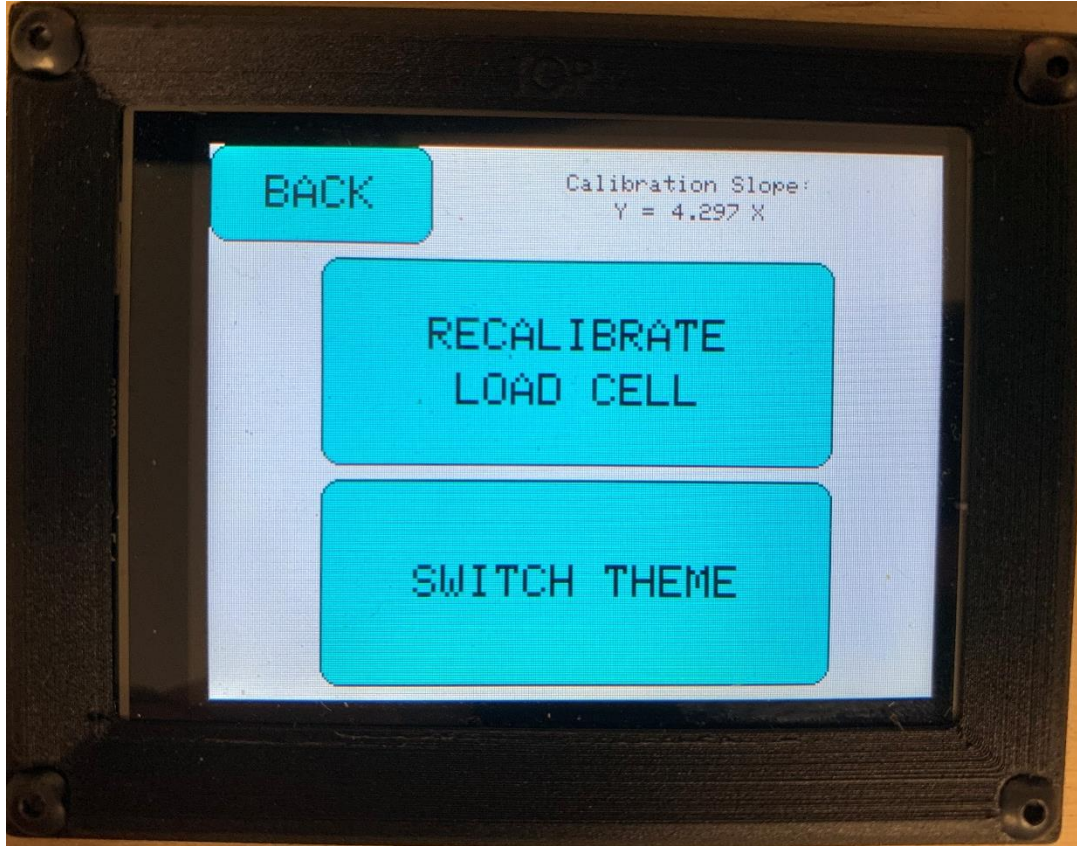


Figure 2.82 Settings menu with alternate theme colors.

### 2.5.3 Hardware Check Screen

To access the **hardware check** screen press the HARDWARE CHECK button from the **main menu**. The **hardware check** screen shows a live reading of the linear scale and load cell, as seen in Figure 2.83. Shuttle movement is also enabled while on this screen so the user can verify the linear scale functionality. Shuttle movement is always controlled using both of the bottom buttons for user safety. Instructions for shuttle movement can be seen on the hardware check screen. There is also a TARE button available to zero the force.

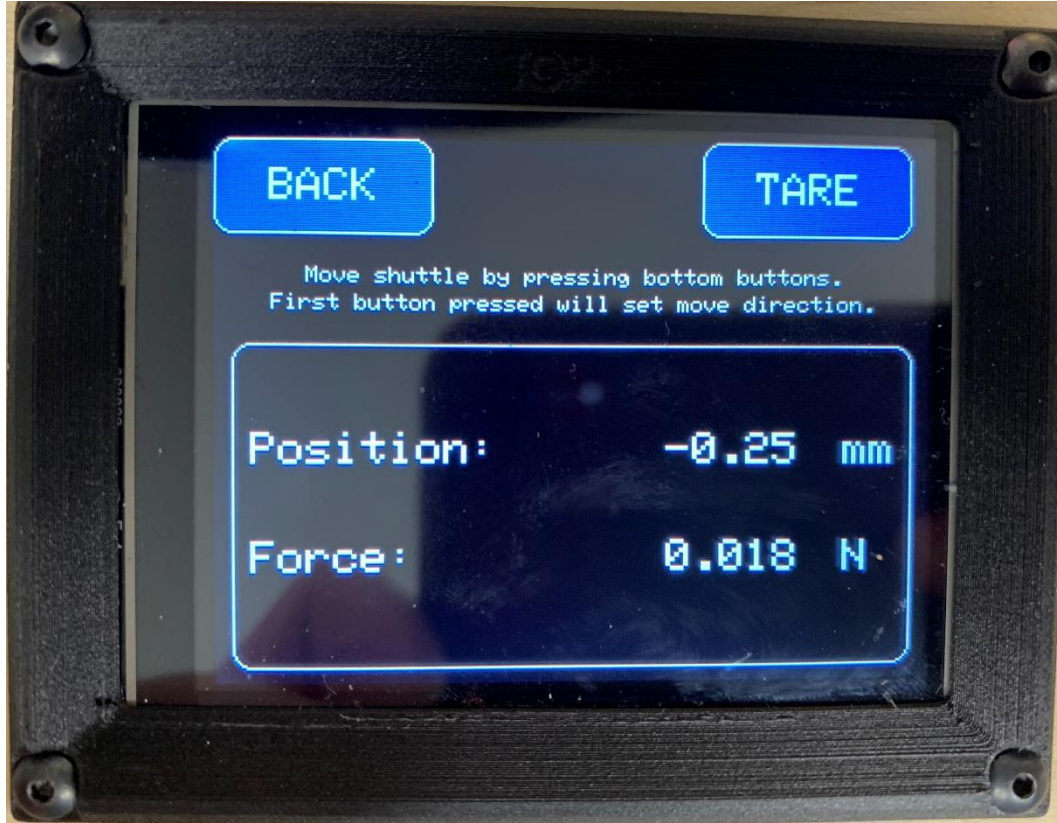


Figure 2.83 Hardware check screen.

#### 2.5.4 Testing Menu

To access the **testing menu** screen press the TESTING button from the **main menu**. The **testing menu** screen displays the current filename that will be generated if a test begins and shows the start position relative to the zero position. Before testing can begin a start position and a zero must be set. Attempting to begin a test before these are set will display an error and direct the user to set them.

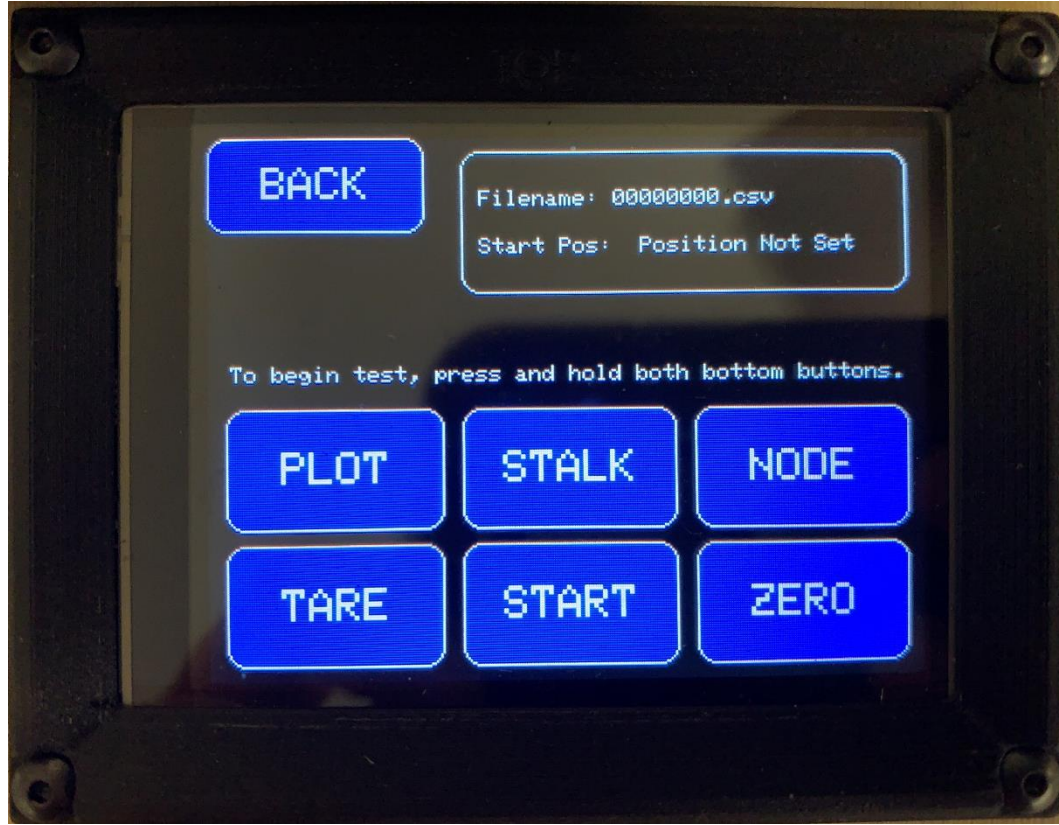


Figure 2.84 Testing menu screen.

#### 2.5.5 Setting Zero and Start Positions

To set the zero position press the ZERO button on the **testing menu** screen. Use the bottom buttons and the on screen arrow buttons to move the tip of the needle until it is flush with the inside face of the backplane. Then press SAVE to record that location and return to the **testing menu**.



Figure 2.85 Set zero position screen.

To set the start position press the START button on the **testing menu** screen. Use the bottom buttons and the on screen arrow buttons to move the tip of the needle to the desired start location. Start position is not as critical as zero position, but setting it allows the user to choose a shorter travel distance for each test if they are testing smaller stalks. The current position relative to the set zero will be displayed on the screen as well. Press SAVE to record the start position and return to the **testing menu**.

At this point a test could be run from the **testing menu** by holding the two bottom buttons down, but the user will likely need to set the Plot, Stalk, and Node number first so the test data is saved under a recognizable file name.

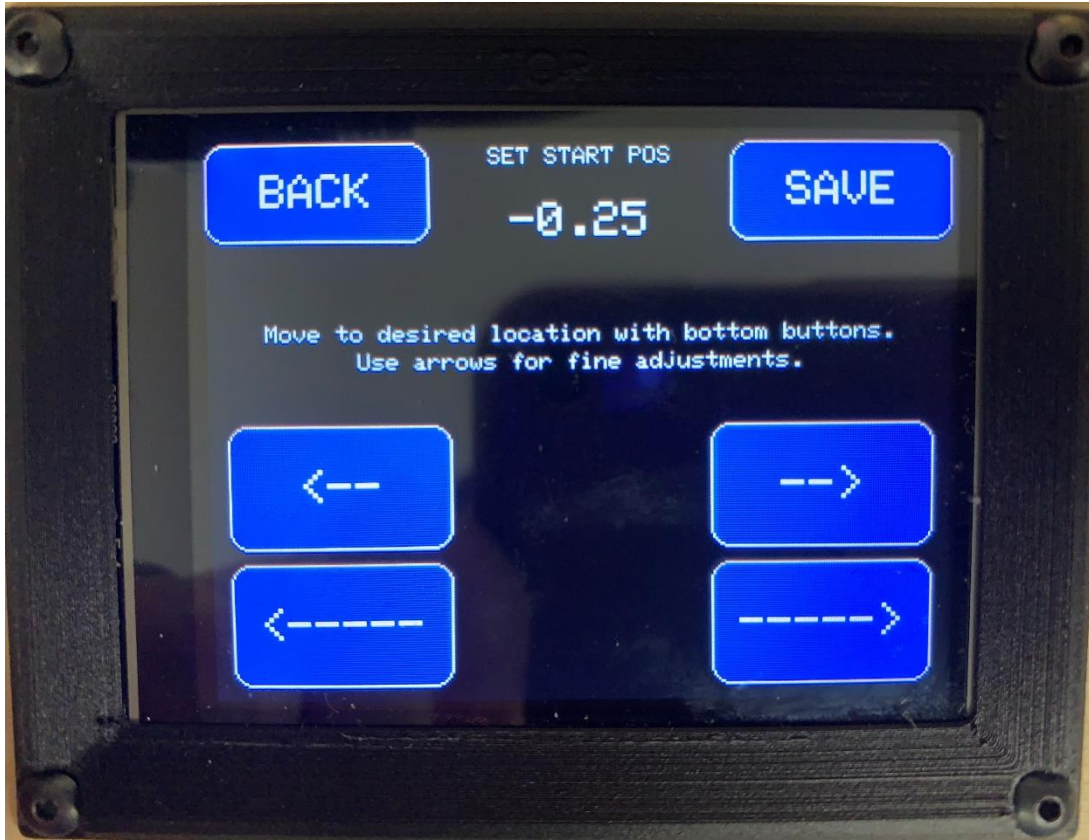


Figure 2.86 Set start position screen.

#### 2.5.6 Setting Plot, Stalk, and Node

The SD breakout board restricts file names to eight characters before the .csv. The SPuD generates the file name by concatenating the four digit plot number, two digit stalk number, and two digit node number into a single 8-digit number. When the **testing menu** is first accessed after powering up or restarting the SPuD it will default the plot, stalk, and node fields to zeros.

To set the plot number press the PLOT button on the **testing menu** screen. Use the keypad to enter the plot number. Pressing the plus button will increment the entered value by one. Once the plot number has been entered press SAVE to save the value and return to the **testing menu**. The first four digits of the filename should now match the plot number.

Both stalk and node number are set similarly by pressing on their corresponding buttons on the **testing menu**. Though both of these only have two digits to enter instead of four. Once the user has finished inputting these values the file name should be a unique 8-digit name corresponding to a specific plot, stalk, and node. Now the user can begin testing.



Figure 2.87 Set plot number screen.

#### 2.5.7 Testing

To begin testing the SPuD should be brought over to a corn stalk and placed so that the stalk is between the inside face of the backplane and the pusher arms. Make sure the minor axis of the stalk internode is aligned to be punctured. Press and hold both bottom buttons while on the testing menu to begin the test.

When testing begins the SPuD will first move the shuttle to the start location if it is not already there. Once the shuttle reaches the start it will immediately begin the test and run the needle all the way to the left until the shuttle hits the left limit switch. As this left movement begins the pusher arms should move forward slightly ahead of the needle and contact the stalk first to help align it and keep the device from shifting along the stalk during the test and damaging the needle. During this left movement of the shuttle the Arduino Mega will be constantly measuring the force and position and saving those values to the micro SD card. During all of this movement the screen will update the user on what is happening and remind them that the bottom buttons must be held during the test. If the user stops pressing one or both of the bottom buttons during a test they will have the option to resume the test by pressing both buttons again or cancel it by touching the screen. The full test movement of

the needle takes approximately 15 seconds (measured with needle at start position of -37.1 mm from zero).



Figure 2.88 SPuD during test.

Once a test is complete the shuttle will return to the start position and display the screen shown in Figure 2.89. This post test screen will display the maximum force encountered during the test, the file name, and a graph of the data collected. The graph shows displacement along the x axis and force along the y axis and is shown to help the user determine if they acquired accurate test data. The three buttons on this screen allow the user to save the data acquired and increment the stalk number by one, save the data acquired and increment the node number by one, or delete the data acquired based on the data preview. After pressing any of these buttons the user will be returned to the testing menu screen where they can begin the next test or adjust test inputs as needed. Cycle time for a full puncture test is approximately 37 seconds which means that the SPuD can take nearly 100 tests per hour.

The SPuD user interface provides the user with quick access to hardware checks, recalibration options, meta data entry, and post test data visualization on a bright touch screen display that is readable in direct sunlight. The only non-touch screen controls are the bottom push buttons which are included to promote user safety during needle movement.

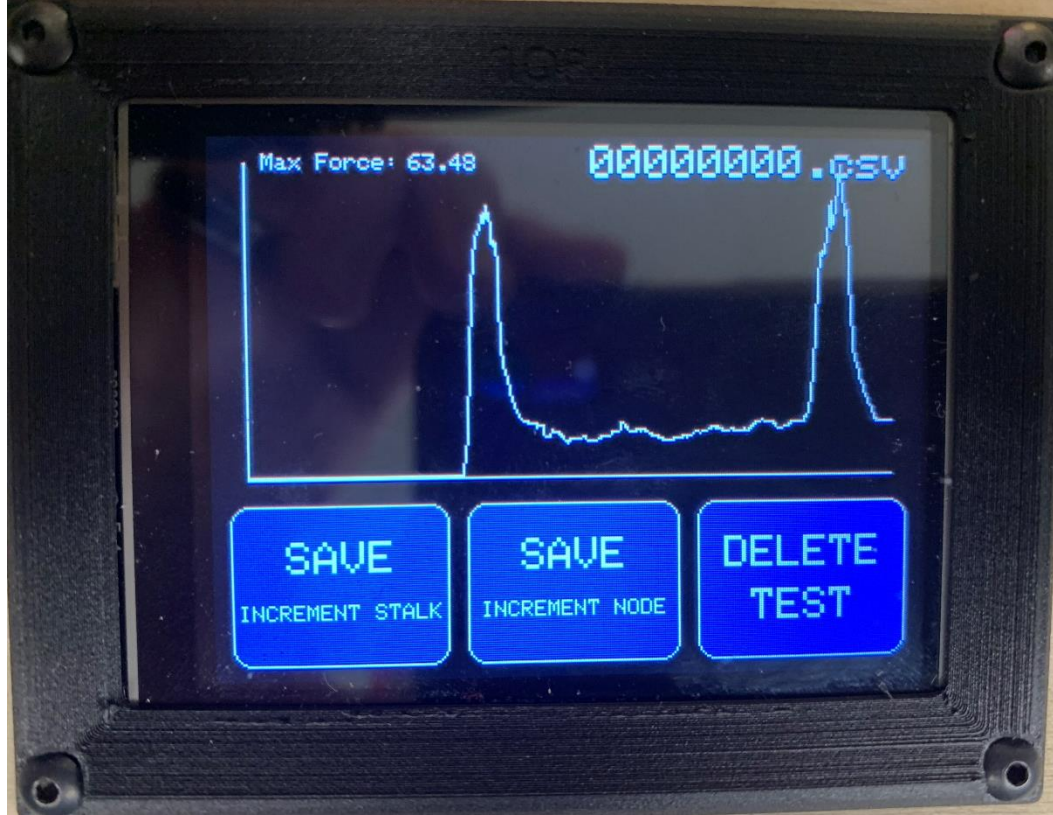


Figure 2.89 Post-test screen.

## 2.6 Validation

Validation for the SPuD was performed by comparing the results of SPuD puncture tests to puncture tests completed using an Instron Universal Testing System (Model # 5944).

### 2.6.1 Methods

Forty-four hybrid maize stalks were used to compare results between the Instron and SPuD puncture tests. These maize plants were grown in Clemson, South Carolina and include 31 stalks from two Mo45 x Mo17 plots and 13 stalks from one M045 x B73 plot. These forty-four maize stalks were harvested from the field at full maturity by cutting them just below the ear and above the ground. They were then moved to forced air dryers where they were dried to a stable state before testing to avoid deterioration over time. The stalks were then shipped from Clemson, South Carolina to Moscow, Idaho for testing. Across the forty-four stalks 123 nodes were punctured by both devices, first by the Instron and then by the SPuD. Internodes with noticeable damage were not tested. The Instron punctured through the minor diameter of the stalk at the middle of each internode. SPuD puncture tests cannot be performed at the same location along the internode due to interference from

the previous test hole. SPuD puncture tests were therefore performed 25 mm or more away from the Instron test location to prevent interference or crack propagation from the previous test hole.

Instron tests were performed using a 2 kN load cell and the custom puncture fixtures detailed in [29].

The SPuD is intended to be used on vertical stalks in the field so a stalk holder, seen in Figure 2.90, was assembled to hold stalks during testing.

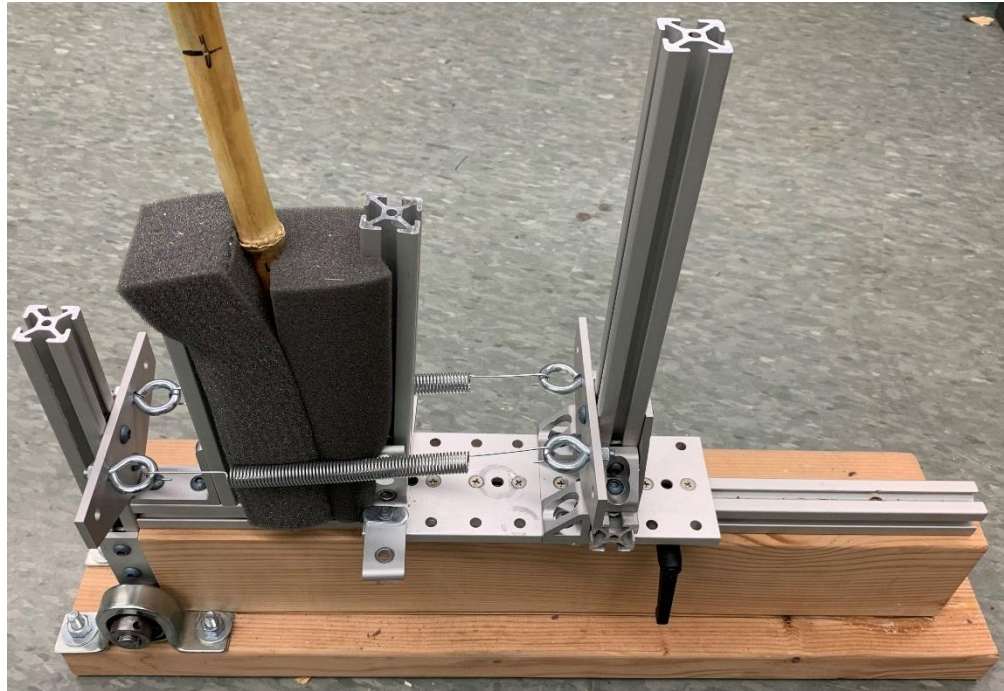


Figure 2.90 Stalk holder for validation tests.

#### 2.6.2 Validation Results

The outputs of both the Instron and SPuD puncture tests are continuous measurements of the displacement and force. Figure 2.91 shows three comparisons of Instron and SPuD data for puncture tests on the same internode. Figure 2.91(A) shows an example of poor SPuD data, likely caused by an incorrectly zeroed needle. This graph had the highest percent error, 5.695%, of all 123 tests when comparing the area under the curve for the SPuD versus the Instron area under the curve. Figure 2.91(B) is the graph from the test with the median error, 1.862%. Figure 2.91(C) shows a graph with one of the lowest percent errors of any test, 0.009%. As seen in the graphs the SPuD data appears more noisy while the Instron data appears smooth. This behavior can be seen throughout the rest of the tests, as well as the presence of the occasional “V” shapes noticeable during the peak rind forces in the SPuD data. These “V” shapes in the data are common but can range in height from just one to

two N, as seen in Figure 2.91(B), to more than 10 N in the most extreme cases. Qualitative analysis of the graphs shows that the Vs tends to be larger when the forces are larger, which likely points to an issue with the rigidity of the device. Running the SPuD without a stalk present showed that the noise during the test was only plus or minus 0.2 N. So it is unlikely that these V shapes are a result of noise.

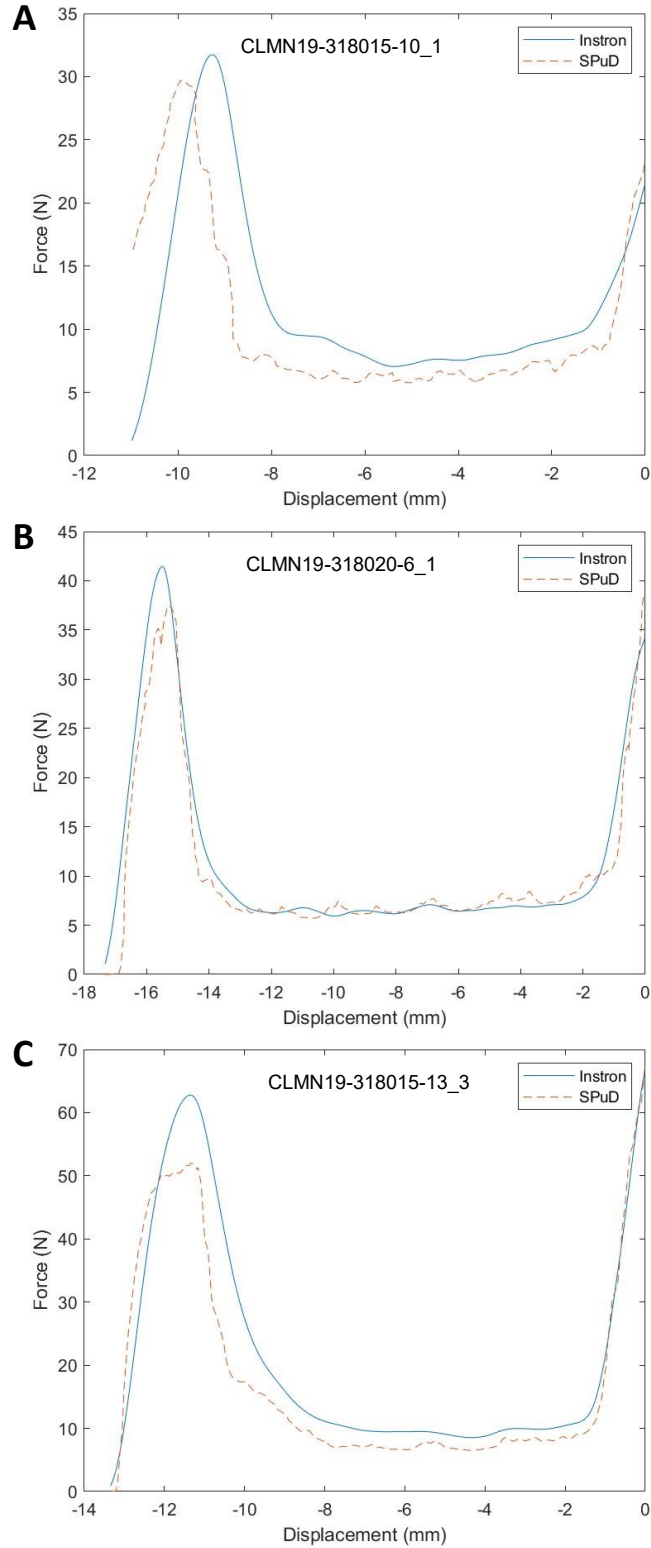


Figure 2.91 Three graphs comparing SPuD and Instron data for the same internodes. A) Graph with high error between SPuD and Instron area under the curve values; likely caused by incorrect zero on SPuD. B) Median error graph of all tests. C) Graph with low error.

A custom Matlab code was used to calculate the internode diameter of each test specimen using both the Instron and SPuD data. Results for each internode were then compared in the scatter plot shown in Figure 2.92. A line of best fit from the XY intercept showed a distinct correlation between the diameter values ( $R^2 = .9997$ ).

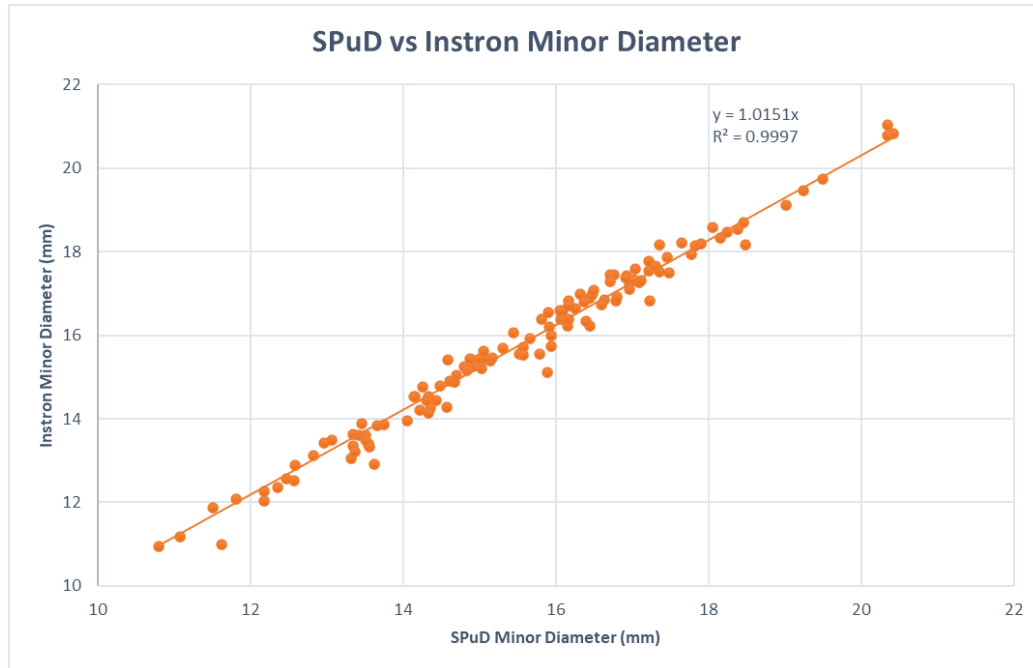


Figure 2.92 Scatter plot comparing minor diameter calculations for the Instron and SPuD.

Integrated puncture score values were calculated for both SPuD and Instron tests and the results have been plotted as seen in Figure 2.94. The line of best fit through the origin shows a strong correlation ( $R^2 = .97$ ) between the tests. The scatter plot of the data, seen in Figure 2.94, shows some heteroscedastic behavior to the data. This behavior is likely tied to the V shapes in the raw data plots discussed earlier, since the size of the Vs in the data seemed to increase with larger peak forces.

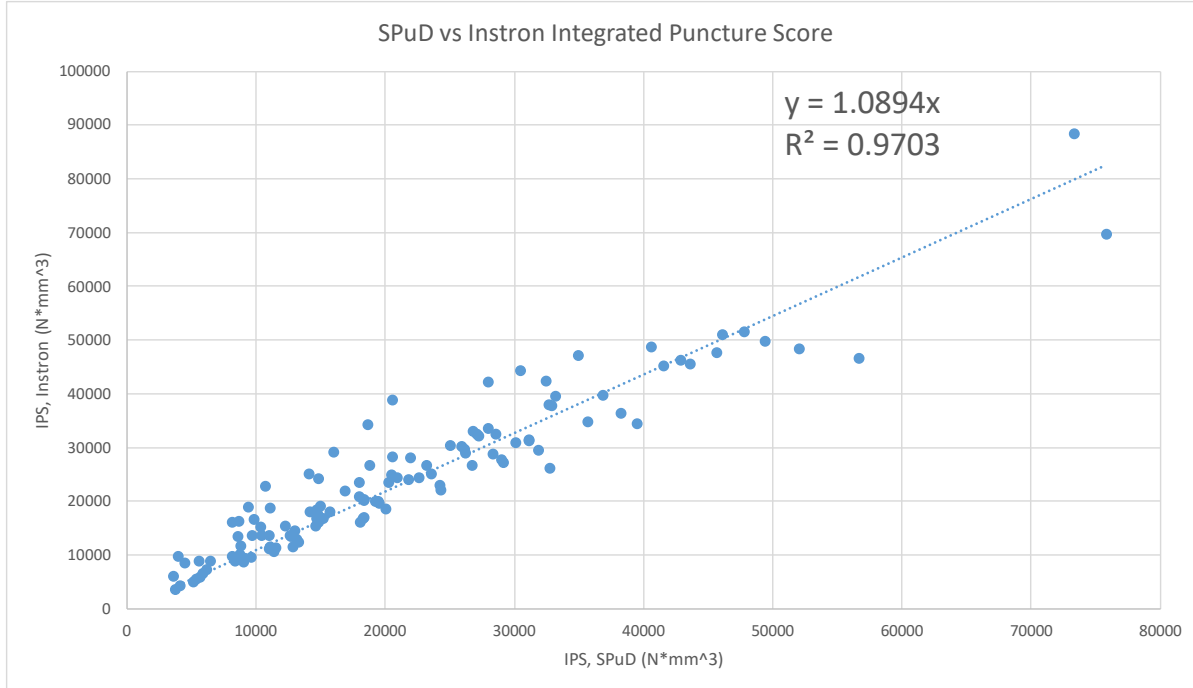


Figure 2.93 Scatter plot comparing SPuD and Instron IPS values.

The tests run on the SPuD device show more noise and have distinctive V shapes during peak forces that are likely a result of a lack of rigidity when compared with the Instron. Despite this, the data from the SPuD correlates strongly with Instron results and shows that the device can categorize the strength of maize stalks. Addressing the rigidity of the SPuD will only make the correlation stronger.

## Chapter 3: Conclusion

### 3.1 Design Challenges

Balancing the portability, functionality, stiffness, and robustness of the SPuD was a unique design challenge.

The portability of the SPuD is key because the ability to obtain data in vivo is the selling point of the device. Portability was considered by attempting to minimize the size and weight of the device. High quality 3D prints were utilized to reduce the weight, time, and cost of parts that would have otherwise been machined. The top and bottom covers on the SPuD are laser cut out of eighth inch birch to reduce weight and allow for rapid modification. The device currently weighs 6.062 kg and fits within a 39 cm by 22 cm by 16 cm box (with the batteries and sling mounts attached). The ergonomics of the device were also considered to increase portability and ease of use. The chest strap and sling mounts help hold the weight of the device between tests and allow users to rest their arms when they are not actively running a test.

The functionality of the SPuD is also key since the device must be capable of fully puncturing a stalk and logging the data required for each test. Some physical requirements, such as the puncture force being up to 200 Newtons with some maize stalks, actively worked against the portability of the device. The linear system, including the NEMA23 stepper motor, required to output this force makes up a significant portion of the SPuD's overall weight.

The stiffness of the SPuD is important to ensure the accuracy of the device. A previous iteration of the SPuD, designed by a senior design team, failed to test effectively largely in part to its lack of stiffness, which made measurements unpredictable. The extruded aluminum frame of the SPuD and the quarter inch thick aluminum back plate help ensure minimal deflection during the forces of testing. Calculations show that less than .02 mm of deflection would occur in the backplane with a force of 270 Newtons (max needle force experienced during historical Instron tests [200 Newtons] plus maximum possible spring forces from pusher arms [2 \* 35 Newtons]). However, measures to increase stiffness decrease the portability of the device by adding weight.

The robustness of the SPuD promotes the longevity and usability of the device. The SPuD is well enclosed and has a minimal amount of exterior wires that could be caught while using the device. Enclosing the device adds weight but increases the usability and reliability of the device during field testing.

Focusing on any one of these design criteria tended to negatively affect the others, which made designing the SPuD a balancing act. Choosing to use the AccuRemote linear scale instead of the more accurate glass scales was done because of the weight and size of glass scales, which made them unreasonable for a handheld device. The linear system was chosen because of its form factor and power output. It is necessary for the function and aids in the stiffness of the device but added a significant amount of weight. Many decisions that sacrificed one design criterion in favor of another were made throughout the design of the SPuD. Ultimately a balance was maintained that allows the device to be both portable and functional.

### **3.2 Next Steps**

The SPuD is portable and capable of gathering the required data to categorize stalk strength, but there is still more that can be done to improve this device.

The most necessary improvement will be for the overheating of the stepper motor driver. During the testing of the 123 stalks for validation it was noticed that the stepper motor began to chatter when changing directions after a number of continuous tests, approximately 35. Note that the rate of tests was significantly slowed during validation since the device was being set down between every few tests to manually change out the corn stalks being tested. The sporadic behavior of the stepper motor has been attributed to the overheating of the motor driver and/or motor because significant heat could be felt on the exterior of the device where the motor driver was mounted and because the chattering would cease after powering down the device and waiting. This issue was mitigated successfully throughout the remainder of testing by powering down the 24 V battery between tests to prevent the idle power from heating the motor and motor driver. As a future improvement an Arduino controlled relay should be added between the 24 V battery and the motor driver to prevent idle power from being transmitted to the driver and motor. Upgrading the motor driver to a more robust driver or finding a way to improve the heat dissipation from the motor driver would also be advised.

The rigidity of the SPuD could be improved to prevent the force drops in the data during testing. Many different methods could be used to improve the stiffness of the SPuD. Reworking the mounting configuration of the linear system, load cell mount, and other key components could improve the stiffness. Simpler fixes, such as ensuring all the screws are thoroughly tightened and locked with thread locker, could also improve the rigidity.

The Arduino programming could be improved in the future to enhance the robustness of the Arduino to Arduino communication. Adding more connections between the Arduinos would help prevent rare instances where partially written communications are read by adding “communication ready” checks before reading. Altering the test procedure code could also reduce the cycle time of tests by beginning to process the acquired data during the return movement of the needle, rather than waiting until movement is complete.

SPuD components could be altered to reduce the BOM and decrease the price of the device. There is a wide array of different hardware throughout the SPuD, in part due to it containing purchased components with both SI and English units, but this assortment of hardware could be refined by altering the design. This would not only simplify the BOM and construction process, but likely reduce the cost of the device. The price could be further decreased by finding alternatives for some of the more expensive components, such as the slides or the NEMA23 stepper included in the linear system. Additionally, some of the more costly 3D printed components, such as the motor cover body (CAD08), could be refined or printed with cheaper materials.

Once some of these improvements are considered, the device should be further tested by taking field data. Field testing the device will help ensure the usability and robustness of the device in its intended setting. These tests may expose flaws that can be addressed before the device is duplicated and changes become more costly. These puncture tests could be performed not only on late season maize stalks, but on green stalk for the first time. These could allow us to determine the efficacy of these tests across the full life of a maize plant.

### **3.3 Conclusion**

The Stalk Puncture Device is a portable battery operated device capable of performing nearly 100 puncture tests an hour on maize stalks. The user interface allows users to operate the device quickly and visualizes the acquired data after each test to improve data quality. Data acquired on the SPuD is more noisy than Instron data and includes regular V shaped dips in the force that are likely caused by a lack of rigidity in the device. Despite the presence of these dips the raw data and calculated values from the SPuD correlate strongly with Instron puncture test results. Improvements to the rigidity, hardware, and programming of the SPuD may improve its data’s correlation and its capabilities in the future, but the device is already capable of being a valuable tool for plant breeders and farmers to identify stronger more lodging resistant maize stalks.

## Literature Cited

- [1] J. M. Awika, “Major Cereal Grains Production and Use around the World,” in *Advances in Cereal Science: Implications to Food Processing and Health Promotion*, American Publisher Society, 2011, pp. 1–13.
- [2] “USDA Coexistence Fact Sheets Corn,” Feb. 2015.  
<https://www.usda.gov/sites/default/files/documents/coexistence-corn-factsheet.pdf> (accessed Aug. 23, 2021).
- [3] M. D. Edgerton, “Increasing Crop Productivity to Meet Global Needs for Feed, Food, and Fuel,” *Plant Physiol.*, vol. 149, no. 1, pp. 7–13, Jan. 2009, doi: 10.1104/pp.108.130195.
- [4] “World Agricultural Production,” *USDA Foreign Agricultural Service*.  
<https://www.fas.usda.gov/data/world-agricultural-production> (accessed Aug. 22, 2021).
- [5] D. J. Robertson, M. Julias, B. W. Gardunia, T. Barten, and D. D. Cook, “Corn Stalk Lodging: A Forensic Engineering Approach Provides Insights into Failure Patterns and Mechanisms,” *Crop Sci.*, vol. 55, no. 6, p. 2833, 2015, doi: 10.2135/cropsci2015.01.0010.
- [6] R. Elmore, D. Marx, R. Klein, and L. Abendroth, “Wind Effect on Corn Leaf Azimuth,” *Crop Sci. - CROP SCI*, vol. 45, Nov. 2005, doi: 10.2135/cropsci2004.0586.
- [7] H. Mizuno, S. Kasuga, and H. Kawahigashi, “Root lodging is a physical stress that changes gene expression from sucrose accumulation to degradation in sorghum,” *BMC Plant Biol.*, vol. 18, no. 1, p. 2, Jan. 2018, doi: 10.1186/s12870-017-1218-9.
- [8] S. Telkar, S. Solanki, S. Chouhan, R. Kumar, and S. Nikas, “Crop Lodging on Cereals: Causes, Effect and Control Introduction,” Nov. 2017.
- [9] M. Hanna, “Harvesting lodged corn | Integrated Crop Management,” *Iowa State University*.  
<https://crops.extension.iastate.edu/encyclopedia/harvesting-lodged-corn> (accessed Aug. 23, 2021).
- [10] N. Barnard, “Why does maize lodge?,” *Why does maize lodge?* <https://www.grainsa.co.za/why-does-maize-lodge> (accessed Aug. 22, 2021).
- [11] L. Erndwein, D. D. Cook, D. J. Robertson, and E. E. Sparks, “Field-based mechanical phenotyping of cereal crops to assess lodging resistance,” *Appl. Plant Sci.*, vol. 8, no. 8, p. e11382, 2020.
- [12] D. Rosenow *et al.*, “Proceedings of the International Conference on Genetic Improvement of Sorghum and Pearl Millet,” *INTSORMIL Impacts Bull.*, Sep. 1996, [Online]. Available: <https://digitalcommons.unl.edu/intsmilimpacts/79>
- [13] P. M. Berry and J. Spink, “Predicting yield losses caused by lodging in wheat,” *Field Crops Res.*, vol. 137, pp. 19–26, 2012.
- [14] S. A. Flint-Garcia, C. Jampatong, L. L. Darrah, and M. D. McMullen, “Quantitative trait locus analysis of stalk strength in four maize populations,” *Crop Sci.*, vol. 43, pp. 13–22, Feb. 2003, doi: DOI 10.2135/cropsci2003.0013.
- [15] D. N. Duvick, “The Contribution of Breeding to Yield Advances in maize (*Zea mays L.*),” *Adv. Agron.*, vol. 86, pp. 83–145, 2005, doi: 10.1016/S0065-2113(05)86002-X.
- [16] Q. Guo *et al.*, “A Non-Destructive and Direction-Insensitive Method Using a Strain Sensor and Two Single Axis Angle Sensors for Evaluating Corn Stalk Lodging Resistance,” *Sensors*, vol. 18, no. 6, p. 1852, 2018.
- [17] Q. Guo *et al.*, “Classification of Corn Stalk Lodging Resistance Using Equivalent Forces Combined with SVD Algorithm,” *Appl. Sci.*, vol. 9, no. 4, p. 640, 2019.
- [18] D. D. Cook, W. de la Chapelle, T.-C. Lin, S. Y. Lee, W. Sun, and D. J. Robertson, “DARLING: a device for assessing resistance to lodging in grain crops,” *Plant Methods*, vol. 15, no. 1, p. 102, 2019.
- [19] D. J. Robertson, S. Y. Lee, M. Julias, and D. D. Cook, “Maize Stalk Lodging: Flexural Stiffness Predicts Strength,” *Crop Sci.*, vol. 56, no. 4, p. 1711, 2016, doi: 10.2135/cropsci2015.11.0665.

- [20] K. L. Khanna, "An improved instrument for testing rind hardness in sugarcane," *Agr Live Stock India*, vol. 5, pp. 156–8, 1935.
- [21] E. M. Sibale, L. L. Darrah, and M. S. Zuber, "Comparison of two rind penetrometers for measurement of stalk strength in maize," *Maydica*, vol. 37(1), pp. 111–114, 1992.
- [22] S. A. Martin, L. L. Darrah, and B. E. Hibbard, "Divergent Selection for Rind Penetrometer Resistance and Its Effects on European Corn Borer Damage and Stalk Traits in Corn," *Crop Sci.*, vol. 44, no. 3, pp. 711–717, 2004, doi: 10.2135/cropscli2004.7110.
- [23] D. Cozzolino, A. Fassio, and A. Gimenez, "The use of near-infrared reflectance spectroscopy (NIRS) to predict the composition of whole maize plants," *J. Sci. Food Agric.*, vol. 81, no. 1, pp. 142–146, 2001, doi: 10.1002/1097-0010(20010101)81:1<142::AID-JSFA790>3.0.CO;2-I.
- [24] B. Anderson and D. G. White, "Evaluation of Methods for Identification of Corn Genotypes with Stalk Rot and Lodging Resistance," *Plant Dis.*, vol. 78, pp. 590–593, Jun. 1994.
- [25] J. W. Dudley, "Selection for Rind Puncture Resistance in Two Maize Populations," *Crop Sci.*, vol. 34, no. 6, pp. 1458–1460, 1994, doi: 10.2135/cropscli1994.0011183X003400060007x.
- [26] D. J. Robertson, D. D. Cook, K. Meehan, and L. Asatiani, "The Effect of Probe Geometry on Rind Puncture Resistance Testing of Maize Stalks," 2020.
- [27] R. S. Sekhon, C. N. Joyner, A. J. Ackerman, C. S. McMahan, D. D. Cook, and D. J. Robertson, "Stalk bending strength is strongly associated with maize stalk lodging incidence across multiple environments," *Field Crops Res.*, vol. 249, p. 107737, 2020.
- [28] Y. Oduntan, C. Stubbs, and D. Robertson, "High Throughput Phenotyping of Cross-sectional Morphology to Assess Stalk Lodging Resistance," *Researchsquare*, doi: 10.21203/rs.3.rs-650790/v1.
- [29] W. H. Seegmiller, J. Graves, and D. J. Robertson, "A novel rind puncture technique to measure rind thickness and diameter in plant stalks," *Plant Methods*, vol. 16, no. 1, p. 44, Apr. 2020, doi: 10.1186/s13007-020-00587-4.
- [30] C. J. Stubbs, C. McMahan, W. Seegmiller, D. D. Cook, and D. J. Robertson, "Integrated Puncture Score: force–displacement weighted rind penetration tests improve stalk lodging resistance estimations in maize," *Plant Methods*, vol. 16, no. 1, pp. 1–12, 2020.